

# Complex conformal spin partial wave expansion of generalized parton distributions and distribution amplitudes

D. Müller<sup>a,b</sup> and A. Schäfer<sup>a</sup>

<sup>a</sup> *Institut für Theoretische Physik, Universität Regensburg  
D-93040 Regensburg, Germany*

<sup>b</sup> *Department of Physics and Astronomy, Arizona State University  
Tempe, AZ 85287-1504, USA*

## Abstract

We introduce a new representation of generalized parton distributions and generalized distribution amplitudes that is based on the partial wave decomposition with respect to the *complex* collinear conformal spin. This decomposition leads us to a versatile parameterization of these non-perturbative functions in terms of conformal moments, which are measurable for integer value on the lattice. This new representation has several advantages: basic properties and crossing relations are automatically implemented, a rather flexible parameterization is possible, the numerical treatment of evolution is simple and analytic approximation of scattering amplitudes can be given. We demonstrate this for simple examples. In particular, phenomenological considerations indicate that the  $t$ -dependence of Mellin moments is governed by Regge trajectories. The new representation is vital to push the analysis of deeply virtual Compton scattering to next-to-next-to-leading order.

# Contents

<b>1</b>	<b>Introduction</b>	<b>1</b>
<b>2</b>	<b>Features and parameterization of GPDs</b>	<b>4</b>
2.1	The anatomy of GPDs . . . . .	4
2.2	Generalized distribution amplitudes and crossing . . . . .	10
2.3	Complex collinear conformal spin partial wave expansion . . . . .	11
2.3.1	Conformal partial wave expansion . . . . .	12
2.3.2	Sommerfeld-Watson transformation . . . . .	15
2.3.3	GPDs represented as Mellin-Barnes integral . . . . .	21
<b>3</b>	<b>Evolution kernels and coefficient functions in a manifest conformal scheme</b>	<b>25</b>
3.1	Convolution of GPDs with conformal kernels . . . . .	26
3.2	Mellin-Barnes representation for amplitudes . . . . .	29
<b>4</b>	<b>Evaluation and parameterization of conformal moments</b>	<b>32</b>
4.1	Numerical treatment of the Mellin-Barnes integral . . . . .	32
4.2	Ansätze for conformal moments . . . . .	37
4.2.1	Ansätze for reduced conformal moments . . . . .	38
4.2.2	Implementation of momentum squared dependence . . . . .	45
4.2.3	Numerical consequences for the probabilistic interpretation of GPD $H$ . . . . .	47
<b>5</b>	<b>Summary and conclusions</b>	<b>50</b>
<b>A</b>	<b>Integrals</b>	<b>53</b>
<b>B</b>	<b>Gluonic sector</b>	<b>55</b>
<b>C</b>	<b>Mellin–Barnes representation of conformal kernels</b>	<b>58</b>

# 1 Introduction

Generalized parton distributions (GPDs) [1, 2, 3, 4, 5] and their analog, obtained by crossing, generalized distribution amplitudes (GDAs) [2, 6] are non-perturbative functions that are accessible in certain hard exclusive processes such as the hard electroproduction of photons and mesons off a nucleon or nucleus or hadron pair production by two photon fusion in  $e^+e^-$  colliders. These functions are related to parton densities, form factors, and distribution amplitudes but contain additional non-perturbative information about the internal structure of hadrons and nuclei. Some of this information can even not be obtained in any other way than through a global fit of GPDs. This has been widely realized for the first time in connection with the proton spin puzzle. Here the second moment of a certain combination of GPDs provides the orbital angular momentum fraction carried by quarks of a given flavour [3]. Moreover, GPDs simultaneously possess a longitudinal and transverse momentum dependence and so it has been pointed out that they encode a three dimensional femto-holographic picture of the probed hadron or nucleus [7]. Indeed, it could be shown that a partonic density interpretation holds in the infinite momentum frame as long as the longitudinal momentum fraction in the  $t$ -channel is vanishing [8, 9], see also Refs. [10, 11]. More precisely, in the impact parameter space GPDs are interpreted as the probability to find a parton species  $i$  with momentum fraction  $x$  at a relative distance  $\mathbf{b}_\perp$  from the proton center. Even an interpretation of the three dimensional Fourier transform of GPDs in the rest frame has been suggested within the concept of phase space (Wigner) distributions [12, 13]. For further details we refer to the comprehensive reviews in Ref. [14, 15].

At present generalized parton distributions are one of the main topics of collider and fixed target experiments at DESY and JLAB. Further experiments are planned or proposed for COMPASS and ERIC. Also it should be mentioned that information on generalized distribution amplitudes has, e.g., been extracted from LEP data. Unfortunately, the wealth of information encoded in GPDs and GDAs goes along with their functional complexity. For instance, GPDs depend on both the momentum fractions in the  $s$ - and  $t$ -channel,  $x$  and  $\eta$ , the momentum transfer squared  $t$ , the resolution scale  $Q$ , and the quantum numbers of the target and the probed parton. This multitude of functional dependencies is, however, very strongly constrained by their relation to parton densities, form factors, and distribution amplitudes and even more so by crossing relations, positivity bounds and Lorentz invariance in general. The latter implies in particular that the Mellin  $x$ -moments of GPDs must be polynomials of given order in the skewness parameter  $\eta$ .

Unfortunately, there is still another complication. Typically experimental observables allow only to determine convolutions including GPDs or GDAs and a formal deconvolution can practically not be done for most of the processes<sup>1</sup>. To determine GPDs or GDAs from experimental data one therefore needs ansätze for them which involve only a minimal number of parameters.

---

<sup>1</sup>This is actually only possible if the hadron is probed with two virtual photons and the virtuality of both photons can be independently varied, which is experimentally an extremely challenging task [16, 17, 18].

Although, on the theoretical side GPDs have been intensively studied in the last few years, only a few of such parameterizations have been proposed and used in phenomenology. Perhaps the most popular parameterization is based on the ansatz suggested by Radyushkin, in which by construction the relation to parton densities, form factors, and polynomiality is assured. However, this advantages arise from the simplicity of this ansatz which also might implement a certain rigidity. Especially, it is widely used in combination with a factorized  $t$ -dependence although the latter is known to be wrong. This factorization does not respect the disappearance of the  $t$ -dependence for  $x \rightarrow 1$  [19, 20] and is also basically ruled out by lattice results [21, 22, 23]. How far the employed versions of this ansatz are suited for the kinematics accessible in present experiments remains an open question. Obviously, it is highly desired to have a versatile parameterization of GPDs and GDAs, which respects all of their formal properties.

The main idea guiding the search for a more appropriate parameterization of GPDs and GDAs is that the relevant kinematic variables should be separated in this new representation. Let us remind how helpful the representation of parton densities by Mellin moments has proven to be for the analysis of hard inclusive processes. Mellin moments are given by the analytic continuation of the forward expectation values of leading twist-two operators with given spin  $J$ . The main advantage of the Mellin space is that operators with different spin  $J$  do not mix under evolution and so the solution of the evolution equations is trivial. In the case of GPDs and GDAs leading twist-two operators can contain total derivatives and so the operator basis has to be chosen differently, in such a way that the operators again do not mix under evolution. The appropriate operator basis is given in terms of collinear conformal operators that are labelled by the (collinear) conformal spin and the normal spin of the operator. The former quantum number characterize the irreducible multiplets or conformal towers of the collinear conformal algebra while the latter denotes the members of a given multiplet. Group theoretically we are dealing with the representation of the so-called collinear conformal algebra  $so(2, 1)$  which is a subalgebra of the full conformal algebra  $so(4, 2)$ . Let us remark that except for the trace anomaly, which is proportional to the renormalization group coefficient  $\beta(\alpha_s)$ , conformal symmetry is preserved in perturbative QCD. Even in the case of a non-vanishing  $\beta$  function the conformal representations can be changed in such a way that the evolution operator is diagonal. The evolution equation can then be solved trivially. The conformal moments at the input scale depend on the skewness parameter and can be expanded in an appropriate orthogonal polynomial basis where the expansion coefficients depend on the momentum transfer squared. In other words, GPDs and GDAs can be represented by a conformal partial wave expansion, where the expansion coefficients are characterized by form factors that are labelled by the conformal spin and by an appropriate second quantum number, e.g., the angular momentum. Most importantly, it has been demonstrated that the first few form factors are measurable on the lattice. Moreover, the crossing relation between GPDs and GDAs are reduced in this representation of the continuation of these form factors from the space- to the time-like region and reverse.

Group theoretical discussions based on discrete conformal spin have a long history in QCD. However, in practice, they seemed to be only useful for distribution amplitudes and GDAs, where the resulting series convergence [24, 25]. Combined with conformal symmetry predictions, the perturbative corrections for (virtual) two photon processes in the generalized Bjorken limit can be worked out, e.g., for the photon-to-pion transition form factor, to next-to-next-to-leading (NNLO) order accuracy [26, 27].

For GPDs the conformal partial wave expansion, where the conformal spin is a non-negative integer, is represented by a series in terms of mathematical distributions, which only converges if it is convoluted with suitable test functions. An appropriate resummation of this series has been proposed in Ref. [28] and the details are presented here. There are also several other suggestions in the literature to define out of this divergent series. One might insert the identity expanded in terms of polynomials, which is however only applicable for a certain kinematical region [29, 30], and for a next-to-leading (NLO) analysis see Refs. [31, 32]. One can also represent the identity by its Fourier transform which makes contact to the group theoretical representation with complex valued conformal spin [33], later adopted for GPDs in Ref. [34] and more recently in Ref. [35]. Also a resummation by an integral transformation has been suggested [36], which, however, under close scrutiny turned out to be unpracticable or at least rather complicated [37]. An attempt to approximately resum the conformal partial wave expansion within a Taylor expansion of conformal moments has been suggested in Ref. [38]. Of course, all these proposals can be related to each other. However, because of the intricate mathematics involved a correct, complete and efficient resummation of conformal partial waves has not yet been worked out.

In this paper we employ the Sommerfeld-Watson transformation to resum the conformal partial wave expansion of GPDs, finally yielding a Mellin-Barnes integral for GPDs. The resulting representation is similar to the one recently proposed in Ref. [35], however, not identical. The Sommerfeld-Watson transformation requires the analytic continuation of the conformal spin, which plays here the analogous role to the complex spin  $J$  in the inverse Mellin representation of parton densities. While the analytic continuation of Mellin moments for parton distribution functions is a rather simple task, it is a highly non-trivial one for the conformal moments of GPDs. This central problem is solved by us to an extent such that the framework can be applied as soon as a GPD ansatz is given. Although the final GPD representation as a Mellin-Barnes integral over the complex conformal spin seems to be rather complicated it has several advantages. The dependence on kinematic variables is separated in this representation, it allows a simple and stable numerical treatment of GPDs and their convolution with hard-scattering amplitudes, and can be used for the analytic approximation of scattering amplitudes. Moreover, the evolution equations to leading order (LO) accuracy are trivially solved and the conformal approach in Ref. [26, 27] can be adopted for the study of higher order corrections in perturbative QCD. Especially, the NNLO corrections to deeply virtual Compton scattering (DVCS) are calculable in a rather economic manner [39]. Also the use of the crossing relation between GDAs and GPDs is possible in our representation

and should be very valuable for phenomenology.

The paper is organized as following. Sect. 2 is devoted to the conformal partial wave decomposition of GPDs for complex conformal spin. We start with a review on the anatomy of GPDs in Sect. 2.1 and discuss the extension of the GPD support [28]. To the best of our knowledge this issue has not been presented in detail so far. Here it will guide us to find the correct treatment of partial waves with complex conformal spin. We consider then the crossing relation between GDAs and GPDs and derive in Sect. 2.3 the new GPD and GDA representations in terms of Mellin-Barnes integrals. In Sect. 3 we consider evolution kernels and their convolution with GPDs in a scheme that preserves conformal symmetry. Moreover, we present the Mellin-Barnes integral for the scattering amplitude in DVCS and discuss its analytic approximation. In Sect. 4 we have a closer look to the analytic continuation procedure of conformal moments for a simple GPD toy ansatz. Then we address the issue of ansätze for conformal moments and explore the features of the resulting GPDs and GDAs. Furthermore, for vanishing longitudinal momentum fraction in the  $t$  channel we have a short look at valence quark GPDs. Motivated by lattice results [21, 22, 23], we introduce a parameterization for which the experimental constraints on GPDs indicate that leading Regge trajectories are present in conformal moments. Finally, we summarize and conclude. In Appendix A integrals, which are used in the main text, and the rotation from ordinary Mellin moments to conformal ones are presented. Appendices B and C contain the Mellin-Barnes integrals for gluonic GPDs and conformal evolution kernels, respectively.

## 2 Features and parameterization of GPDs

### 2.1 The anatomy of GPDs

GPDs are defined as Fourier transform of light-ray operators, sandwiched between the initial and final hadronic states. There is a whole compendium of GPDs for each hadron. In addition the initial and final states can have different quantum numbers (transition GPDs), and one even can replace the hadrons by nuclei (nucleus GPDs). Once the initial and final states are specified, GPDs are classified with respect to the twist of the operators and the spin content of fields. At leading twist-two level three different types of quark and gluon GPDs can be defined (here the gauge link is omitted):

$$\left\{ \begin{matrix} qF^V \\ qF^A \\ qF^T \end{matrix} \right\} (x, \eta, \Delta^2, \mu^2) = \int \frac{d\kappa}{2\pi} e^{i\kappa x P_+} \langle P_2, S_2 | \bar{\psi}_q^r(-\kappa n) \left\{ \begin{matrix} \gamma_+ \\ \gamma_+ \gamma_5 \\ i\sigma_{+\perp} \end{matrix} \right\} \psi_q^r(\kappa n) | P_1, S_1 \rangle, \quad (1)$$

$$\left\{ \begin{matrix} GF^V \\ GF^A \\ GF^T \end{matrix} \right\} (x, \eta, \Delta^2, \mu^2) = 2 \int \frac{d\kappa}{\pi P_+} e^{i\kappa x P_+} \langle P_2, S_2 | G_{+\mu}^a(-\kappa n) \left\{ \begin{matrix} g_{\mu\nu} \\ i\epsilon_{\mu\nu-+} \\ \tau_{\mu\nu;\rho\sigma} \end{matrix} \right\} G_{\nu+}^a(\kappa n) | P_1, S_1 \rangle, \quad (2)$$

with  $P_+ = n \cdot (P_1 + P_2)$ ,  $V_- = n^* \cdot V$ ,  $n^2 = (n^*)^2 = 0$ ,  $n \cdot n^* = 1$ . In the first (vector) and second (axial-vector) entry the in- and outgoing partons have the same helicities, and the sum (vector) and difference (axial-vector) of left- and right-handed partons is taken, respectively. For the third entry, called transversity, a helicity flip appears. GPDs depend on the momentum fraction  $x$ , conjugated to the light-cone distance  $2\kappa$ , the longitudinal momentum fraction  $\eta = (P_1 - P_2)^+ / (P_1 + P_2)^+$  in the  $t$ -channel<sup>2</sup>, the momentum transfer  $\Delta^2 \equiv t = (P_2 - P_1)^2$ , and the renormalization scale  $\mu^2$ . The latter is induced by the renormalization prescription of the operators, which is part of the GPD definition. To deal with the polarization of the hadronic states, one might introduce a form factor decomposition [40, 41]. For instance, for the nucleon GPD Dirac and Pauli-like form factors appear in the vector case [40]:

$${}^iF^V = \overline{U}(P_2, S_2) \gamma_+ U(P_1, S_1) H_i(x, \eta, \Delta^2) + \overline{U}(P_2, S_2) \frac{i\sigma_{+\nu} \Delta^\nu}{2M} U(P_1, S_1) E_i(x, \eta, \Delta^2), \quad (3)$$

where  $i = u, d, s, \dots, G$ . To avoid confusion, let us note that for the process  $\gamma^*(q_1) + p(P_1) \rightarrow \gamma^*(q_2) + p(P_2)$  two scaling variables exist. They are denoted as  $\xi$  and  $\eta$  and are defined by [2]:

$$\xi = \frac{-q^2}{P \cdot q}, \quad \eta = -\frac{\Delta \cdot q}{P \cdot q} \quad \text{with} \quad q = \frac{1}{2}(q_1 + q_2). \quad (4)$$

Both variable coincide, up to power suppressed corrections  $\mathcal{O}(\Delta^2/Q^2)$ , when the outgoing photon is real, i.e., for DVCS one can simply replace  $\eta$  by  $\xi$ . In this paper we will treat the general case.

The definitions (1)–(3) imply the basic properties of GPDs:

- In the forward limit  $\Delta \rightarrow 0$  helicity non-flip GPDs reduce to parton densities [2, 3, 4, 5], e.g.,

$$q_i(x, \mu^2) = \lim_{\Delta \rightarrow 0} H_i(x, \eta, \Delta^2, \mu^2) \quad (5)$$

and the helicity flip GPDs  $E_i$  decouple, but

$$\lim_{\Delta \rightarrow 0} E_i(x, \eta, \Delta^2, \mu^2) \neq 0. \quad (6)$$

- The  $\mu^2$ -dependence is governed by linear evolution equations [1, 2], which can be derived from the renormalization group equation of the light-ray operators [42, 43].
- Hermiticity [2] together with time reversal invariance [40] leads to a definite symmetry with respect to the skewness parameter  $\eta$ , e.g.,  $H_i(x, \eta) = H_i(x, -\eta)$ .
- The Mellin moments of GPDs are expectation values of local twist-two operators:

$$\int dx x^n {}^qF^V(x, \eta, \Delta^2, Q^2) = \frac{1}{P_+^{n+1}} n^{\mu_0} \dots n^{\mu_n} \langle P_2, S_2 | \mathbf{S} \bar{\psi}_q^r \gamma_{\mu_0} i \overleftrightarrow{D}_{\mu_1} \dots i \overleftrightarrow{D}_{\mu_n} \psi_q^r | P_1, S_1 \rangle, \quad (7)$$

---

<sup>2</sup>In the literature  $\eta$  is now denoted as  $\xi$ , which also is the Bjorken like scaling variable in hard inelastic exclusive processes. To be precise, we distinguish between both variables. The sign convention for  $\xi$  is fixed, for  $\eta$  it is changing. For quantities which are even under reflection, i.e.,  $\eta \rightarrow -\eta$ , the sign convention is irrelevant. Here we define  $\eta$  in such a way that it corresponds to the variable  $\xi$ , commonly used in the definition of GPDs, too.



where  $\overleftrightarrow{D}_\mu = \overrightarrow{D}_\mu - \overleftarrow{D}_\mu$  is the covariant derivative, acting as indicated by the arrows, and the operator  $\mathbf{S}$  symmetrizes all indices and subtracts the traces. Lorentz covariance enforces that this moments are polynomials in  $\eta$ .

Furthermore, GPDs are constrained in the region  $x \geq |\eta|$  by the positivity of the norm in the Hilbert space of states. The most general form of such positivity bounds [44, 45, 46], known so far, are given as an infinite set of constraints [47, 48]. Such constraints can be alternatively understood within the representation of GPDs as overlap of light-cone wave functions [49].

Let us consider the support of a GPD in more detail<sup>3</sup>. A generic quark GPD  $F(x, \eta, \Delta^2)$ , e.g., in the vector case, is related to a double distribution (DD)  $D(y, z, \Delta^2)$  by the integral transformation [2, 51]

$$F(x, \eta, \Delta^2) = \int_{-1}^1 dy \int_{-1+|y|}^{1-|y|} dz x^p \delta(x - y - \eta z) D(y, z, \Delta^2), \quad p = \{0, 1\}. \quad (8)$$

Here  $D(y, z, \Delta^2)$  is an even function in  $z$  so that  $F(x, \eta, \Delta^2)$  has the proper symmetric behavior under the exchange  $\eta \rightarrow -\eta$ . Obviously, its Mellin moments, i.e.,  $\int dx x^n F(x, \eta, \Delta^2)$  are even polynomials in  $\eta$ , since the support of  $D(y, z, \Delta^2)$  is restricted. Depending on the form factors appearing in the decomposition of the GPDs (1) and (2), see, for instance, Eq. (3), the order of the polynomial is  $n$  or  $n+1$ . To treat both cases in a convenient and generic manner, we have included in Eq. (8) the factor  $x^p$  with  $p = 0$  ( $p = 1$ ) in the former (latter) case [52]. This restores the correct order of the polynomials<sup>4</sup>. We can now fix  $\eta$  to be positive and decompose the integration with respect to  $y$  into  $y > 0$  and  $y < 0$ . This results into a decomposition of  $F(x, \eta, \Delta^2)$  in its quark  $q$  and anti-quark  $\bar{q}$  part:

$$F(x, \eta, \Delta^2) = q(x, \eta, \Delta^2) \mp \bar{q}(-x, \eta, \Delta^2). \quad (9)$$

Here both functions separately satisfy the polynomiality condition:

$$q(x, \eta, \Delta^2) = \int_0^1 dy \int_{-1+y}^{1-y} dz x^p \delta(x - y - \eta z) D(y, z, \Delta^2), \quad p = \{0, 1\} \quad (10)$$

and analogous for the anti-quark GPD  $\bar{q}(x, \eta, \Delta^2)$ , where  $D(y, z, \Delta^2)$  is replaced by  $\bar{D}(-y, z, \Delta^2) = \pm(-1)^p D(-y, z, \Delta^2)$

$$\bar{q}(x, \eta, \Delta^2) = \int_0^1 dy \int_{-1+y}^{1-y} dz x^p \delta(x - y - \eta z) \bar{D}(y, z, \Delta^2), \quad p = \{0, 1\}. \quad (11)$$

---

<sup>3</sup>The GPD support might be directly derived by means of a partonic Fock state decomposition and the so-called  $\alpha$ -representation for Feynman diagrams, see for instance Ref. [50]. Equivalently, a GPD can be expressed in terms of a DD [2, 51], which has a simpler structure, and one might consider it as more convenient to derive the support of the former from that of the latter.

<sup>4</sup>Note that within  $p = 0$  an additive so-called  $D$ -term was proposed to generate  $\eta^{n+1}$  terms [53]. It is only non-zero in the restricted region  $|x| \leq |\eta|$  and is contained in our representation with  $p = 1$  as an additive term of  $D(y, z, \Delta^2)$  that is proportional to  $\delta(y)$ . Our parameterization offers the possibility that the  $\eta^{n+1}$  terms arise from an uniform GPD.



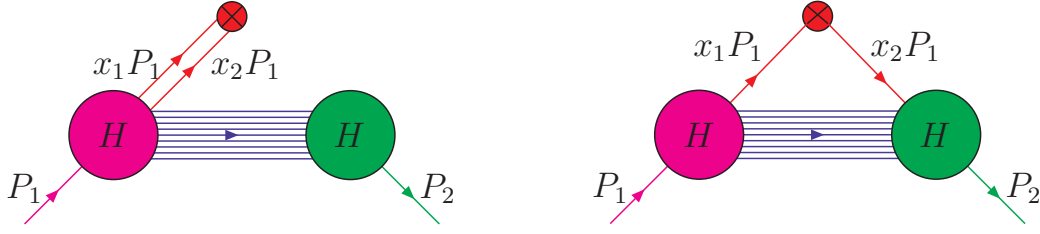


Figure 1: Partonic interpretation of GPDs in the central (left) and outer (right) region.

Obviously, both quark and anti-quark GPDs have the same mathematical representation and so we will in the following mainly deal with the quark one. The results for anti-quark GPDs are easily obtained by replacements  $D \rightarrow \overline{D}$ .

In the central (exclusive or ER-BL) region  $-\eta \leq x \leq \eta$ ,  $q(x, \eta, \Delta^2)$  might be interpreted as probability amplitude to have a meson like configuration inside the hadron, while the outer (inclusive or DGLAP) region  $\eta \leq x \leq 1$  can be viewed as probability amplitude for emission and absorbtion of a quark with momentum fraction  $x_1 P_1 = \frac{x+\eta}{1+\eta} P_1$  and  $x_2 P_1 = \frac{x-\eta}{1+\eta} P_1$ , respectively, see Fig. 1. Remarkably, both regions have a dual interpretation, namely, as meson and parton exchange in the  $t$  and  $s$  channel, respectively.

Lorentz invariance ties both dual regions, which can be read off from the representation (10) that ensures polynomiality. Suppose  $\eta \geq 0$ , the  $z$  integration in the double distribution representation (10) can be trivially performed<sup>5</sup> and leads to the support

$$q(x, \eta, \Delta^2) = \theta(-\eta \leq x \leq 1) \omega(x, \eta, \Delta^2) + \theta(\eta \leq x \leq 1) \omega(x, -\eta, \Delta^2). \quad (12)$$

The function  $\omega$  follows from the  $y$  integration in Eq. (10)

$$\omega(x, \eta, \Delta^2) = \frac{1}{\eta} \int_0^{\frac{x+\eta}{1+\eta}} dy x^p D(y, (x-y)/\eta, \Delta^2). \quad (13)$$

The GPD representation (12) is manifestly invariant under the transformation  $\eta \rightarrow -\eta$ , especially, the support  $-\eta \leq x \leq 1$  remains untouched.

In the central region the GPD is given by  $\omega(x, \eta, \Delta^2)$  from which the outer region, determined by the symmetrized function  $\omega(x, \eta, \Delta^2) + \omega(x, -\eta, \Delta^2)$ , can be restored, see Fig. 2. Let us have a closer look at this continuation. In the central region the integration variable in the integral (13) takes the values  $0 \leq y \leq \frac{x+\eta}{1+\eta} \leq 1$ . The restriction of the second argument in the double distribution  $|z| = |(x-y)/\eta| \leq 1-y$  is ensured by the values of the lower and upper limit, see solid line in Fig. 2(a). The integration path, starting at  $y = 0$  and  $z = x/\eta$ , lies inside of the DD support as it must be. At the cross-over point  $x = \eta$  it starts at the support edge  $y = 0$  and

<sup>5</sup> Since  $\eta > 0$ , we have set  $\delta(x-y-z\eta) = 1/\eta \delta(x/\eta - y/\eta - z)$  rather than to indicate the modulus  $1/|\eta|$ . The sign convention of  $\omega(x, -\eta)$  and its transformation under reflection  $\eta \rightarrow -\eta$  avoids an overall  $\text{sign}(\eta)$  factor in Eq. (12). This allows us to treat  $\omega(x, \eta)$  as a holomorphic function in the complex  $\eta$  plane.

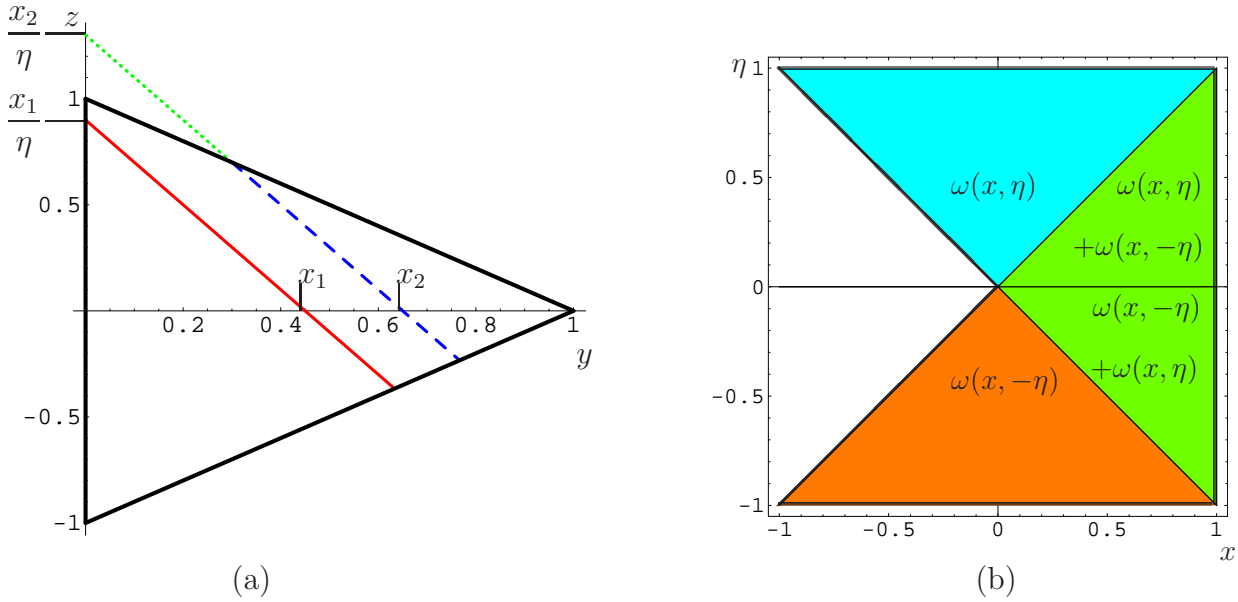


Figure 2: Support of a DD (the area surrounded by thick lines) and integration path for the calculation of  $\omega(x, \eta)$ , see Eq. (13), for the central region  $x_1 < \eta$  (solid) and the outer region  $\eta < x_2$  (dashed) are shown in Fig. (a). The continuation of the integration path over the support boundary is indicated as dotted line. In Fig. (b) the support of the resulting GPD (12) is depicted.

$z = 1$  and in the outer region the lower limit is  $y = \frac{x-\eta}{1-\eta}$  rather than zero. We can now define an (ambiguous) continuation of the DD support for  $|z| > 1 - y$  by any smooth function  $\tilde{D}(y, z, \Delta^2)$  symmetric in  $z$ .

$$D(y, (x-y)/\eta, \Delta^2) \rightarrow D(y, (x-y)/\eta, \Delta^2) \theta\left(y - \frac{x-\eta}{1-\eta}\right) + \tilde{D}(y, (x-y)/\eta, \Delta^2) \theta\left(\frac{x-\eta}{1-\eta} - y\right). \quad (14)$$

This provides the (ambiguous) continuation of  $\omega(x, \eta, \Delta^2)$  into the outer region.  $\omega(x, -\eta, \Delta^2)$  is obtained by reflection symmetry  $\eta \rightarrow -\eta$  and adding both contributions leads to the integral representation

$$\omega(x, \eta, \Delta^2) + \omega(x, -\eta, \Delta^2) = \frac{1}{\eta} \int_{\frac{x-\eta}{1-\eta}}^{\frac{x+\eta}{1+\eta}} dy x^p D(y, (x-y)/\eta, \Delta^2), \quad (15)$$

in which the integration runs only over the original support of the DD. Hence, the ambiguity in the continuation of  $\omega(x, \eta, \Delta^2)$  and  $\omega(x, -\eta, \Delta^2)$  drops out in their sum.

Let us suppose that  $D(y, z, \Delta^2)$  can be viewed as a holomorphic function of  $y$  and  $z$  inside its support and has branch cuts outside of it. Then the integration path in Fig. (2) (a) can cross or go along such branch cuts. To deal with a unique definition of  $\omega(x, \eta)$  for all values of  $x$  we might define its value within its integral representation (13) for  $\eta \leq x$  by the principal value prescription

$$\frac{1}{2} \omega(x + i\epsilon, \eta) + \frac{1}{2} \omega(x - i\epsilon, \eta) \quad \text{for } \eta < x. \quad (16)$$

For illustration we give a simple example for the Radyushkin ansatz

$$q(x, \eta) = \int_0^1 dy \int_{-1+y}^{1-y} dz \delta(x - y - \eta z) \frac{q(y)}{1-y} \Pi(|z|/(1-y)), \quad (17)$$

where the  $\Delta^2$  dependence is disregarded. The parton density is parameterized by a toy ansatz  $q(y) = y^\alpha(1-y)^\beta/B(\alpha+1, \beta+1)$ , which can be considered as building block for realistic parameterizations. A popular ansatz for the profile function is

$$\Pi(z) = \Pi(z|b) = \frac{(1-z^2)^b}{B(b+1, 1/2)}, \quad B(x, y) = \frac{\Gamma(x)\Gamma(y)}{\Gamma(x+y)}, \quad (18)$$

where the parameter  $b$  controls the strength of the skewness effect. This GPD ansatz can be evaluated in an analytical form in terms of hypergeometric functions for non-negative integer value of the parameter  $b$ . We might choose here for simplicity  $b = 0$ , i.e.,  $\Pi(z, 0) = 1/2$ . In the central region this toy GPD reads

$$q(x, \eta) = \frac{\Gamma(2+\alpha+\beta)}{2\eta\Gamma(2+\alpha)\Gamma(1+\beta)} \left(\frac{x+\eta}{1+\eta}\right)^{1+\alpha} {}_2F_1\left(\begin{matrix} 1+\alpha, 1-\beta \\ 2+\alpha \end{matrix} \middle| \frac{x+\eta}{1+\eta}\right) \quad \text{for } -\eta \leq x \leq \eta. \quad (19)$$

The extension of the DD support corresponds to the analytic continuation of  $\omega(x, \eta)$  into the outer region and so we find:

$$q(x, \eta) = \frac{\Gamma(2+\alpha+\beta)}{2\eta\Gamma(2+\alpha)\Gamma(1+\beta)} \left[ \left(\frac{x+\eta}{1+\eta}\right)^{1+\alpha} {}_2F_1\left(\begin{matrix} 1+\alpha, 1-\beta \\ 2+\alpha \end{matrix} \middle| \frac{x+\eta}{1+\eta}\right) - \left(\frac{x-\eta}{1-\eta}\right)^{1+\alpha} {}_2F_1\left(\begin{matrix} 1+\alpha, 1-\beta \\ 2+\alpha \end{matrix} \middle| \frac{x-\eta}{1-\eta}\right) \right] \quad \text{for } x \geq \eta. \quad (20)$$

We remark that the rescaled distribution

$$Y^{p-1}q\left(\frac{X}{Y}, \frac{1}{Y}, \Delta^2\right) = \int_0^1 dy \int_{-1+y}^{1-y} dz X^p \delta(X - yY - z) D(y, z, \Delta^2), \quad p = \{0, 1\} \quad (21)$$

has technically the same support as it appears in evolution kernels. Defining  $\varpi$  by

$$\varpi(X, Y, \Delta^2) = \int_0^{\frac{1+X}{1+Y}} dy X^p D(y, X - Yy, \Delta^2), \quad p = \{0, 1\}, \quad (22)$$

we have

$$Y^{p-1}q\left(\frac{X}{Y}, \frac{1}{Y}, \Delta^2\right) = \text{sign}(1+Y)\theta\left(\frac{1+X}{1+Y}\right)\theta\left(\frac{Y-X}{1+Y}\right)\varpi(X, Y, \Delta^2) + \left\{ \begin{matrix} X \rightarrow -X \\ Y \rightarrow -Y \end{matrix} \right\}. \quad (23)$$

The evolution kernels have the form (23) in the collinear limit  $\Delta^2 = 0$ . This enables us to adopt results for the representation of GPDs to the representation of GDAs (see next section) and of kernels. Needless to say, the GPD (12) follows from  $X = x/\eta$  and  $Y = 1/\eta$ , where  $\omega(x, \eta, \Delta^2)$ , see Eq. (13), is related to  $\varpi(X, Y, \Delta^2)$  by the formula

$$\omega(x, \eta, \Delta^2) = \eta^{p-1} \varpi\left(\frac{x}{\eta}, \frac{1}{\eta}, \Delta^2\right). \quad (24)$$

## 2.2 Generalized distribution amplitudes and crossing

Another ingredient we need for our derivation of a Mellin-Barnes representation of GPDs is their extension to  $1 < \eta$ . This immediately leads us to further non-perturbative distributions, the so-called GDAs [2, 6], which are related to GPDs by crossing [54]. The GDAs, denoted as  $\Phi(z, \zeta, W^2)$ , are defined in analogy to the GPDs in Eqs. (1) and (2), however, the initial state is replaced by the vacuum and the final one contains two hadrons. For instance, the crossing analog of  ${}^qF^V$  for a spin-zero target reads

$${}^q\Phi^V(z, \zeta, W^2, \mu^2) = \int \frac{d\kappa}{2\pi} e^{i\kappa(1-2z)P_+} \langle 0 | \bar{\psi}_q^r(-\kappa n) \gamma_+ \psi_q^r(\kappa n) | P_1, P_2 \rangle \quad (25)$$

with  $P_+ = n \cdot (P_1 + P_2)$ . Here  $0 \leq z \leq 1$  and  $1 - z$  are the momentum fractions of the quark and anti-quark, respectively, which produce the hadron pair with invariant mass squared  $W^2$ .  $0 \leq \zeta \leq 1$  is the momentum fraction of one of the hadrons.

In the following we give a rather generic discussion of the crossing relation to GPDs, which neglects details about form factor decomposition or quantum numbers. We consider also only a quark GPD and its analog. For anti-quarks the only additional aspect, that one has to implement, is the sign convention in the decomposition (9). The GDA reads in terms of the rescaled distribution (21) with  $X = 1 - 2z$ ,  $Y = 1 - 2\zeta$ , and  $\Delta^2 = W^2$  as

$$\Phi(z, \zeta, W^2) = Y^{p-1} q\left(\frac{X}{Y}, \frac{1}{Y}, \Delta^2\right) \Big|_{X=1-2z, Y=1-2\zeta, \Delta^2=W^2}. \quad (26)$$

Consequently, from Eq. (23) we read off its representation

$$\Phi(z, \zeta, W^2) = \theta(z - \zeta) \varpi(1 - 2z, 1 - 2\zeta, W^2) + \theta(\zeta - z) \varpi(2z - 1, 2\zeta - 1, W^2), \quad (27)$$

where the function  $\varpi$  is given by the integral (22). Having in mind that in Eq. (26) a rescaled GPD appears, it remains a trivial exercise to directly relate GPDs and GDAs<sup>6</sup>:

$$\left\{ \begin{array}{c} \Phi(z, \zeta, W^2), \\ \varpi(1 - 2z, 1 - 2\zeta, W^2) \end{array} \right\} \leftrightarrow \left\{ \begin{array}{c} \eta^{1-p} q(x, \eta, \Delta^2) \\ \eta^{1-p} \omega(x, \eta, \Delta^2) \end{array} \right\}, \quad 1 - 2z \leftrightarrow \frac{x}{\eta}, 1 - 2\zeta \leftrightarrow \frac{1}{\eta}, W^2 \leftrightarrow \Delta^2, \quad (28)$$

where the lower line is in fact the relation (24).

Let us shortly discuss this crossing relation. A GDA is obtained from the GPD analog by

$$\varpi(1 - 2z, 1 - 2\zeta, W^2) = (1 - 2\zeta)^{p-1} \omega\left(\frac{1 - 2z}{1 - 2\zeta}, \frac{1}{1 - 2\zeta}, W^2\right). \quad (29)$$

Since  $0 \leq \zeta \leq 1$ , the second argument of  $\omega$  covers the region  $|1/(2\zeta - 1)| \geq 1$ . Thus, the crossing relation requires to enter a kinematic region which is unphysical for GPDs, except for the point

---

<sup>6</sup>Note that the upper line in Eq. (28) is only valid for  $1 < \eta$ , i.e.,  $\zeta < 1/2$ . For  $1/2 < \zeta$  one must replace  $\eta^{1-p}$  by  $\text{sign}(\eta)\eta^{1-p}$ . It is more convenient to use the second line, valid for all values of  $\eta$ , together with the explicit representations (12) and (27), see also footnote 5.

$\eta = 1$ , i.e.,  $\zeta = 0$ . However, for a given functional form of a GPD, the relation (29) allows to fix its phenomenological parameters. So for instance, the same function appears after factorization in hard exclusive electroproduction of a photon or mesons on a hadron target as GPD and in the production of a hadron pair due to two photon fusion as GDA. The knowledge of the analytic form of the GPD in the central region is sufficient to perform the symmetry transformation (29) to obtain the corresponding GDA. Reversely, a GPD follows from a given GDA using the symmetry transformation (24). As expected from general reasons, the physical and unphysical regions are again connected by crossing. Moreover, as we realized above,  $\omega(x, \eta, \Delta^2)$  is not uniquely defined in the outer region. As explained above this problem is artificial and does not affect the net contribution in this region.

Let us stress ones more that the extension procedure of the support is unique, which was shown in connection with the support extension of evolution kernels [1, 2]. Here we adopt the same arguments. Suppose we know the function  $\varpi(1 - 2z, 1 - 2\zeta, \Delta^2)$  in the region  $0 \leq \zeta \leq z \leq 1$ , which is equivalently to the knowledge of the GDA  $\Phi(z, \zeta, W^2)$ , see Eq. (27). Next representing the GDA (26) in terms of the DD (21), we realize that its convolution with any holomorphic test function  $\tau(z)$  yields an holomorphic function in  $\zeta$ . For instance, one finds for  $p = 0$

$$\int_0^1 dz \tau(z) \Phi(z, \zeta, W^2) = \frac{1}{2} \int_0^1 dy \int_{-1+y}^{1-y} dz \tau\left(\frac{1 - y(1 - 2\zeta) - z}{2}\right) D(y, z, W^2). \quad (30)$$

Hence, also the Fourier transform of the GDA with respect to  $z$  is a holomorphic function in the conjugate variables  $\lambda$  and  $\zeta$ . Consequently, we can employ analytic continuation. Then the inverse Fourier transform together with the crossing relation (28) yields the result we desire,

$$q(x, \eta, \Delta^2) = \text{sign}(\eta) \eta^{p-1} \int_{-\infty}^{\infty} \frac{d\lambda}{2\pi} e^{-i\lambda x/\eta} \text{AC} \left[ 2 \int_0^1 dz e^{i\lambda(1-2z)} \Phi(z, \zeta, W^2) \right], \quad (31)$$

where  $\zeta = (\eta - 1)/2\eta$ ,  $W^2 = \Delta^2$  and AC denotes the analytic continuation of both variables  $\lambda$  and  $\zeta$ . (Actually, the variables stays real and analytic continuation is only used to extend their numerical values on the real axis, e.g., for  $\lambda$  up to  $\pm$  infinity.)

### 2.3 Complex collinear conformal spin partial wave expansion

We derive now a new representation for GPDs which has several advantages, already mentioned in the introduction. In fact we will deal with a partial wave decomposition of GPDs, where the partial waves are labelled by the complex conformal spin, the quantum number which characterize the multiplets (towers) of conformal operators. This is rather analogous to the partial wave expansion of scattering amplitudes with respect to the complex angular momentum, however, requires a more attentive consideration. Irrespectively, of whether the symmetry is preserved or not, one can introduce such an expansion. Certainly, conformal symmetry is broken in the non-perturbative QCD sector. Fortunately, up to calculable corrections proportional the non-vanishing  $\beta$  function, it holds true in the perturbative sector and thus has nevertheless still predictive power.

In the following we consider only quark GPDs, the gluon case can be treated analogously and the results are collected in Appendix B. To derive the partial wave decomposition of GPDs, the following steps will be performed:

- First the conformal moments and partial wave expansion of GPDs are introduced for discrete conformal spin. Here GPDs are represented as a divergent series in terms of mathematical distributions.
- This series will be summed in the unphysical region, where it can be viewed as an ordinary expansion in terms of orthogonal polynomials, by means of the Sommerfeld–Watson transformation, which requires the analytic continuation of the conformal spin.
- Finally, we complete the Sommerfeld-Watson transformation and derive a representation of GPDs in terms of a Mellin–Barnes integral for the central region. The outer region follows from a suitable continuation in  $x$  that arises from the analytic structure of GPDs.

### 2.3.1 Conformal partial wave expansion

So-called conformal moments of quark GPDs are formed with respect to Gegenbauer polynomials  $\eta^n C_n^{3/2}(x/\eta)$  with index  $3/2$  and order  $n$ . These moments are given by the expectation value of local conformal operators, see below Eq. (37). Relevant group theoretical aspects can be found in Appendix B and in the review [55]. These moments can be viewed as an appropriate generalization of the ordinary forward Mellin moments, used in the analysis of deep inelastic scattering. The Gegenbauer polynomials are orthogonal polynomials, possess a definite reflection symmetry  $C_n^{3/2}(x) = (-1)^n C_n^{3/2}(-x)$ , and are the only solution of the second order differential equation

$$\frac{d^2}{dx^2}(1-x^2)C_n^{3/2}(x) = -(n+1)(n+2)C_n^{3/2}(x) \quad (32)$$

that is finite at the singular points  $x = \pm 1$ . These polynomials form a complete basis in the interval  $[-1, 1]$ . Here we rescale the polynomials and choose the normalization

$$c_n(x, \eta) = \eta^n c_n\left(\frac{x}{\eta}\right) \quad \text{with} \quad c_n(x) = \frac{\Gamma(3/2)\Gamma(1+n)}{2^n \Gamma(3/2+n)} C_n^{3/2}(x) \quad (33)$$

in such a way that in the forward case the ordinary Mellin moments appear:

$$\lim_{\eta \rightarrow 0} c_n(x, \eta) = x^n. \quad (34)$$

There are several possibilities to express  $c_n(x, \eta)$  in terms of hypergeometric functions, which might provide different prescriptions for the analytic continuation of the discrete variable  $n$ . Below we will use

$$c_j(x, \eta) = \frac{\Gamma(3/2)\Gamma(3+j)}{2^{1+j}\Gamma(3/2+j)} \eta^j {}_2F_1\left(\begin{matrix} -j, j+3 \\ 2 \end{matrix} \middle| \frac{\eta-x}{2\eta}\right) \quad (35)$$

for complex valued  $j$ . Equivalently, we can express it in terms of (associated) Legendre functions of the first kind.

The conformal moments of a GPD, separated into quark and anti-quark ones, are defined as

$$m_n(\eta, \Delta^2) = \int_{-\eta}^1 dx c_n(x, \eta) q(x, \eta, \Delta^2), \quad \overline{m}_n(\eta, \Delta^2) = \int_{-\eta}^1 dx c_n(x, \eta) \overline{q}(x, \eta, \Delta^2). \quad (36)$$

They are given by the expectation values of collinear conformal operators, e.g., in the vector case,

$$m_n(\eta, \Delta^2) - (-1)^n \overline{m}_n(\eta, \Delta^2) = \frac{\Gamma(3/2)\Gamma(1+n)\eta^n}{2^n\Gamma(3/2+n)P_+} \langle P_2, S_2 | \bar{\psi}_q^r \gamma_+ C_n^{3/2} \left( \frac{i \overleftrightarrow{D}_+}{\eta P_+} \right) \psi_q^r | P_1, S_1 \rangle. \quad (37)$$

The rotation to the ordinary Mellin moments (7) and its inversion are given in Appendix A by Eqs. (169) and (170). The operators are characterized by the conformal spin, which in our case is  $n+2$ . The (conformal) moments can be either calculated on the lattice<sup>7</sup>, can be directly modelled, or evaluated from a given GPD ansatz. In the latter case they are naturally decomposed as, e.g., for quarks,

$$m_n(\eta, \Delta^2) = \mu_n(\eta, \Delta^2) + \mu_n(-\eta, \Delta^2), \quad \mu_n(\eta, \Delta^2) = \int_{-\eta}^1 dx c_n(x, \eta) \omega(x, \eta, \Delta^2). \quad (38)$$

This is a simple consequence of the symmetry relations  $c_n(x, \eta) = c_n(x, -\eta)$  together with the representation (12). The  $\mu_n(\eta, \Delta^2)$  are only defined in terms of  $\omega(x, \eta, \Delta^2)$  and, thus, they can be quite general functions of  $\eta$ . However, after symmetrization with respect to  $\eta$ , see first formula in Eq. (38), one obtains the polynomial  $m_n(\eta, \Delta^2)$ .

Now we would like to invert the transformation (36). As mentioned above the polynomials  $c_n(x, \eta)$ , see Eqs. (33) and (34), form only a complete basis in the central region  $[-\eta, \eta]$ . Let us denote by  $p_n(x, \eta)$  the polynomials that include the weight  $(1-x^2)$  and an appropriate normalization

$$p_n(x, \eta) = \eta^{-n-1} p_n\left(\frac{x}{\eta}\right), \quad p_n(x) = \theta(1-|x|) \frac{2^n \Gamma(5/2+n)}{\Gamma(3/2)\Gamma(3+n)} (1-x^2) C_n^{3/2}(-x). \quad (39)$$

The orthogonality relation for Gegenbauer polynomials reads in our notation

$$\int_{-1}^1 dx p_n(x, \eta) c_m(x, \eta) = (-1)^n \delta_{nm}. \quad (40)$$

The minus sign in the argument of Gegenbauer polynomials in Eq. (39) is conventionally and induces the factor  $(-1)^n$  in the orthogonality relation. This sign convention is appropriate to perform the steps which follow. Note also that the support restriction is explicitly contained in

---

<sup>7</sup>The separation of valence quarks and sea quarks is done by measuring even and odd moments. For instance, in the vector case: if the quark and anti-quark sea is equivalent, in even moments the complete sea drops out, while for odd moments valence and sea quarks are added.



the definition (39) and so the integration region in the integral (40) is restricted to the central region. We might now expand a GPD in terms of such polynomials (39)

$$q(x, \eta, \Delta^2) = \sum_{n=0}^{\infty} (-1)^n p_n(x, \eta) m_n(\eta, \Delta^2). \quad (41)$$

It is easily to see that the conformal moments (36) of a GPD are reproduced by this series (41). However, it is divergent as expansion in terms of polynomials<sup>8</sup>. Especially, the restricted support property of each individual term does not imply that the GPD vanishes in the outer region. Rather one should understand this expansion as an ill-convergent sum of distributions (in the mathematical sense) that yields a result which is non-zero in the outer region. Indeed,  $p_n(x, \eta)$  can be considered as the  $n$ th derivative of a smeared  $\delta$  function:

$$p_n(x, \eta) = \frac{\Gamma(5/2 + n)}{n! \Gamma(1/2) \Gamma(2 + n)} \int_{-1}^1 du (1 - u^2)^{n+1} \delta^{(n)}(x - u\eta). \quad (42)$$

Taking now the forward limit  $\lim_{\eta \rightarrow 0} p_n(x, \eta) = \delta^{(n)}(x)/n!$ , the series (41) turns out to be the expansion of parton densities in terms of derivatives of  $\delta(x)$ .

On the other hand, Eq. (41) might be a convergent series for  $\eta > 1$  and by means of the crossing relation (28) we find for a GDA the partial wave decomposition:

$$\Phi(z, \zeta, W^2) = \sum_{n=0}^{\infty} (-1)^n p_n(1 - 2z, 1) M_n(\zeta, W^2), \quad (43)$$

where the polynomials  $M_n(\zeta, W^2) = (1 - 2\zeta)^n m_n(1/(1 - 2\zeta), W^2)$  are of order  $n$ . If  $\Phi(z, \zeta, W^2)$  is a smooth function that vanishes at the end-points  $z = \{0, 1\}$ , the series converges and the moments  $M_n(\zeta, W^2)$  behave for  $n \rightarrow \infty$  as  $\sim 2^{-n} n^{-1/2-\epsilon}$  with  $\epsilon > 0$ . Here the exponential suppression by  $2^{-n}$  is a consequence of our normalization, which has been adopted from the Mellin moments of GPDs respectively parton densities.

The series (41) and (43) are the conformal partial wave expansions with respect to the conformal spin  $n + 2$ . They have the advantage that in perturbative QCD the conformal spin is, to some extend, a good quantum number. So for instance the LO evolution kernels are diagonal with respect to Gegenbauer polynomials. Furthermore, in this expansion the  $x$  and  $\Delta^2$  (respectively  $z$  and  $W^2$ ) dependence factorizes. In the case of GPDs the  $(x, \eta)$  dependence is decomposed in an intrinsic  $x/\eta$  and a remaining  $(\eta, \Delta^2)$  dependence contained in the conformal moments. The  $(\eta, \Delta^2)$  or  $(\zeta, W^2)$  dependencies can be separated by an expansion of the moments with respect to an appropriate set of orthogonal polynomials. It has been proposed to expand  $M_n(\zeta, W^2)$  in terms of Legendre polynomials  $P_l(\cos(\theta))$  [38], the eigenfunctions of the rotation group  $SO(3)$  for spinless states. Here  $\cos(\theta) \simeq 1 - 2\zeta = 1/\eta$  and  $\theta$  is the scattering angle in the center-of-mass system. Certainly, it is appealing to have such an expansion with respect to angular momentum  $l$ , which

---

<sup>8</sup>This is also the case in the central region  $[-\eta, \eta]$ , since the coefficients in front of the Gegenbauer polynomials are enhanced by the factor  $\eta^{-j-1}$ , which diverges for  $|\eta| < 1$  at  $j \rightarrow \infty$ .

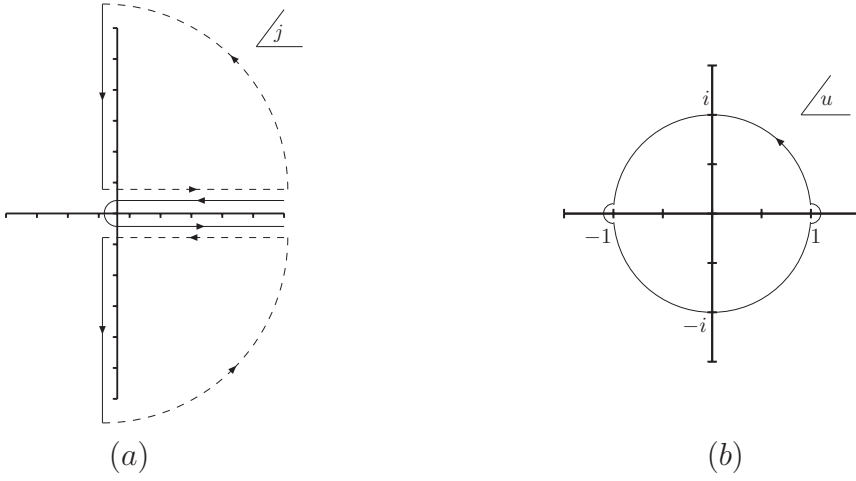


Figure 3: (a) The integration contour in Eq. (45) enclosing the real axis in the complex  $j$ -plane. Adding semicircles results in an integration path which is parallel to the imaginary axis. (b) The contour of the Schläfli integral (46) in the complex  $u$ -plane.

makes contact to the  $SO(3)$  partial wave expansion. When spin is involved, the expansion is rather given in terms of Wigner functions, expressible in terms of associated Legendre polynomials. To be not specific on the spin content and in view of the definition in terms of conformal operators, it appears also natural to expand conformal moments with respect to Gegenbauer polynomials with index  $3/2$ :

$$m_n(\eta, \Delta^2) = \sum_{k=0}^n F_{nk}(\Delta^2) \eta^n c_k(1/\eta), \quad M_n(\zeta, W^2) = \sum_{k=0}^n F_{nk}(W^2) c_k(1 - 2\zeta), \quad (44)$$

where all  $\Delta^2$  and  $W^2$  dependence is absorbed into the form factors<sup>9</sup>  $F_{nk}$ . Obviously, the crossing of GPDs and GDAs, i.e., the transfer from the space-like to the time-like region, concerns now only these form factors. The form factors, appearing in a specific partial wave expansion with respect to the angular momentum, are simply obtained by a rotation from the conformal ones, i.e.,  $F_{nk}(\Delta^2)$ .

### 2.3.2 Sommerfeld-Watson transformation

As already mentioned, the series (41) can not be directly used in practical calculation. Rather, it must be either resummed or the individual terms must be smeared by inserting the identity, expanded with respect to an appropriate basis. However, the latter method is only applicable in a restricted kinematical region and has been performed only approximately. So we chose to resum the conformal partial waves series for GPDs instead. We consider it first in the unphysical region  $\eta > 1$  and rewrite  $q(x, \eta, \Delta^2)$  as a contour integral in the complex plane that includes the positive

<sup>9</sup>We note that in this expansion the scaling invariance and so the conformal symmetry is broken, since in general the form factors contain now a massive parameter for dimensional reason. This is not surprising, since in non-perturbative QCD this symmetry does not hold – otherwise there would exist only massless hadrons.

real axis, see Fig. 3:

$$q(x, \eta, \Delta^2) = \frac{1}{2i} \oint_{(0)}^{(\infty)} dj \frac{1}{\sin(\pi j)} p_j(x, \eta) m_j(\eta, \Delta^2). \quad (45)$$

Here we included a factor  $1/\sin(\pi j)$ , which has the residue  $\text{Res}_{j=n} 1/\sin(\pi j) = (-1)^n/\pi$  for  $n = 0, 1, 2, \dots$ . Thus, if no other singularities are present inside the integration contour, the residue theorem leads to the conformal partial wave expansion (41). The main difficulty is to find an appropriate analytic continuation<sup>10</sup> of both functions  $p_j(x, \eta)$  and  $m_j(\eta, \Delta^2)$  with respect to the conformal spin  $n + 2$ .

First let us define the analytic continuation of  $p_j(x, \eta)$ . This can be done using its definition (39) in terms of hypergeometric functions. To include also the support restriction, we represent the analytic continuation of the Gegenbauer polynomials by the Schläfli integral

$$p_j(x, \eta) = -\frac{\Gamma(5/2 + j)}{\Gamma(1/2)\Gamma(2 + j)} \frac{1}{2\pi i} \oint_{(-1+\epsilon)}^{(+1-\epsilon)} du \frac{(u^2 - 1)^{j+1}}{(x + u\eta)^{j+1}}. \quad (46)$$

Here the integration contour is essentially the unit circle in the complex  $u$ -plane where the points  $-1$  and  $+1$  are included, see Fig. 3 (b). The integrand has four branch points in the complex  $u$ -plane, namely at  $\{-\infty, -1, -x/\eta, 1\}$ . These points will be connected by a single branch cut that goes along the real axis from  $-\infty$  to  $\text{Max}(-x/\eta, 1)$ . It is easy to see that for non-negative integer  $j = n$  the Schläfli integral is equivalent to the definition (39). The integrand possesses now only a pole of order  $n + 1$  at  $u = -x/\eta$  (and at infinity). For  $|x| < \eta$  the pole is inside the integration contour and the residue theorem gives  $p_n(x, \eta)$ . On the other hand for  $|x| > \eta$  the pole is moved out of the contour and so the integral vanishes.

Before we evaluate the integral (46) in general, let us consider the forward case  $\eta = 0$ . Here the integrand is essentially reduced to the function  $(u^2 - 1)^{j+1}$  and possesses for non-integer  $j$  a discontinuity on the real axis in the interval  $-1 \leq u \leq 1$ . We might now deform the contour so that the real axis is pinched. For  $|\Re u| \leq 1$  we pick up a phase factor  $e^{\pm i\pi(j+1)}$  for  $\Im u \gtrless 0$  and so we can write

$$p_j(x, \eta = 0) = x^{-j-1} \frac{\Gamma(5/2 + j)}{\Gamma(1/2)\Gamma(2 + j)} \frac{1}{2\pi i} (e^{i\pi(j+1)} - e^{-i\pi(j+1)}) \int_{-1}^1 du (1 - u^2)^{j+1}. \quad (47)$$

The remaining integral represents just  $\Gamma(1/2)\Gamma(2 + j)/\Gamma(5/2 + j)$ , which results in

$$p_j(x, \eta = 0) = \frac{\sin(\pi[j + 1])}{\pi} x^{-j-1}. \quad (48)$$

This is, up to the conventional factor  $\sin(\pi[1 + j])/\pi$ , nothing else but the integral kernel of the inverse Mellin transform, widely used in deep inelastic scattering.

---

<sup>10</sup>We remind that the analytic continuation of a function that depends on a discrete variable is not unique. For instance, a term proportional to  $\sin(\pi j)$  could be added, which drops out for  $j = n = 0, 1, 2, \dots$ .

For  $\eta > 0$  and non integer values  $j$  the integrand in Eq. (46) has no discontinuity for  $x \leq -\eta$ . For  $x \geq -\eta$  we will pick up phase factors by surrounding the branch points at  $-x/\eta$  and  $x = 1$ . They appear in the following interval above or below the real axis:

$$\left\{ \begin{array}{l} [-x/\eta, 1] \\ [-1, 1] \end{array} \right\} \quad \text{for} \quad \left\{ \begin{array}{l} -\eta < x \leq \eta \quad \text{and} \quad \eta > 0 \\ \eta < x \end{array} \right. . \quad (49)$$

Consequently, at the endpoint  $x = -\eta$  and for  $x < -\eta$  the integral vanishes

$$p_j(x \leq -\eta, \eta) = 0 . \quad (50)$$

For both the central and the non-vanishing outer region the complex integral can be evaluated by deforming the contour as before so that the real axis is pinched. Taking the discontinuity yield the following integrals along the real axis

$$\begin{aligned} p_j(x, \eta) &= \frac{\Gamma(5/2 + j)}{\Gamma(1/2)\Gamma(2 + j)} \frac{\sin(\pi[j + 1])}{\pi} \int_{-x/\eta}^1 du \frac{(1 - u^2)^{j+1}}{(x + u\eta)^{j+1}}, \quad -\eta \leq x \leq \eta, \quad \eta > 0 \\ &= \frac{\Gamma(5/2 + j)}{\Gamma(1/2)\Gamma(2 + j)} \frac{\sin(\pi[j + 1])}{\pi} \int_{-1}^1 du \frac{(1 - u^2)^{j+1}}{(x + u\eta)^{j+1}}, \quad 0 \leq \eta \leq x. \end{aligned} \quad (51)$$

At the cross over point  $x = \eta$  both integrals have the same value and represent a Beta function. So  $p_j(x = \eta, \eta)$  is smooth in the vicinity of this point and takes the value

$$p_j(x = \eta, \eta) = \frac{2^{1+j}}{\eta^{j+1}} \frac{\Gamma(5/2 + j)}{\Gamma(3/2)\Gamma(3 + j)} \frac{\sin(\pi[j + 1])}{\pi}. \quad (52)$$

The integrals in Eq. (51) define hypergeometric functions. The analytic continuation of the mathematical distributions  $p_n(x, \eta)$  with respect to the conformal spin is expressed by them as following:

$$p_j(x, \eta) = \theta(\eta - |x|)\eta^{-j-1}\mathcal{P}_j\left(\frac{x}{\eta}\right) + \theta(x - \eta)\eta^{-j-1}\mathcal{Q}_j\left(\frac{x}{\eta}\right) \quad (53)$$

where

$$\mathcal{P}_j(x) = \frac{2^{j+1}\Gamma(5/2 + j)}{\Gamma(1/2)\Gamma(1 + j)}(1 + x) {}_2F_1\left(\begin{matrix} -j - 1, j + 2 \\ 2 \end{matrix} \middle| \frac{1 + x}{2}\right), \quad (54)$$

$$\mathcal{Q}_j(x) = -\frac{\sin(\pi j)}{\pi} x^{-j-1} {}_2F_1\left(\begin{matrix} (j + 1)/2, (j + 2)/2 \\ 5/2 + j \end{matrix} \middle| \frac{1}{x^2}\right). \quad (55)$$

Here, a few comments are in order. First, for  $j = n = 0, 1, 2, \dots$  only the central region contributes and the relation

$${}_2F_1\left(\begin{matrix} -j, j + 3 \\ 2 \end{matrix} \middle| \frac{1 + x}{2}\right) = \frac{2}{1 - x} {}_2F_1\left(\begin{matrix} -j - 1, j + 2 \\ 2 \end{matrix} \middle| \frac{1 + x}{2}\right) \quad (56)$$

establishes the definition (39) of  $p_n$  in terms of Gegenbauer polynomials, cf. Eqs. (33) - (35). Obviously, in the central region the analytic continuation is based on the definition of hypergeometric

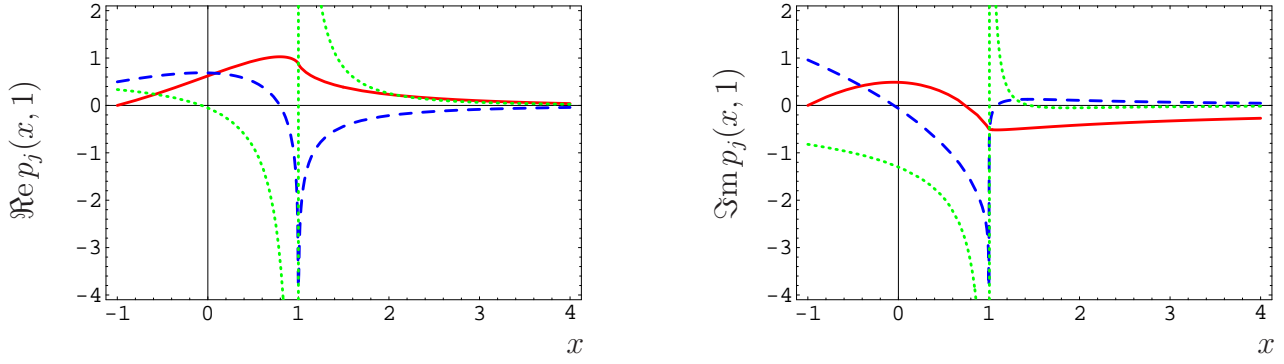


Figure 4: The real (left) and imaginary (right) part of the conformal partial wave  $p_j(x, \eta = 1)$  (solid), its first (dashed), and second (dotted) derivative for  $j = -1/4 + i/2$ .

functions. In the outer region, however, the result might be surprising. To clarify its meaning, we decompose the integral (51) for  $\eta < x$  as  $\int_{-1}^1 du \dots = \int_{-x/\eta}^1 du \dots - \int_{-x/\eta}^{-1} du \dots$  and realize that it can be expressed by the function  $\mathcal{P}_j$ . Thus, we can write Eq. (53) as

$$p_j(x, \eta) = \theta(-\eta \leq x) \eta^{-j-1} \mathcal{P}_j\left(\frac{x}{\eta}\right) + \theta(\eta \leq x) \cos(\pi[j+1]) \eta^{-j-1} \mathcal{P}_j\left(-\frac{x}{\eta}\right). \quad (57)$$

Here it is understood that the principal value is taken at the branch cut, which starts at  $x = \eta$ , i.e., we insert  $[\mathcal{P}_j(x+i\epsilon) + \mathcal{P}_j(x-i\epsilon)]/2$  for  $x \geq 1$ . The  $\cos(\pi[j+1])$  term in the second expression on the r.h.s. arise from the continuation of  $\eta$  to  $-\eta$ , again by taking the principal value. Hence, one realizes that this result precisely fits the structure of the representation (12) for  $q(x, \eta, \Delta^2)$  in terms of the functions  $\omega$ . We remark that the identity

$$\mathcal{Q}_j(x) = \frac{1}{2} \mathcal{P}_j(x+i\epsilon) + \frac{1}{2} \mathcal{P}_j(x-i\epsilon) + \cos(\pi[j+1]) \mathcal{P}_j(-x) \quad \text{for } x \geq 1, \quad (58)$$

we derived here, is a known relation between associated Legendre functions of the first and second kind.

The function  $p_j(x, \eta)$  is continuous at the cross-over point  $x = \eta$ , however, the imaginary part of the first derivative has a jump, while the real part is still continuous, see Fig. 4. It satisfies the second order differential equation for conformal partial waves with complex valued conformal spin  $j+2$ :

$$(1-x^2) \frac{d^2}{dx^2} p_j(x, \eta=1) = -(j+1)(j+2) p_j(x, \eta=1). \quad (59)$$

The expressions for the conformal partial waves in Eqs. (53), (54), and (55), turn out to be in agreement with a representation, given recently in Ref. [35], in terms of associated Legendre functions for the gluonic GPDs. In fact, up to some normalization factors and shift in both the conformal spin and the index, the same functions appear in the central and outer region. For the former one we, however, prefer to work with complex conformal spin, too. This incorporates the underlying duality between central and outer region in a manifest manner and yields a uniform representation of scattering amplitudes, see below Sect. 3.2. This is essential for the perturbative QCD analysis at higher orders.

The analytic continuation of the polynomials  $m_n(\eta, \Delta^2)$  is denoted as  $m_j(\eta, \Delta^2)$ . These functions will be also analytic in  $\eta$ , however, might have branch points at  $\eta = 0$ ,  $\eta = \pm 1$ , and  $\eta = \infty$ . It would be desirable to have an integral representation that makes this property transparent and might allow the continuation from  $\eta \geq 1$  to  $\eta \leq 1$  or even to negative values. Moreover, we will also require that the moments  $m_j(\eta, \Delta^2)$  are bounded at large  $j$ . It turned out that with these requirements the analytic or numerical calculation of moments from a given GPD is a rather intricate task. We have to admit that this mathematical problem is also not solved here for any conceivable GPD. In the following we give, however, some recipes to evaluate the conformal moments for complex conformal spin in the region  $|\eta| \leq 1$ .

To derive an appropriate integral representation, we decompose here, in contrast to Eq. (38), the conformal moments into contributions that arise from the outer and the central region:

$$m_n(\eta, \Delta^2) = \mu_n^{\text{cen}}(\eta, \Delta^2) + \mu_n^{\text{out}}(\eta, \Delta^2). \quad (60)$$

Again polynomiality is only manifest for the sum but not for the separate terms on the r.h.s. The analytic continuation of  $\mu_n^{\text{out}}(\eta, \Delta^2)$  is defined in terms of hypergeometric functions (35)

$$\mu_j^{\text{out}}(\eta, \Delta^2) = \int_{\eta}^1 dx c_j(x, \eta) [\omega(x, \eta, \Delta^2) + \omega(x, -\eta, \Delta^2)]. \quad (61)$$

From the asymptotics of the hypergeometric functions

$$c_j(x, \eta) \sim \left( \frac{x + \sqrt{x^2 - \eta^2}}{2} \right)^j \quad \text{for } j \rightarrow \infty, \quad |\arg(j)| \leq \pi/2, \quad (62)$$

we can estimate the large  $j$ -behavior of conformal moments

$$\mu_j^{\text{out}}(\eta, \Delta^2) \sim \int_{\eta}^1 dx \left( \frac{x + \sqrt{x^2 - \eta^2}}{2} \right)^j [\omega(x, \eta, \Delta^2) + \omega(x, -\eta, \Delta^2)]. \quad (63)$$

For  $0 < \eta < 1$  the integrand and thus the conformal moments are exponentially suppressed for  $j \rightarrow \infty$  with  $|\arg(j)| < \pi/2$ . In the limit  $\eta = 0$  we arrive at the parton densities and get the power like suppression factor  $j^{-p}$ .

The contribution from the central region reads for integer values  $n$

$$\mu_n^{\text{cen}}(\eta, \Delta^2) = \int_{-\eta}^{\eta} dx c_n(x, \eta) \omega(x, \eta, \Delta^2). \quad (64)$$

The analytic continuation of the conformal spin, as done for the central region above, would yield terms proportional to  $\sin(\pi j)$  that exponentially grow at large  $\Im j$ . The presence of such terms can also be read off from the integral (161), in the appendix, together with our final GPD representation (77), given below. In the case that this integral can be evaluated in an analytic form for integer  $n$  these terms drop out and the analytic continuation can be performed by means

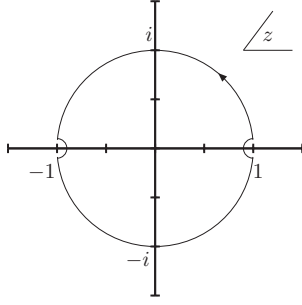


Figure 5: The integration contour in Eq. (65).

of the substitution  $n \rightarrow j$ . We remark that the explicit knowledge of  $\mu_j^{\text{out}}(\eta, \Delta^2)$  allows to restore the contribution from the central region by means of the polynomiality condition. Obviously, within such a procedure one might miss some terms that satisfy the polynomiality condition, but contribute only in the central region. Nevertheless, this procedure offers in principle a way to restore the polynomiality of a GPD that is only known in the outer region, e.g., from an ansatz within the overlap representation [49].

Another possibility for the analytic continuation of the conformal spin, appropriate for numerical calculations, arises from the definition of the conformal moments in the central region by the following contour integral (see Fig 5):

$$\mu_n^{\text{cen}}(\eta, \Delta^2) = \frac{\eta^{n+1}}{2i} \oint_{-1+\epsilon}^{1-\epsilon} dz d_n(z) \omega(z\eta, \eta, \Delta^2). \quad (65)$$

Here the function  $d_n(z)$  is defined in the complex plane by the integral

$$d_n(z) = \frac{1}{\pi} \frac{1}{(1-z^2)} \int_{-1}^1 dx \frac{(1-x^2)c_n(x, 1)}{x-z}. \quad (66)$$

It has a branch cut on the real axis in the interval  $[-1, 1]$  and in addition single poles at  $x = \{-1, 1\}$ . Thus, we excluded in the integration contour of the integral (65) the points  $x = \{-1, 1\}$ . Obviously, inserting Eq. (66) into Eq. (65) yield by means of the residue theorem and taking the limit  $\epsilon \rightarrow 0$  to the original definition of the conformal moments (64). The function  $d_n(z)$  can be expressed through Legendre functions of the second kind and an appropriate continuation of the conformal spin  $n$  is given in terms of a hypergeometric function

$$d_j(x) = \frac{2^{-2j-2}\Gamma(1+j)\Gamma(3+j)}{\Gamma(3/2+j)\Gamma(5/2+j)} \frac{x^{-j-1}}{x^2-1} {}_2F_1\left(\begin{matrix} (j+1)/2, (j+2)/2 \\ 5/2+j \end{matrix} \middle| \frac{1}{x^2}\right). \quad (67)$$

The function  $d_j(x)$  behaves at large  $x$  as  $x^{-j-3}$  and has a pole at  $x = \pm 1$ . At large  $j$  it is bound in the whole region  $1 \leq x \leq \infty$  by

$$d_j(x, \eta) \sim 2^{-j} \frac{x^{-1-j}}{x^2-1}. \quad (68)$$

Let us suppose that the function  $\omega(x\eta, \eta)$  is a regular function that has only a branch cut along the real axis  $[-\infty, -1]$  and has a power like behavior at infinity. We can expand the upper and lower



part of the integration contour in Fig. 5 to semicircles encompassing the complete half-planes such that the real axis is pinched in the intervals  $[-\infty, -1]$  and  $[1, \infty]$ . For a certain value of  $\Re j$ , the contributions at infinity are negligible and so we pick up the discontinuity along the negative real axis and the pole at  $x = 1$ . This result serves now for the definition of the analytic continuation in  $j$ :

$$\begin{aligned} \mu_j^{\text{cen}}(\eta, \Delta^2 | \sigma) &= \sigma \eta^{j+1} \int_{-\infty}^{-1} dx d_j(-x) \frac{1}{2i} [\omega(x\eta - i\epsilon, \eta, \Delta^2) + \omega(x\eta + i\epsilon, \eta, \Delta^2)] \\ &+ \left(\frac{\eta}{2}\right)^{j+1} \frac{\Gamma(1/2)\Gamma(1+j)}{\Gamma(3/2+j)} \omega(\eta, \eta, \Delta^2). \end{aligned} \quad (69)$$

Our choice of  $\Re j$  guarantees the convergence of the integral and, moreover, we assumed here that  $\omega(x = -\eta, \eta)$  vanishes. The choice of  $\Re j$  can be relaxed by introducing appropriate subtraction terms that improve the power behavior of  $\omega(\eta x, \eta)$  at  $x = \infty$ . On the r.h.s. of Eq. (69) the last term arises from the pole at  $x = 1$  and the first term contains a phase factor  $\sigma = e^{\pm i\pi j}$ , that depends on the continuation procedure from positive to negative real valued  $x$ . To get rid of this factor we define for even and odd  $n$  the analytic continuation as

$$\mu_n^{\text{cen}}(\eta, \Delta^2) \rightarrow \begin{cases} \mu_j^{\text{cen}}(\eta, \Delta^2 | \sigma = 1) \\ \mu_j^{\text{cen}}(\eta, \Delta^2 | \sigma = -1) \end{cases} \quad \text{for } n = \begin{cases} \text{even} \\ \text{odd} \end{cases}. \quad (70)$$

Note that the appearance of the phase factor is strongly connected to the analytic properties of GPDs and is only absent if the GPD has no branch point at  $x = -\eta$ .

Finally, we have for the analytic continuation of the conformal moments

$$m_n(\eta, \Delta^2) \rightarrow \begin{cases} m_j^{\text{even}}(\eta, \Delta^2) \\ m_j^{\text{odd}}(\eta, \Delta^2) \end{cases} = \mu_j^{\text{out}}(\eta, \Delta^2) + \begin{cases} \mu_j^{\text{cen}}(\eta, \Delta^2 | \sigma = 1) \\ \mu_j^{\text{cen}}(\eta, \Delta^2 | \sigma = -1) \end{cases} \quad \text{for } n = \begin{cases} \text{even} \\ \text{odd} \end{cases}. \quad (71)$$

It is obvious that  $m_j^{\text{even}}$  and  $m_j^{\text{odd}}$  lead only for even and odd integer values of  $j = n$  to polynomials, which are even in  $\eta$ . The difference of even and odd moments arises only from the central region and is expressed by a function in  $\eta$  which does not degenerate into a polynomial for integer values of  $j = n$ .

### 2.3.3 GPDs represented as Mellin-Barnes integral

Now we like to change the integration contour in Eq. (45), in such a way that it becomes parallel to the imaginary axis in the  $j$ -plane, i.e., extends from  $c - i\infty$  to  $c + i\infty$ . Here the constant  $c < 0$  is chosen such that all singularities contained in the conformal moments  $m_j(\eta, \Delta^2)$  are on the left hand side of the integration path. Let us assume for the moment that  $m_j(\eta, \Delta^2)$  degenerates for all non-negative integer values of  $j$  to polynomials. As displayed in Fig. 3 (a), we add two quarters of circles in the first and fourth quadrant so that the integration contour includes the imaginary axis and is closed by the arc that includes the points  $c + i\infty$ ,  $\infty$ , and  $c - i\infty$ .

It remains to show that within our definition of conformal moments the contribution from the arc vanishes. Suppose that  $\eta \geq 1$  and that the variable  $x$  is rescaled by  $\eta$ , i.e.,  $x = \eta X$ . Hence, we must study the behavior of  $p_j(\eta X, \eta)$  for  $j \rightarrow \infty$  in the interval  $|X| \leq 1$ . The asymptotic expansion of the partial waves for large  $j$  with  $|\arg(j)| \leq \pi/2$  can be read off from the behavior of hypergeometric functions [56] and is

$$p_j(X\eta, \eta) \sim \left(\frac{2}{\eta}\right)^j \left[ e^{j \operatorname{arccosh}(-X \pm i\epsilon)} \pm i e^{-(j+3) \operatorname{arccosh}(-X \pm i\epsilon)} \right] \quad \text{for } |X| \leq 1. \quad (72)$$

For  $-1 \leq X \leq 1$  the function  $\operatorname{arccosh}(-X \pm i\epsilon)$  has a monotonously increasing or decreasing imaginary part that lies in the interval  $[0, \pi]$  and  $[-\pi, 0]$  for the  $+i\epsilon$  and  $-i\epsilon$  prescription, respectively. Thus, within both prescriptions

$$\frac{1}{\sin(\pi j)} p_j(\eta X, \eta) m_j(\eta, \Delta^2) \quad (73)$$

exponentially vanishes for  $-1 < X < 1$  on the arc, specified above, as long as  $m_j(\eta, \Delta^2)$  behaves for  $\eta > 1$  as

$$m_j(\eta, \Delta^2) \sim \left(\frac{\eta}{2}\right)^j \quad \text{for } j \rightarrow \infty. \quad (74)$$

This remains true, if we replace  $p_j(x, \eta)$  by the symmetric and antisymmetric combinations

$$p_j^{\text{even}}(x, \eta) = \frac{1}{2} [p_j(x, \eta) + p_j(-x, \eta)], \quad p_j^{\text{odd}}(x, \eta) = \frac{1}{2} [p_j(x, \eta) - p_j(-x, \eta)] \quad (75)$$

and  $m_j(\eta, \Delta^2)$  by the corresponding even and odd moments, respectively. Since  $p_n(x, \eta) = (-1)^n p_n(-x, \eta)$  has definite symmetry, the residues of

$$\frac{1}{\sin(\pi j)} p_j^{\text{even}}(x, \eta) m_j^{\text{even}}(\eta, \Delta^2) \quad \text{and} \quad \frac{1}{\sin(\pi j)} p_j^{\text{odd}}(x, \eta) m_j^{\text{odd}}(\eta, \Delta^2) \quad (76)$$

only contribute for even and odd values of  $j = n$ , respectively, and, thus, the polynomiality is implemented in a manifest manner.

Unfortunately, we did not give in the previous section a representation for  $m_j(\eta, \Delta^2)$  that allows the analytic continuation in  $\eta$  to the region  $\eta > 1$  and simultaneously satisfies the requirement that  $m_j(\eta, \Delta^2)$  fulfills the bound (74). This can be read off from Eq. (63), where obviously, we will pick up an additional phase. It seems that such a representation can not easily be found rather we encounter here similar problems as for the continuation to the region  $\eta < 0$ .

This difficulty can be avoided once we replace in  $m_j(\eta, \Delta^2)$  the variable  $\eta$  by  $\eta^*$  with  $\eta^* \leq 1$ . It is sufficient to consider the cross-over point, since for all other  $x$  values inside the central region we will have an additional exponential suppression due to the phases of  $p_j(\eta, \eta)$ , see Eq. (72). For  $X = 1$  we find from Eq. (52) that  $p_j(\eta, \eta)$  behaves on the cross-over point as  $\sim (2/\eta)^j \sin(\pi j)/\sqrt{j}$ . To get rid of the exponential growth, induced by the real part of  $j$ , we might choose  $\eta > 2$  and can

arrange in this way even an exponential suppression. If now the conformal moments  $m_j(\eta^*, \Delta^2)$  for given  $\eta^*$  do not grow faster than  $(\eta/2)^j/\sqrt{j}$  for  $j \rightarrow \infty$ , the integral on the infinite arc does not contribute for  $x = 1$ , too. Thus, after appropriate scaling of  $x$  with  $\eta$ , analytic continuation to the region  $0 \leq \eta \leq 1$ , and setting  $\eta^* = \eta$  we find for all values  $|x| \leq \eta$  the following Mellin–Barnes integral representation for GPDs:

$$q(x, \eta, \Delta^2) = \frac{i}{2} \int_{c-i\infty}^{c+i\infty} dj \frac{1}{\sin(\pi j)} p_j(x, \eta) m_j(\eta, \Delta^2). \quad (77)$$

Finally, we extend this integral into the outer region. For  $p_j(x, \eta)$  this is done by means of the definition (53).

The Mellin–Barnes integral (77) can be used when the analytic continuation of even and odd moments leads to the same function  $m_j(\eta, \Delta^2)$ . If this is not the case, we separately introduce the Mellin–Barnes integral for the even and odd part of

$$q(x, \eta, \Delta^2) = q^{\text{even}}(x, \eta, \Delta^2) + q^{\text{odd}}(x, \eta, \Delta^2) \quad (78)$$

Since the representation (77) remains valid if we substitute  $p_j(x, \eta)$  by the symmetrized partial waves  $p_j^{\text{even}}(x, \eta)$  and  $p_j^{\text{odd}}(x, \eta)$ , we have the same form of the Mellin–Barnes integral as before:

$$q^{\text{even/odd}}(x, \eta, \Delta^2) = \frac{i}{2} \int_{c-i\infty}^{c+i\infty} dj \frac{1}{\sin(\pi j)} p_j^{\text{even/odd}}(x, \eta) m_j^{\text{even/odd}}(\eta, \Delta^2). \quad (79)$$

Bearing in mind that  $p_j(x, \eta)$  is set to zero for  $x < -\eta$ , the extension of  $p_j^{\text{even}}(x, \eta)$  and  $p_j^{\text{odd}}(x, \eta)$ , defined in Eq. (75) in terms of  $p_j(x, \eta)$  and  $p_j(-x, \eta)$ , is consistently done by the procedure (53). The original GPD (78) is restored by adding its even and odd parts:

$$q(x, \eta, \Delta^2) = \frac{i}{2} \int_{c-i\infty}^{c+i\infty} dj \frac{1}{\sin(\pi j)} [p_j^{\text{even}}(x, \eta) m_j^{\text{even}}(\eta, \Delta^2) + p_j^{\text{odd}}(x, \eta) m_j^{\text{odd}}(\eta, \Delta^2)] . \quad (80)$$

The extension into the outer region is not based on analytic continuation and the reader might wonder whether this prescription (53) is indeed correct. Besides the arguments we gave in Sect. 2.3.2, we provide next some further support. Let us first verify that the GPD representation (80) has the correct support property, i.e., it contributes only for  $-\eta < x$ . As mentioned above, the difference of odd and even moments arise only from the central region and has thus the functional form  $(\eta/2)^{j+1} f_j(\eta, \Delta^2)$ , where  $f_j(\eta, \Delta^2)$  has a power-like behavior at  $j \rightarrow \infty$ , see Eq. (69). We expect that such a term does not contribute to the outer region. Indeed this can be read off from the Mellin–Barnes integral, which takes the form

$$\frac{i}{2} \int_{c-i\infty}^{c+i\infty} dj \frac{2^{-j-1}}{\sin(\pi j)} Q_j(x/\eta) f_j(\eta, \Delta^2),$$

see definitions (53) and (55). For  $x > \eta$  the term  $2^{-j-1} Q_j(x/\eta)/\sin(\pi j)$  contains an exponential damping factor  $(\eta/x)^j$  for  $j \rightarrow \infty$  with  $|\arg(j)| < \pi/2$ , while the remaining factor in the integrand

is bounded. So we can close the integration contour by an infinite arc that includes the first and forth quadrant. Since the whole integrand is analytic in these two quadrants, Cauchy theorem gives zero. Note that  $Q_j(x/\eta)/\sin(\pi j)$  contains no singularities on the real positive axis. Consequently, even and odd contributions are the same in the outer region and will add for  $x > \eta$ , while they cancel for  $x < -\eta$ .

Alternatively, we can represent the GPD as

$$q(x, \eta, \Delta^2) = \frac{i}{2} \int_{c-i\infty}^{c+i\infty} dj \frac{1}{\sin(\pi j)} [\theta(|x| \leq \eta) p_j(-x, \eta) m_j^\Delta(\eta, \Delta^2) + p_j(x, \eta) m_j^\Sigma(\eta, \Delta^2)] , \quad (81)$$

where  $m_j^\Sigma = (m_j^{\text{even}} + m_j^{\text{odd}})/2$  and  $m_j^\Delta = (m_j^{\text{even}} - m_j^{\text{odd}})/2$ . Here the polynomiality is not manifest in the conformal moments, rather it is separately restored for  $m_{2n}^\Sigma + m_{2n}^\Delta$  and  $m_{2n+1}^\Sigma - m_{2n+1}^\Delta$ .

Let us next show that the Mellin-Barnes integral vanishes for  $|x| > 1$ . Here the expression  $\eta^{-j-1} Q_j(x/\eta)/\sin(\pi j)$  in the integrand vanishes on the infinite arc, due to the damping factor  $(1/x)^j$ , see Eqs. (53) and (55). As in the previous paragraph, we can close the integration contour and find that the integral gives zero. If we would have allowed an additional term proportional to  $\mathcal{P}_j(-x, \eta)$  in the extension of the support for  $x > \eta$ , it would in general contribute in the unphysical region  $x > 1$ , too.

Finally, the correctness of the GPD representations as Mellin-Barnes integral is deduced from the fact that for non-negative integers the conformal moments are reproduced. Employing the symmetry with respect to  $x \rightarrow -x$ , we find from the representation (80), e.g., for even moments,

$$\int_{-\infty}^{\infty} dx c_n(x, \eta) q(x, \eta, \Delta^2) = \int_{-\eta}^{\infty} dx c_n(x, \eta) \frac{i}{2} \int_{c-i\infty}^{c+i\infty} dj \frac{1}{\sin(\pi j)} p_j(x, \eta) m_j^{\text{even}}(\eta, \Delta^2) \quad (82)$$

for  $n = 0, 2, \dots$ . From the moments separately calculated in the outer and central region, given in Eqs. (159) and (161), respectively, it follows<sup>11</sup>

$$\int_{-\infty}^{\infty} dx c_n(x, \eta) q(x, \eta, \Delta^2) = \lim_{\epsilon \rightarrow +0} \frac{1}{2i\pi} \int_{n-i\infty}^{n+i\infty} dj \left( \frac{\mathcal{N}_{nj}(\eta)}{n-j+\epsilon} + \frac{\mathcal{N}_{nj}(\eta)}{j-n+\epsilon} \right) m_j^{\text{even}}(\eta, \Delta^2), \quad (83)$$

for  $n = 0, 2, \dots$ . The integration path can be parameterized by  $j = n + i\lambda$  and making use of the identity  $1/(\lambda - i\epsilon) - 1/(\lambda + i\epsilon) = 2i\pi\delta(\lambda)$ , the integral yields finally the conformal moment  $m_n^{\text{even}}(\eta, \Delta^2)$  for  $n = 0, 2, \dots$ . Analogously, the conformal moments  $m_n^{\text{odd}}(\eta, \Delta^2)$  arise for odd values of  $n$ .

We complete this section with the Mellin-Barnes representation for GDAs, which follows now by crossing from Eq. (77) with the constrain  $z \geq \zeta$ , which arises from  $-1/\eta \leq x/\eta \leq 1$ . Employing

---

<sup>11</sup>The  $x$ -integral over the outer region only exist for  $\Re j > n$ . Since here the integrand has no singularities on the positive real axis, we can first shift the Mellin-Barnes integration path to the imaginary axis to the right. Then with  $\Re j = n + \epsilon$  the  $x$ -integration is performed. On the other hand the  $x$ -integration over the central region must be performed within the original contour. It produces a  $\sin(\pi j)$  term, which removes the poles on the real axis and so we can shift the Mellin-Barnes integration path along the positive real axis, too. Both remaining integrals can then be combined in the limit that is indicated in Eq. (83).

the symmetry transformation  $z \rightarrow 1 - z$  and  $\zeta \rightarrow 1 - \zeta$  we get the remaining contribution, see Eq. (27):

$$\Phi(z, \zeta, W^2) = \frac{i}{2} \int_{c-i\infty}^{c+i\infty} dj \frac{1}{\sin(\pi j)} \left[ \theta(z - \zeta) p_j(1 - 2z, 1) M_j(\zeta, W^2) + \left\{ \begin{array}{l} z \rightarrow 1 - z \\ \zeta \rightarrow 1 - \zeta \end{array} \right\} \right], \quad (84)$$

where  $M_j(\zeta, W^2)$  is the analytic continuation of the conformal GPD moments, obtained by crossing, see below Eq. (43). If  $M_j(\zeta, W^2)$  is bounded along the integration path for  $0 \leq \zeta \leq 1$ , the integral of the first term in the square brackets in this formula exist for all values of  $0 \leq z \leq 1$ . So we can drop both the restriction  $\theta(z - \zeta)$  and the second term in the square brackets, obtained by symmetry. This latter term follows now from analytic continuation and so we arrive at the representation:

$$\Phi(z, \zeta, W^2) = \frac{i}{2} \int_{c-i\infty}^{c+i\infty} dj \frac{1}{\sin(\pi j)} p_j(1 - 2z, 1) M_j(\zeta, W^2). \quad (85)$$

Suppose that  $M_j(\zeta, W^2)$  vanishes for  $j \rightarrow \infty$  with  $|\arg j| \leq \pi/2$ , it is straightforward to see that the conformal moments for non-negative integer conformal spin are reproduced. Employing Eq. (161) with  $\eta = 1$  and  $k = n = \{0, 1, 2, \dots\}$ , we can then close the contour so that it now encircles the positive real axis. The residue theorem yields then  $M_n(\zeta, W^2)$ .

### 3 Evolution kernels and coefficient functions in a manifest conformal scheme

To LO accuracy the evolution kernels and coefficient functions for exclusive processes respect conformal symmetry, which is the symmetry of the QCD Lagrangian at the classical level for massless quarks. Conformal symmetry find, in fact, many practical applications in QCD. It allows for instance to solve the mixing problem of light-ray operators, caused by renormalization, and by means of the conformal operator product expansion it predicts the hard-scattering amplitude. The breaking of conformal symmetry beyond LO has been studied with perturbative methods in great detail [57, 58, 26, 59, 60, 61]. The main lesson from these studies is that the only physical contributions violating conformal symmetry are generated by the non-zero  $\beta$  function. All other terms violating conformal symmetry (in the perturbative sector) are mainly artifacts introduced by the standard renormalization/factorization prescription for the light-ray operators, which is based on some version of minimal subtraction within the dimensional regularization scheme. Within the standard scheme the conformal symmetry is separately broken in the evolution kernels and the hard-scattering amplitude for two-photon processes. However, it can be restored by a finite renormalization providing a scheme in which conformal symmetry is manifest, except for terms proportional to  $\beta$  that are induced by the trace anomaly of the energy momentum tensor. Thus, we will restrict us in the following two subsections not to LO accuracy. Rather, the results can be

(at least partly) applied to all orders of perturbation theory. Of course, terms proportional to  $\beta$  need special consideration. A first discussion of this issue can be found in Ref. [27], see also Ref. [62].

### 3.1 Convolution of GPDs with conformal kernels

In this section we consider the convolution

$$K \otimes q(x, \eta) \equiv \int_{-\infty}^{\infty} \frac{dy}{|\eta|} K\left(\frac{x}{\eta}, \frac{y}{\eta}\right) q(y, \eta, \Delta^2) \quad (86)$$

of a GPD with a generic kernel  $K(x, y)$  that respects conformal symmetry. Here the integration region is defined by the combined restrictions for the GPDs and the kernels. The requirement of conformal symmetry means in fact that the kernel has for  $|x|, |y| \leq 1$  the following spectral representation

$$K(x, y) = \sum_{n=0}^{\infty} (-1)^n p_n(x) k_n c_n(y) \quad \text{for } |x|, |y| \leq 1, \quad (87)$$

where  $k_n$  are the eigenvalues of  $K(x, y)$  and the polynomials  $p_n(x)$  and  $c_n(y)$  are defined in Eqs. (33) and (39), respectively. Suppose that even and odd eigenvalues have the same sign and provide after analytic continuation with respect to the conformal spin the same holomorphic function  $k_j$  so that it satisfies a bound for all values of  $j$  with  $\arg(j) \leq \pi/2$ . In fact the eigenvalues  $k_n$  coincide with the Mellin moments of the DGLAP kernel, given by rational functions and harmonic sums, and so we know their analytic continuation. We remark that the support in the  $(x, y)$ -plane is defined in Eq. (193) and the extension to the full region is unique, see Appendix C. The convolution of a GPD confined to  $[-\eta, 1]$  with this kernel leads to a function that has also the support  $-\eta \leq x \leq 1$ .

To proceed in the simplest possible manner let us extend the representation (87) to the whole region by the series

$$\frac{1}{\eta} K\left(\frac{x}{\eta}, \frac{y}{\eta}\right) = \sum_{n=0}^{\infty} (-1)^n p_n(x, \eta) k_n c_n(y, \eta). \quad (88)$$

Again, here we understand that  $p_n(x, \eta)$  are mathematical distributions with the restricted support  $-\eta \leq x \leq \eta$  for integer values of  $n$ , while  $c_n(y, \eta)$  are the polynomials (33), which can be extended to the whole  $y$  region. Taking the Mellin-Barnes integral (77) and the spectral representation (88), the convolution (86) leads to a divergent series

$$K \otimes q(x, \eta) = \sum_{n=0}^{\infty} (-1)^n p_n(x, \eta) k_n m_n(\eta, \Delta^2). \quad (89)$$

Here we employed the integrals (159) and (161) for discrete conformal spin, as has been explained at the end of Sect. 2.3.3. Since the analytic continuation of  $k_n$  does not spoil our assumptions for

the Sommerfeld-Watson transform, we can proceed as in Sect. 2.3.3. As expected, for a conformal kernel the convolution

$$K \otimes q(x, \eta) = \frac{i}{2} \int_{c-i\infty}^{c+i\infty} dj \frac{1}{\sin(\pi j)} p_j(x, \eta) k_j m_j(\eta, \Delta^2) \quad (90)$$

is in the Mellin momentum space given by a multiplication of the conformal GPD moments with the corresponding eigenvalues.

In those cases in which we must distinguish between even and odd eigenvalues of the kernel, we write  $K$  as

$$\frac{1}{\eta} K \left( \frac{x}{\eta}, \frac{y}{\eta} \right) = \sum_{n=0}^{\infty} (-1)^n \left[ p_n^{\text{even}}(x, \eta) k_n^{\text{even}} c_n(y, \eta) + p_n^{\text{odd}}(x, \eta) k_n^{\text{odd}} c_n(y, \eta) \right], \quad (91)$$

where  $p_n^{\text{even}}(x)$  and  $p_n^{\text{odd}}(x)$  are defined as in Eq. (75), and employ the GPD representation (80). Since even and odd Gegenbauer polynomials and partial waves have definite symmetry under reflection, they can not mix. Hence, the convolution leads to

$$K \otimes q(x, \eta) = \frac{i}{2} \int_{c-i\infty}^{c+i\infty} dj \frac{1}{\sin(\pi j)} \left[ p_j^{\text{even}}(x, \eta) k_j^{\text{even}} m_j^{\text{even}}(\eta, \Delta^2) + \{\text{even} \rightarrow \text{odd}\} \right]. \quad (92)$$

If the support of the GPD was in the interval  $[-\eta, 1]$  and the eigenvalues are different in the even and odd sector, the convolution certainly gives us a function that lives now in the whole region  $[-1, 1]$ . The support extension is caused by the mixing with an anti-quark GPD. With  $k_j^{\text{even}} = k_j^{\Sigma} + k_j^{\Delta}$  and  $k_j^{\text{odd}} = k_j^{\Sigma} - k_j^{\Delta}$ , we can decompose the convolution as

$$K \otimes q(x, \eta) = \delta q(x, \eta) + \delta \bar{q}(-x, \eta). \quad (93)$$

Based on the representation (81), we interpret the terms on the r.h.s. as contributions to a quark GPD, with  $-\eta \leq x \leq 1$ ,

$$\delta q(x, \eta) = \frac{i}{2} \int_{c-i\infty}^{c+i\infty} dj \frac{k_j^{\Sigma}}{\sin(\pi j)} \left[ \theta(|x| \leq \eta) p_j(-x, \eta) m_j^{\Delta}(\eta, \Delta^2) + p_j(x, \eta) m_j^{\Sigma}(\eta, \Delta^2) \right] \quad (94)$$

and an anti-quark GPD, with  $-1 \leq -x \leq \eta$ ,

$$\delta \bar{q}(-x, \eta) = \frac{i}{2} \int_{c-i\infty}^{c+i\infty} dj \frac{k_j^{\Delta}}{\sin(\pi j)} \left[ \theta(|x| \leq \eta) p_j(x, \eta) m_j^{\Delta}(\eta, \Delta^2) + p_j(-x, \eta) m_j^{\Sigma}(\eta, \Delta^2) \right]. \quad (95)$$

For the convolution of a conformal kernel with a GDA we would obtain the analogous results. The convolution is conventionally defined as

$$K \otimes^e \Phi(z, \zeta, W^2) = \int_0^1 dy K(1-2z, 1-2y) \Phi(y, \zeta, W^2). \quad (96)$$

Note that the change of variable  $(1-2y) \rightarrow y$ , induces a factor 2 in comparison to the definition (86). We can now represent the GDA by the convergent series (43), and the convolution immediately leads to

$$K \otimes^e \Phi(z, \zeta, W^2) = \sum_{n=0}^{\infty} (-1)^n p_n(1-2z, 1) \frac{k_n}{2} M_n(\zeta, W^2). \quad (97)$$



Within the Mellin-Barnes representation the solution of the evolution equation is a trivial task to LO accuracy, where the conformal symmetry is manifest in any scheme. The restoration of this symmetry is well understood to NLO and even the terms proportional to  $\beta$  can be diagonalized with respect to conformal partial waves. Relying on this symmetry and borrowing the eigenvalues of the evolution kernels from the Mellin moments of the DGLAP kernel from Ref. [63, 64] one can even proceed to NNLO.

The simplest example is given by the flavor non-singlet sector and LO accuracy. Here the evolution equation reads

$$\mu \frac{d}{d\mu} q(x, \eta, \Delta^2, \mu^2) = -\frac{\alpha_s(\mu)}{2\pi} \gamma^{(0)} \otimes q(x, \eta, \Delta^2, \mu^2), \quad (98)$$

where the evolution kernel is

$$\gamma^{(0)}(x, y) = \left[ \Theta(x, y) \frac{1+x}{1+y} \left( 1 + \frac{2}{y-x} \right) + \Theta(-x, -y) \frac{1-x}{1-y} \left( 1 + \frac{2}{x-y} \right) \right]_+, \quad (99)$$

with the +-prescription  $[K(x, y)]_+ = K(x, y) - \delta(x-y) \int dz K(z, y)$  and the shorthand notation

$$\Theta(x, y) = \text{sign}(1+y) \theta \left( \frac{1+x}{1+y} \right) \theta \left( \frac{y-x}{1+y} \right).$$

Its eigenvalues can be simply calculated for discrete conformal spin  $n$ . If one did this for complex conformal spin  $j$ , one would encounter the same problems as for moments of GPDs. Namely, terms proportional to  $\sin(\pi j)$  would appear. The analytic continuation of the discrete eigenvalues can, however, be defined without such terms:

$$\gamma_j^{(0)} = C_F \left( 4\psi(j+2) - 4\psi(1) - 3 - \frac{2}{(j+1)(j+2)} \right), \quad C_F = \frac{4}{3}, \quad \psi(z) = \frac{d}{dz} \ln \Gamma(z). \quad (100)$$

This is just the forward anomalous dimensions of twist-two operators, well-known from deep inelastic scattering. The evolution of the conformal moments is thus governed by the ordinary differential equation

$$\mu \frac{d}{d\mu} m_j(\eta, \Delta^2, \mu^2) = -\frac{\alpha_s(\mu)}{2\pi} \gamma_j^{(0)} m_j(\eta, \Delta^2, \mu^2), \quad (101)$$

which is easily solved. Equating the renormalization scale  $\mu$  with the resolution scale  $\mathcal{Q}$  and inserting the solution into the Mellin-Barnes integral (81) leads to

$$q(x, \eta, \Delta^2, \mathcal{Q}^2) = \frac{i}{2} \int_{c-i\infty}^{c+i\infty} dj \frac{1}{\sin(\pi j)} p_j(x, \eta) \exp \left\{ -\frac{\gamma_j^{(0)}}{2} \int_{\mathcal{Q}_0^2}^{\mathcal{Q}^2} \frac{d\sigma}{\sigma} \frac{\alpha_s(\sigma)}{2\pi} \right\} m_j(\eta, \Delta^2, \mathcal{Q}_0^2), \quad (102)$$

where the moments  $m_j(\eta, \Delta^2, \mathcal{Q}_0^2)$  belongs to a given GPD at the input scale  $\mathcal{Q}_0$ .

### 3.2 Mellin-Barnes representation for amplitudes

We study next the convolution of a GPD with a given hard-scattering amplitude. To have a concrete example at hand we deal here with the so-called Compton form factors that appear in the perturbative description of DVCS:

$$\mathcal{F}(\xi, \Delta^2, \mathcal{Q}^2) = \sum_{p=u,d,s,g} \int_{-1}^1 \frac{dx}{\xi} \left[ C_p^{(0)\mp} \left( \frac{x}{\xi} \right) + \frac{\alpha_s(\mu)}{2\pi} C_p^{(1)\mp} \left( \frac{x}{\xi}, \frac{\mu}{\mathcal{Q}} \right) + \mathcal{O}(\alpha_s^2) \right] F_p(x, \xi, \Delta^2, \mu^2). \quad (103)$$

For this process the skewness parameter is equal to the Bjorken like scaling variable, i.e.,  $\eta = \xi$ . The same kinematic constraint appears also in the hard exclusive electroproduction of mesons. In fact, the result for the Compton factors, we will give below in Eq. (106), can be adopted for this process, too. This is trivial to LO and requires some additional work beyond this order.

Let us consider the partonic Compton form factors to LO accuracy,

$$\mathcal{F}_p(\xi, \Delta^2, \mathcal{Q}^2) = \int_{-1}^1 dx \left[ \frac{Q_p^2}{\xi - x - i\epsilon} \mp \frac{Q_p^2}{\xi + x - i\epsilon} \right] F_p(x, \xi, \Delta^2, \mathcal{Q}^2), \quad (104)$$

where  $Q_p$  is the electric charge of the parton. Employing the decomposition (9) of GPDs into quark and anti-quark parts, the partonic Compton form factor (104) reads

$$\mathcal{F}_p(\xi, \Delta^2, \mathcal{Q}^2) = \int_{-\xi}^1 dx \left[ \frac{Q_p^2}{\xi - x - i\epsilon} \mp \frac{Q_p^2}{\xi + x - i\epsilon} \right] [q_p(x, \xi, \Delta^2, \mathcal{Q}^2) + \bar{q}_p(x, \xi, \Delta^2, \mathcal{Q}^2)]. \quad (105)$$

Next we employ the Mellin-Barnes representation (81) for GPDs and perform the momentum fraction integration by means of Eq. (171). Then the Compton form factors are expressed in terms of the conformal moments

$$\mathcal{F}_p = \frac{Q_p^2}{2i} \int_{c-i\infty}^{c+i\infty} dj \xi^{-j-1} \frac{2^{j+1} \Gamma(5/2 + j)}{\Gamma(3/2) \Gamma(3 + j)} \left( i - \frac{\cos(\pi j) \mp 1}{\sin(\pi j)} \right) [m_j + \bar{m}_j](\xi, \Delta^2, \mathcal{Q}^2), \quad (106)$$

where the sum of  $m_j + \bar{m}_j$  is given by the analytic continuation of odd and even conformal moments for the vector and axial-vector case, respectively. As we realize by comparing with Eq. (77) and Eq. (52) the imaginary part of  $\mathcal{F}_p$  is  $\pi [q + \bar{q}](\xi, \xi, \Delta^2)$  as it must be. The real part of the amplitude, given by a principal value integral in the momentum fraction representation, contains in the integrand an additional factor  $\tan(\pi j/2)$  and  $-\cot(\pi j/2)$  for the vector and axial-vector case, respectively.

In a conformal subtraction scheme the inclusion of perturbative corrections is straightforward. Higher order corrections can be written as convolution of the LO hard-scattering amplitude (104) with certain kernels, which are conformally covariant. Hence, in analogy to the discussion in Sect. 3.1, this yields in the Mellin-Barnes representation a multiplication with the corresponding eigenvalues, which are known from deep inelastic scattering. For instance, to NLO accuracy the partonic form factor  $\mathcal{H}_p$  for quarks in the parity even sector of DVCS on a nucleon target reads

for  $\mu = \mathcal{Q}$

$$\mathcal{H}_p = \frac{Q_p^2}{2i} \int_{c-i\infty}^{c+i\infty} dj \xi^{-j-1} \frac{2^{j+1}\Gamma(5/2+j)}{\Gamma(3/2)\Gamma(3+j)} \left[ i + \tan\left(\frac{\pi j}{2}\right) \right] \left[ 1 + \frac{\alpha_s(\mathcal{Q})}{2\pi} \mathcal{C}_j^{(1)} \right] [h_j + \bar{h}_j] (\xi, \Delta^2, \mathcal{Q}^2) \quad (107)$$

with the NLO coefficients

$$\begin{aligned} \mathcal{C}_j^{(1)} = C_F & \left[ S_1^2(1+j) + \frac{3}{2} S_1(j+2) - \frac{9}{2} + \frac{5 - 2S_1(j)}{2(j+1)(j+2)} - S_2(j+1) \right. \\ & \left. + \frac{1}{2} \gamma_j^{(0)} \{ 2S_1(2j+3) - S_1(j+2) - S_1(j+1) \} \right], \end{aligned} \quad (108)$$

where the analytic continuation of harmonic sums is defined by derivatives of the  $\Gamma$  function

$$S_1(z) = \psi(z+1) - \psi(1), \quad S_2(z) = -\frac{d}{dz} \psi(z+1) + \frac{\pi^2}{6}, \quad \psi(z) = \frac{d}{dz} \ln \Gamma(z). \quad (109)$$

The first line in Eq. (108) is up to an overall normalization factor the well-known perturbative correction to the Wilson coefficients of the structure function  $F_1$  in deep inelastic scattering [65], while the addenda in the second line is induced by the non-forward kinematics. This result is verified by a direct rotation from the minimal subtraction scheme to the conformal one and coincides with the prediction of the conformal operator product expansion [26, 59].

Another advantage of the Mellin-Barnes representation is that it might be useful for an analytic approximation of the Compton factors at smaller values of  $\xi$ , lets say  $\xi \lesssim 10^{-2}$ , which should lead to a rather good approximation of the scattering amplitude for the kinematics in Collider experiments. Such an approximation has been already studied within the DD formalism, see [66] and references therein, however, it remained restricted to the perturbative LO approximation and only the term containing the leading power in  $\xi$  could be extracted. The main idea here is to shift the integration path in Eq. (107) to the left, so that one picks up the leading order contribution for  $\xi \rightarrow 0$ . Suppose that for the vector case the first singularity on the l.h.s. is a pole at  $j = \alpha_0$  with  $-1 < \alpha_0 < c < 1$ , which might depend on  $\Delta^2$ . We recall that in this case only the analytic continuation of odd moments enters and, thus,  $c$  can also be chosen to be positive, however, it must be smaller than one. The integration path can then be shifted further to the left such that  $-1 < c' < \alpha_0$  and all other singularities remain to the left of the new integration path, while the leading pole contribution ( $j = \alpha_0$ ) is explicitly taken into account. To LO accuracy the partonic Compton form factors thus read

$$\begin{aligned} \mathcal{H}_p = & Q_p^2 \xi^{-\alpha_0-1} \frac{2^{\alpha_0+1}\Gamma(5/2+\alpha_0)}{\Gamma(3/2)\Gamma(3+\alpha_0)} \left[ i + \tan\left(\frac{\alpha_0\pi}{2}\right) \right] \pi \text{Res} [h_j + \bar{h}_j] (\xi, \Delta^2, \mathcal{Q}^2) \Big|_{j=\alpha_0} \\ & + \frac{Q_p^2}{2i} \int_{c'-i\infty}^{c'+i\infty} dj \xi^{-j-1} \frac{2^{j+1}\Gamma(5/2+j)}{\Gamma(3/2)\Gamma(3+j)} \left[ i + \tan\left(\frac{\pi j}{2}\right) \right] [h_j + \bar{h}_j] (\xi, \Delta^2, \mathcal{Q}^2). \end{aligned} \quad (110)$$

This result could even be improved by further shifts of the integration contour. A more systematic expansion, requires that also the conformal moments  $m_j(\xi, \Delta^2)$  are expanded in  $\xi$  in the vicinity

of  $\xi = 0$ . We remind that  $\xi$  is related to the Bjorken variable by  $\xi \sim x_B/(2 - x_B)$  and is for present fixed target experiments certainly not larger than  $\sim 0.4$ . Hence, already the inclusion of the  $O(\xi^2)$  corrections might be sufficient to obtain a good approximation of the Compton form factors in this kinematics.

Unfortunately, the method for a systematic approximation, pointed out above, must maybe be refined due to the following complication. Namely, we know that in general the conformal moments will have a branch point at  $\xi = 0$  and so a Taylor expansion around this point is not possible, after the analytic continuation is performed. Even worse, it turns out that the appropriate analytic continuation, which guarantees the correctness of the Mellin-Barnes integral, can induce terms that lead to a behavior  $\propto \eta^j$  or even  $\propto \eta^{2j}$ . Certainly, the latter term requires that we shift the integration path to the right, while the former require a consideration of all poles. Corresponding to its behavior at  $j \rightarrow \infty$ , we might close the integration path so that the positive or negative axis is included. For specific conformal moments it is probably still possible to obtain a systematic expansion of the Compton form factors in powers of  $\xi$  up to a certain order. In general, however, this seems to be a serious problem.

One might naively expect that this issue can be resolved, if one goes back to the definition of conformal moments (36); expand first  $c_n(x, \xi)$  in  $\xi^2$  and take then moments with respect to  $x$ , which in turn can be simply continued to complex valued  $j$ . Such an expansion looks like, see Eq. (170),

$$c_j(x, \xi) = x^j \left[ c_{j0} + c_{j2} \frac{\xi^2}{x^2} + c_{j4} \frac{\xi^4}{x^4} + \dots \right]. \quad (111)$$

The coefficients  $c_{jm}$  vanish for integer value  $j = n$  with  $m > n$  and so this expansion degenerates then into a polynomial<sup>12</sup> [67]. in  $\eta$  of degree  $n$ . Hence we can shift from the beginning for each individual term the integration path in the Mellin-Barnes integral to the r.h.s., i.e.,  $c \rightarrow c + m$ . However, one easily realizes that this procedure will also introduce new poles in the complex  $j$  plane that are also shifted to the right of the real axis, remaining, however, to the left of the new integration path. Finally, it turns out that these poles will remove the power in  $\xi^2$  we gained by the expansion (111). With one word, taking the limit  $\xi \rightarrow 0$  in general conformal moments, leads to the correct leading power behavior of the Compton form factors in  $\xi$ , however, the normalization might be wrong.

Let us finally comment on the representation for the scattering amplitude in the case of the production of a hadron pair by photon fusion. For the important phenomenological situation that one photon is on-shell, it is of course related to the DVCS amplitude by crossing. By means of

---

<sup>12</sup>Obviously, for non-negative integer  $n$  we are dealing with integrals of the type  $\int_{-1}^1 dx x^{n-m} q(x, \eta, \Delta^2)$ , well defined for  $n \geq m$ . To avoid divergencies for complex valued  $j$  with  $\Re j \leq m - 1$ , the integral should be defined as a contour integral in the complex  $x$  plane so that it exist and can be viewed as analytic continuation with respect to the variable  $n - m$

the crossing relation (28) the amplitude follows to LO accuracy from Eq. (104):

$$\mathcal{F}_p(\zeta, W^2, \mathcal{Q}^2) = (1 - 2\zeta)Q_p^2 \int_0^1 dz \left[ \frac{1}{z} \mp \frac{1}{1-z} \right] \Phi_p(z, \zeta, W^2, \mathcal{Q}^2). \quad (112)$$

Employing the conformal partial wave decomposition (43) for GDAs, we immediately find the following series for the scattering amplitude

$$\mathcal{F}_p(\zeta, W^2, \mathcal{Q}^2) = (1 - 2\zeta)Q_p^2 \sum_{n=0}^{\infty} \frac{2^{n+1}\Gamma(5/2+n)}{\Gamma(3/2)\Gamma(3+n)} [1 \mp (-1)^n] M_n(\zeta, W^2). \quad (113)$$

As discussed in Sect. 2.2 the conformal moments  $M_n(\zeta, W^2)$  are related to the GPD ones by crossing, cf. Eq. (43). Of course, the inclusion of perturbative corrections and evolution effects is done in an analogous way as in the case of DVCS. The only difference is that we are now dealing with integer  $n$ . The sum (113) converges, just as the partial wave decomposition for the GDA itself. However, the oscillations caused by the polynomials  $p_n(1-2z, 1)$  drop out and so its numerical approximation is easier to handle. This representation can be directly used in phenomenological studies. Knowing an appropriate analytic continuation of  $M_n(\zeta, W^2)$  would also allow to rewrite the conformal partial wave expansion (113) as Mellin-Barnes integral:

$$\mathcal{F}_p(\zeta, W^2, \mathcal{Q}^2) = (1 - 2\zeta) \frac{Q_p^2}{2i} \int_{c-i\infty}^{c+i\infty} dj \frac{2^{j+1}\Gamma(5/2+j)}{\Gamma(3/2)\Gamma(3+j)} \frac{M_j(1-\zeta, W^2) \mp M_j(\zeta, W^2)}{\sin(\pi j)}. \quad (114)$$

Here we employed the symmetry relation  $M_n(\zeta, W^2) = (-1)^n M_n(1-\zeta, W^2)$  and that  $M_j$  is holomorphic in the first and forth quadrant.

## 4 Evaluation and parameterization of conformal moments

This section is devoted to the parameterization of conformal moments and the numerical treatment of GPDs and Compton form factors. We study first the analytic properties of conformal moments for a simple toy GPD ansatz and give then examples for the numerical evaluation. Then we introduce a simple parameterization of the conformal moments with respect to the skewness dependence, i.e., we consider only a reduced GPD and its crossing analog, and discuss its dependence on the momentum transfer squared. Finally, we suggest a simple GPD model, which is rather flexible in its parameterization.

### 4.1 Numerical treatment of the Mellin-Barnes integral

Let us consider the conformal moments in terms of the Radyushkin ansatz (17) for the reduced GPDs. This toy example can be treated for integer values of  $b$  and  $\beta$  in an analytic manner. To represent the results here in an explicit form we choose again  $b = 0$  and our toy model with  $\beta = 1$ .

In this case the function  $\omega(x, \eta)$  is given in terms of Eq. (12) by

$$q(x, \eta) = \theta(-\eta \leq x \leq 1) \frac{2+\alpha}{2\eta} \left( \frac{x+\eta}{1+\eta} \right)^{1+\alpha} + \theta(\eta \leq x \leq 1) \frac{2+\alpha}{-2\eta} \left( \frac{x-\eta}{1-\eta} \right)^{1+\alpha}. \quad (115)$$

The analytic continuation of the function  $\mu_n(-\eta)$ , see Eq. (38), reads

$$\mu_j(-\eta) = -\frac{\Gamma(1/2)\Gamma(3+j)}{2^{3+j}\Gamma(3/2+j)}(1-\eta)\eta^{-1+j} {}_3F_2 \left( \begin{matrix} -j, 3+j, 2+\alpha \\ 2, 3+\alpha \end{matrix} \middle| \frac{-1+\eta}{2\eta} \right). \quad (116)$$

This function has the behavior needed for the derivation of the Mellin-Barnes integral. However, it is not appropriate for an analytic continuation to negative  $\eta$ , since the argument of the hypergeometric function would then become larger than one, i.e.,  $(-1+\eta)/2\eta \rightarrow (1+\eta)/2\eta$ , and so its value is given at the branch cut of the hypergeometric function. To analyse the situation in more detail, we can first express the hypergeometric function in Eq. (116) as a sum of two  ${}_3F_2$  functions with argument  $2\eta/(-1+\eta)$ . This gives

$$\begin{aligned} \mu_j(-\eta) = & -\frac{(2+\alpha)(1-\eta)^{1+j}}{2(2+j+\alpha)\eta} {}_3F_2 \left( \begin{matrix} -j-1, -j, -2-j-\alpha \\ -2j-2, -j-1-\alpha \end{matrix} \middle| \frac{2\eta}{-1+\eta} \right) - \frac{(2+\alpha)\eta^{2(1+j)}}{2^{2(2+j)}(1-\eta)^{2+j}} \\ & \times \frac{\Gamma(1+j)\Gamma(3+j)\tan(\pi j)}{(1+j-\alpha)\Gamma(3/2+j)\Gamma(5/2+j)} {}_3F_2 \left( \begin{matrix} 2+j, 3+j, 1+j-\alpha \\ 4+2j, 2+j-\alpha \end{matrix} \middle| \frac{2\eta}{-1+\eta} \right) \\ & - \frac{\eta^{1+j+\alpha}}{2^{1+j-\alpha}(1-\eta)^{1+\alpha}} \frac{\Gamma(1/2)\Gamma(1+j)}{\Gamma(3/2+j)} \frac{\Gamma(3+\alpha)\Gamma(1+j-\alpha)\sin(\pi j)}{\Gamma(-\alpha)\Gamma(3+j+\alpha)\sin(\pi[j+\alpha])}. \end{aligned} \quad (117)$$

The first term on the r.h.s. contains poles on the real axis at  $j = 1/2, 3/2, \dots$  and for  $\alpha < 0$  at  $j = -\alpha, 1-\alpha, \dots$ . Both of them are cancelled by the second and third term, respectively.

The continuation of this function to negative values of  $\eta$  is obviously not unique, since we have branch points at  $\eta = 0$ , which leads to phase factors  $e^{\pm i\pi(j+1+\alpha)}$  as well as  $e^{\pm i2\pi(j+1)}$ . Such phase factors in  $\mu_j(\eta)$  would, however, violate the assumptions made for the derivation of the Mellin-Barnes representation. To ensure that this does not happen we define the analytic continuation by

$$\mu_j^{\text{AC}}(\eta) = \frac{e^{i\pi j}\mu_j(-\eta e^{-i\pi}) - e^{-i\pi j}\mu_j(-\eta e^{i\pi})}{2i\sin(\pi j)}. \quad (118)$$

were the phase factors  $e^{\pm i\pi j}$  compensate the phases which arise from the  $\eta^j$  terms in the definition (35) of conformal moments, while taking the “discontinuity” and dividing it by  $2i\sin(\pi j)$  ensures that no new singularities appear on the real axis and that  $\mu_j(\eta)$  is bound for  $j \rightarrow \infty$ . In fact the properties of Legendre functions imply that the prescription (118) provides the contribution from the outer region

$$\mu_j^{\text{AC}}(\eta) = \int_{\eta}^1 dx c_j(x, \eta) \frac{2+\alpha}{2\eta} \left( \frac{x+\eta}{1+\eta} \right)^{1+\alpha} + \frac{2+\alpha}{2\eta} \left( \frac{2\eta}{1+\eta} \right)^{1+\alpha} \left( \frac{\eta}{2} \right)^{j+1} \frac{\Gamma(1/2)\Gamma(1+j)}{\Gamma(3/2+j)}, \quad (119)$$

where the second term on the r.h.s. arises from a pole at  $x = \eta$  and cancels the contribution from the lower bound of the integral. Hence, we realize that the central region is still ignored in Eq.

(119) and its contribution might be taken into account within Eq. (69). The term that appears there from the pole at  $x = \eta$  is already contained in Eq. (119) and so only the discontinuity on the negative axis contributes.

Analytic continuation via Eq. (118) leads for our toy ansatz to

$$\begin{aligned} \mu_j^{\text{AC}}(\eta) = & \frac{(2+\alpha)(1+\eta)^{1+j}}{2(2+j+\alpha)\eta} {}_3F_2 \left( \begin{matrix} -j-1, -j, -2-j-\alpha \\ -2j-2, -j-1-\alpha \end{matrix} \middle| \frac{2\eta}{1+\eta} \right) + \frac{(2+\alpha)\eta^{2(1+j)}}{2^{2(2+j)}(1+\eta)^{2+j}} \\ & \times \frac{\Gamma(1+j)\Gamma(3+j)\tan(\pi j)}{(1+j-\alpha)\Gamma(3/2+j)\Gamma(5/2+j)} {}_3F_2 \left( \begin{matrix} 2+j, 3+j, 1+j-\alpha \\ 4+2j, 2+j-\alpha \end{matrix} \middle| \frac{2\eta}{1+\eta} \right) \\ & - \frac{\eta^{1+j+\alpha}}{2^{1+j-\alpha}(1+\eta)^{1+\alpha}} \frac{\Gamma(1/2)\Gamma(1+j)}{\Gamma(3/2+j)} \frac{\Gamma(3+\alpha)\Gamma(1+j-\alpha)\sin(\pi\alpha)}{\Gamma(-\alpha)\Gamma(3+j+\alpha)\sin(\pi[j+\alpha])}. \end{aligned} \quad (120)$$

As before for  $\mu_j(-\eta)$  there are no net singularities in the first and forth quadrant of the complex  $j$  plane, however, individual terms possesses poles on the real axis. The first term on the r.h.s. is needed to restore the polynomiality in the sum  $\mu_n(\eta) + \mu_n^{\text{AC}}(-\eta)$ . However, the third term violates polynomiality and must be cancelled by the contribution from the central region, still missing. We can restore this missing term from the polynomiality condition in such a way that it is free of singularities in the first and forth quadrant of the complex  $j$  plane. The  $\sin(\pi\alpha)/\sin(\pi[j+\alpha])$  term of the third line, however, generates for  $j = n = \{0, 1, 2, \dots\}$ , a sign alternating series and to get rid of it, we separately continue even and odd moments:

$$m_j(\eta|\sigma) = \mu_j(\eta) + \mu_j^{\text{AC}}(-\eta) + \sigma \frac{\eta^{1+j+\alpha}}{2^{1+j-\alpha}(1+\eta)^{1+\alpha}} \frac{\Gamma(1/2)\Gamma(1+j)}{\Gamma(3/2+j)} \frac{\Gamma(3+\alpha)\Gamma(1+j-\alpha)}{\Gamma(-\alpha)\Gamma(3+j+\alpha)}, \quad (121)$$

with  $\sigma = 1$  and  $\sigma = -1$  in the even and odd sector, respectively. We remark that this result for the conformal moments of our toy GPD (115) can be alternatively obtained within the framework given in Sect. 2.3.2. Especially, the term we restored from the polynomiality condition arise from the discontinuity on the negative real axis in Eq. (69).

Now let us come to the numerical treatment of the Mellin-Barnes integrals for GPDs (77,80) and Compton form factors (106). The numerical evaluation can be easily done once the conformal moments are known in analytic or numerical form. Corresponding to the behavior of GPDs at  $x \rightarrow 1$ , they should vanish at large  $j$  rather fast [19]. Hence, the integral converges rather fast, too, and so one can in practice perform the integration over a finite interval. If one includes higher order corrections or the evolution the numerical treatment remains stable.

For our toy model we display in Fig. 6(a) for  $\alpha = -1/2$  and  $\eta = 0.25$  the GPDs arising from odd and even conformal moments, while the sum of them (solid line) provides the original support. The evolution with respect to the renormalization/factorization scale  $\mu^2 = Q^2$  is taken into account simply by including the evolution operator in the Mellin-Barnes integral. For the vector case the even quark moments evolve separately, i.e., they do not mix with the gluonic ones, and so we can employ Eq. (102). For  $\alpha_s(Q)$  we take its LO approximation for three quark flavors and  $\Lambda = 0.22$  GeV. That the numerics is completely unproblematic is demonstrated in Fig. 6(b),



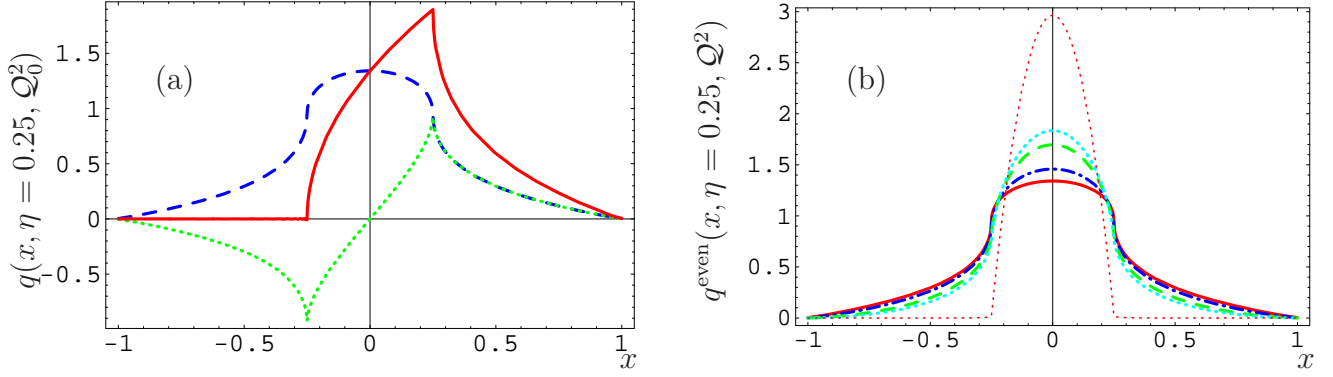


Figure 6: In panel (a) the toy GPD (115) is displayed for  $\alpha = -1/2$  and  $\eta = 0.25$  as solid line and its symmetric and antisymmetric part as dashed and dotted line, respectively. Panel (b) shows the evolution of the symmetric part from the input scale  $Q_0^2 = 0.5 \text{ GeV}^2$  (solid) to the scales  $Q^2 = 1 \text{ GeV}^2$  (dash-dotted),  $Q^2 = 10 \text{ GeV}^2$  (dashed),  $Q^2 = 100 \text{ GeV}^2$  (dotted), and (nearly) asymptotic limit (thin dotted).

where the asymptotic case  $Q^2 \rightarrow \infty$  is nearly reached by setting  $Q^2 = 10^{1000} \text{ GeV}^2$ . We remind that in this limit the outer region will die out and only the lowest conformal moment contributes leading to the asymptotic GPD

$$q^{\text{asy}}(x, \eta) = \theta(\eta - |x|) \frac{3}{4|\eta|} \frac{\eta^2 - x^2}{\eta^2}. \quad (122)$$

The numerical procedure for the calculation of scattering amplitudes is even easier to handle than that for GPDs themselves. As mentioned, a nice feature of the Mellin-Barnes integral is that it can be used to derive an expansion in powers of  $\xi$ . Let us suppose that we like to evaluate the Compton form factor (107) to LO accuracy, where the charge  $Q_p$  is set to one. Here only the analytic continuation of the odd conformal moments is needed. Guided by the small  $x$  behavior of parton densities, we choose the parameter  $\alpha$  to be negative and larger than  $-3/2$ . To ensure that all singularities are on the l.h.s. of the integration path, we take  $-\text{Max}(1/2, -1 - \alpha) < c < \text{Min}(1/2, -\alpha)$ . The first pole which appear in the integrand on the negative axis arises from  $\tan(\pi j/2)$  and is at  $j = -1$ . We remark that the pole which we would have expected in the forward case, namely, at  $j = -1 - \alpha$  is absent for  $\xi > 0$ . Rather there appears a new one at  $j = -1 + \alpha$ , which is associated with the behavior of the GPD at the cross-over point  $x = \eta$ . From our explicit expression for the conformal moments, given in Eqs. (117), (120), and (121) it is obvious that the integrand contains three different pieces, proportional to  $\xi^{-1-j}$ ,  $\xi^{1+j}$ , and  $\xi^\alpha$ . For the term proportional to  $\xi^{-1-j}$  we can arrange a systematic expansion in  $\xi$  by a shift of the integration path to the left. The poles appear here at  $j = \{-1 - \alpha, -2 - \alpha, \dots\}$ ,  $j = \{-1, -2, \dots\}$ , and at  $j = \{-1/2, -3/2, \dots\}$ . In the latter case the contribution will be cancelled by those from the piece proportional to  $\xi^{1+j}$ , which has poles on the positive axis only, at  $j = \{1/2, 3/2, \dots\}$ . This is established by a shift of the integration path to the right. What remains are the terms proportional to  $\xi^\alpha$ . Here we can close the integration path so that the first and forth quadrant is

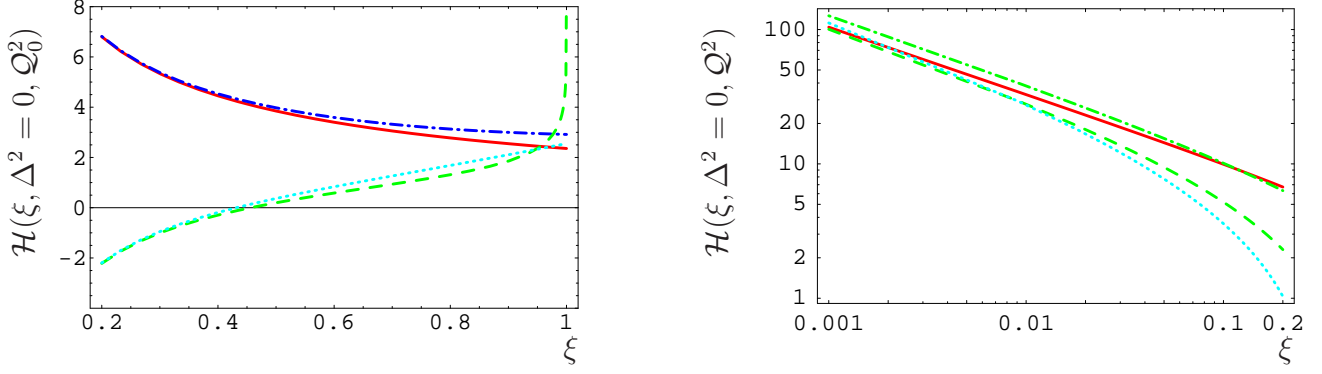


Figure 7: The Compton form factor  $\mathcal{H}(\xi, \Delta^2 = 0, Q^2)$ , arising from the toy GPD (115), to LO accuracy. Left: Exact imaginary (solid) and real (dashed) part of the Compton form factor and their approximation by Eq. (123) (dash-dotted and dotted lines, respectively). Right: The Compton form factor evaluated numerically at the input scale  $Q_0^2 = 0.5 \text{ GeV}^2$  (solid and dashed) and evolved with the flavor non-singlet evolution equation to  $Q^2 = 4 \text{ GeV}^2$  (dash-dotted and dotted). The imaginary part is shown as solid and dash-dotted lines and the absolute value of the real part as dashed and dotted lines.

included and employ then the residue theorem, where the only poles are at  $j = \{-\alpha, 1 - \alpha, \dots\}$ . All of these poles contribute to the leading power behavior and they must be resummed. Finally, collecting the results and neglecting power corrections of order  $\mathcal{O}(\xi^3)$  leads to the approximation

$$\begin{aligned} \mathcal{H}(\xi) = & 2^\alpha \pi (2 + \alpha) \left[ i + \cot\left(\frac{\pi\alpha}{2}\right) \right] \xi^\alpha \left\{ 1 - i(1 + \alpha)\xi \tan\left(\frac{\pi\alpha}{2}\right) \right. \\ & \left. + \frac{(1 + \alpha)(2 + \alpha)}{2} \xi^2 + \mathcal{O}(\xi^3) \right\} - \frac{2(2 + \alpha)}{\alpha} \left\{ 1 + \frac{(2 + \alpha + \alpha^2)}{(1 - \alpha)(2 - \alpha)} \xi^2 + \mathcal{O}(\xi^3) \right\}. \end{aligned} \quad (123)$$

This expansion coincides with that for the exact Compton form factor, which for our toy model (115) is exactly calculable. It is remarkable that this expansion does contain odd powers of  $\xi$ . In fact, the  $\xi$  term in the first line should be especially important in the small  $\xi$  region. Numerically, this approximation works quite well for the region that is of phenomenological interest. The deviation from the exact expression is about 3% for  $\alpha = -1/2$  and  $\xi = 0.4$  for the imaginary part. For the real part the approximation induces a small shift of the zero of the exact expression from  $\xi \sim 0.456$  to  $\xi \sim 0.431$ . The accuracy of the approximation (123) grows with increasing  $\alpha$  and rapidly with decreasing  $\xi$ . It is amazing that this approximation remains qualitatively correct as long as  $\xi$  does not approaches one, see left panel in Fig. 7. In the right panel of this figure we show the imaginary and real part of the Compton form factor, evaluated numerically with the Mellin-Barnes integral, for smaller values of  $\xi$ . Here the difference between the approximate and exact result is even invisible. Let us stress specifically, that we do not encounter any numerical problems in the small  $\xi$  region.

## 4.2 Ansätze for conformal moments

The conformal moments for complex valued conformal spin, appearing in the GPD representation (77), can be expanded in terms of  $c_k(1, \eta)$  using a suitable integral transformation. Such an integral transformation can be viewed as the analytic continuation of the conformal expansion (44) for non-negative integer conformal spin. In such an representation the  $\eta$  and  $\Delta^2$  dependence in the conformal moments separates and only an ansatz for the form factors  $F_{jk}(\Delta^2)$  is required.

Lets have a closer look at these form factors. The GPD Mellin–Barnes integral representation (77) can be interpreted as describing the effective summation of all particle exchanges in the  $t$ -channel. These are labelled by their conformal spin. Of course, conformal symmetry is broken in the non-perturbative sector. However, the conformal spin can still be used for the classification of excitations, just like in quantum mechanics for a non-spherical potential, the partial wave expansion in terms of spherical harmonics can still be employed to solve the Schrödinger equation. For vanishing skewness, i.e.,  $\eta = 0$ , the quantum number of the conformal spin can be replaced by the common spin  $J = j + 1$  and the conformal moments are given by the “diagonal” form factor  $F_{jj}(\Delta^2)$

$$m_j(\eta = 0, \Delta^2) = F_{jj}(\Delta^2), \quad (124)$$

cf. Eq. (44). Having in mind that the conformal partial waves  $p_j(x, \eta = 0)$  are then given by  $(1/x)^J$ , where  $1/x$  plays the role of a (rescaled) energy, the Mellin–Barnes integral for GPDs looks similar to the  $t$ -channel scattering amplitude at large energies. This suggest that there exists a connection with Regge theory or at least with Regge phenomenology. Let us remind that in deep inelastic scattering, i.e., for  $\Delta^2 = 0$ , this connection shows up in the small  $x$  behavior of structure functions, which is governed by the intercept of the corresponding leading Regge trajectories [68]. Note, however, that the small  $x$  behavior of parton densities depends on their conventions, i.e., on the factorization scheme and scale. A more recent analysis for the unpolarized valence quark densities can be found in Ref. [69]. Below it will be demonstrated that for  $\eta = 0$  there exist phenomenological indications that the  $\Delta^2$  dependence in  $F_{jj}(\Delta^2)$  is related to Regge trajectories.

Also for general kinematics, i.e.,  $\eta \neq 0$ , one can take this duality between  $t$ - and  $s$ -channel serious, see the discussion in Sect. 2.1. A description of DVCS in the high-energy limit is given in [70], where the leading Regge trajectory arises from the pomeron exchange in the  $t$ -channel. Moreover, the  $t$ -channel description provides arguments for the so-called  $D$ -term [53], appearing in the nucleon GPDs  $H(x, \eta, \Delta)$  and  $E(x, \eta, \Delta)$ , and for the so-called pion pole term [71], appearing in  $\tilde{E}(x, \eta, \Delta)$ . Note that these effects are taken into account by a modification of GPDs that affects only the central region and so their  $s$ -channel counterpart is absent. On the basis of the conformal partial wave expansion, applied to LO accuracy, and the crossing relation between GPDs and GDAs a dual description of the former ones in terms of  $t$ -channel exchanges has been suggested in Ref. [38]. Here the conformal moments have been decomposed into contributions with definite angular momentum. Since the concept of conformal spin has to the best of our knowledge not been

worked out for applications in hadron spectroscopy, one should focus on this more appropriate quantum number. Nevertheless, let us point out that the form factors  $F_{jk}(\Delta^2)$  for  $j \neq k$ , defined in Eq. (44), measure the strength of (non-perturbative) conformal symmetry breaking. In this paper, however, we do not proceed with the spectroscopic interpretation of these form factors (or some rotated version of them) and the search of an appropriate representation for the conformal moments with complex valued conformal spin in terms of them.

Instead, our aim is now more pragmatic, namely we will introduce and study specific ansätze for the conformal moments. Therefore, we now introduce and explore ansätze that are simpler to handle. We start in Sect. 4.2.1 with a reduced variable dependence by setting  $\Delta^2 = 0$ . Then we implement in Sect. 4.2.2 the  $\Delta^2$  dependence. In Sect. 4.2.3 we especially consider this dependence for the case  $\eta = 0$  and discuss the resulting GPD  $H(x, \eta = 0, \Delta^2)$ , especially, its interpretation as three dimensional parton density.

#### 4.2.1 Ansätze for reduced conformal moments

For our simple toy GPD example (115), studied in Sect. 4.1, the conformal moments appear to be rather complicated functions. Indeed, it is not clear at all whether the complicated structure of  $m_j(\eta, \Delta^2 = 0)$  in our toy model, is an artifact of the analytic continuation procedure or indicates some physics, related to the skewness dependence. So let us explore several “minimal” ansätze for the conformal moments.

To ensure that the forward limit is correctly reproduced, we factorize the poles in the complex  $j$ -plane that survive the limit  $\eta \rightarrow 0$ :

$$m_j(\eta, \Delta^2 = 0 | \alpha, \beta) = \frac{\Gamma(\alpha + 1 + j)\Gamma(\alpha + \beta + 2)}{\Gamma(\alpha + 1)\Gamma(\alpha + \beta + 2 + j)} b_j(\eta^2). \quad (125)$$

Here the normalization of the function is  $b_j(\eta^2 = 0) = 1$  and, moreover, we considered it as convenient to normalize the lowest moment according to  $m_0(\eta, \Delta^2 = 0 | \alpha, \beta) = 1$ . In the forward limit we arrive after an inverse Mellin transform at

$$m_j(\eta = 0, \Delta^2 = 0 | \alpha, \beta) \rightarrow \frac{\Gamma(\alpha + \beta + 2)}{\Gamma(\alpha + 1)\Gamma(\beta + 1)} x^\alpha (1 - x)^\beta, \quad (126)$$

which is well defined for all realistic values of  $\alpha$ , except for  $\alpha = -1$ . For this special value one can first multiply the expression with an appropriate normalization factor that cancels the factor  $1/\Gamma(\alpha + 1)$ . The standard parameterization of a parton density, i.e.,  $Nx^\alpha (1 + A\sqrt{x} + Bx) (1 - x)^\beta$ , can be obtained in Mellin space by the linear combination

$$q_j = N' [m_j(0, 0 | \alpha, \beta) + A' m_j(0, 0 | \alpha + 1/2, \beta) + B' m_j(0, 0 | \alpha + 1, \beta)], \quad (127)$$

where

$$N' = N \frac{\Gamma(1 + \alpha)\Gamma(1 + \beta)}{\Gamma(2 + \alpha + \beta)}, \quad A' = \frac{\Gamma(3/2 + \alpha)\Gamma(2 + \alpha + \beta)}{\Gamma(1 + \alpha)\Gamma(5/2 + \alpha + \beta)} A, \quad B' = \frac{1 + \alpha}{2 + \alpha + \beta} B. \quad (128)$$

It is required that the function  $b_j(\eta^2)$  for non-negative integer values of  $j = n$  reduces to a polynomial of order  $n/2$  and  $(n \pm 1)/2$  for even and odd  $n$ , respectively. Here the order of the odd moments depends on the specific GPD. Moreover, these functions have only singularities in the second and third quadrant of the complex  $j$  plane. We can allow that these functions grow with the real part of  $j$ , however, they must be bounded for large imaginary parts of  $j$ ,  $|\arg(j)| \leq \pi/2$ .

One can classify the conformal moments  $b_n(\eta^2)$  in general and their analytic continuation with respect to their dependence on both variables  $\eta$  and  $j$ , which leads to a classification of reduced GPDs. (We do not know whether this mathematical fact is known already from some other context.) For the time being, we concentrate on functions  $b_j(\eta^2)$  that can be expanded around the point  $\eta^2 = 0$ . Several simple examples can be given in terms of hypergeometric functions

$$b_j \left( \eta^2 \middle| \{a, b\}, \{r, s\}, \{\sigma, p\} \right) = \frac{{}_2F_1 \left( \begin{matrix} -j/2 + (1-2p)(1-\sigma)/4, a \\ b \end{matrix} \middle| r + s\eta^2 \right)}{{}_2F_1 \left( \begin{matrix} -j/2 + (1-2p)(1-\sigma)/4, a \\ b \end{matrix} \middle| r \right)}, \quad (129)$$

where the normalization condition at  $\eta = 0$  is satisfied. Here the parameters  $a$  and  $b$  may depend on  $j$ . For the analytic continuation of even moments we set as above  $\sigma = 1$  in the case of odd ones  $\sigma = -1$  and the choice  $p = 1$  leads for  $j = n$  to polynomials of order  $(\eta^2)^{(n+1)/2}$ , while  $p = 0$  gives polynomials of order  $(\eta^2)^{(n-1)/2}$ . To ensure that no branch cut appears in the interval  $0 \leq \eta^2 \leq 1$ , the parameters  $r$  and  $s$  must fulfill the inequalities  $r \leq 1$  and  $r + s \leq 1$ .

The definition (129) is quite general and contains a number of special cases. For instance, if we set  $\sigma = 1, a = (1-j)/2, b = 2$ , and  $r = 1$ ,

$$b_j \left( \eta^2 \middle| \{(1-j)/2, 2\}, \{1, s\}, \{1, 0\} \right) = \frac{\Gamma(3/2)\Gamma(3+j)}{2^{j+1}\Gamma(3/2+j)} {}_2F_1 \left( \begin{matrix} -j/2, (1-j)/2 \\ 2 \end{matrix} \middle| 1 + s\eta^2 \right), \quad (130)$$

we recover for  $s = -1$  the definition of conformal moments (35) with  $x = 1$ . Here they are expressed in terms of hypergeometric functions that arise from the original ones by a so-called quadratic transformation. These moments can be used for even and odd values of  $j$ . If one needs odd moments that are of order  $(\eta^2)^{(n+1)/2}$ , one should set  $a = (-1-j)/2$ . We remark that the expansion in the vicinity of  $\eta^2 = 0$  exists only as linear combination of two power series in  $\eta^2$ , one of them containing the overall factor  $(\eta^2)^{3/2+j}$ .

Besides the other parameters,  $s$  controls the strength of the skewness dependence. If we set it to zero, the function  $b_j(\eta^2)$  is simply one.

If  $a = b$ ,  $b_j(\eta^2)$  reduces to the simple function

$$b_j \left( \eta^2 \middle| \{a, a\}, \{r, s\}, p \right) = \left( 1 - \frac{s}{1-r} \eta^2 \right)^{(j+p)/2}. \quad (131)$$

Here  $1-r$  appears as a scaling factor and so in the following  $r$  can be set to zero, when simultaneously  $s$  is restricted to  $s \leq 1$ . For negative values of  $s$  the function (129) is even analytic for  $1 \leq \eta$ . To get a clue which values of  $a(j)$  and  $b(j)$  are allowed in the ansatz (130), we generate

cases	parameters of $b_j \left( \eta^2 \left\{ a, b \right\}, \left\{ r, s \right\}, \left\{ 1, 0 \right\} \right)$	explicit expression
	$\{a, b\}$	$\{r, s\}$
(a)	$\{(1-j)/2, 2\}$	$\{1, -1\}$
(b)	$\{a, b\}$	$\{1, 0\}$
(c)	$\{-199/4 + j, 2/3 + 2j\}$	$\{0, -1/4\}$
(d)	$\{-199/4 + j, 2/3 + 2j\}$	$\{0, 1/4\}$
(e)	$\{a, a\}$	$\{0, \pm 1/4\}$

Table 1: The parameters and resulting functions for our ansätze concerning the analytic continuation of even conformal moments (129), classified by case (a) -(e).

“associated” conformal moments of  $b_j \left( \eta^2 \left\{ a, a \right\}, \left\{ 0, s \right\}, p \right)$  by the convolution integral

$$\int_0^1 dz f_j(z) (1 - z s \eta^2)^{(j+p)/2}, \quad \text{with} \quad \int_0^1 dz f_j(z) = 1. \quad (132)$$

Here it is required that  $f_j(z)$  as function of  $j$  is bound for  $j \rightarrow \infty$  with  $|\arg(j)| \leq \pi/2$  for  $0 \leq z \leq 1$ . To arrive at the parameterization in terms of hypergeometric functions we choose

$$f_j(z) = \frac{\Gamma(b(j))}{\Gamma(a(j))\Gamma(b(j) - a(j))} z^{a(j)-1} (1 - z)^{b(j)-a(j)-1}. \quad (133)$$

The requirement for the bound of  $f_j(z)$  is certainly satisfied for  $\Re a(j) > 0$  and  $\Re(b(j) - a(j)) > 0$ . Especially, if  $a(j)$  tends to infinity for  $j \rightarrow \infty$ ,  $b(j)$  has to grow as  $a(j)$  or even faster. The case  $a = (1 - j)/2$  and  $b = 2$ , mentioned above, can be obtained within an analogous treatment. Here, however, one has to choose an integration contour in Eq. (132) in the complex plane that encircles the point  $z = 0$  and so the convergence condition for the integral can be relaxed. We will skip this issue here and refer, for instance, to Ref. [67].

We now explore the resulting GPDs and GDAs. As example we take the reduced valence quark GPDs and GDAs in the vector case with the rather realistic values  $\alpha = -1/2$  and  $\beta = 3$ . The unpolarized parton density is normalized to one and reads, cf. Eqs. (125) and (126),

$$q(x) = \frac{35}{32} x^{-1/2} (1 - x)^3 \quad (134)$$

The function  $b_j(\eta^2)$  is the analytic continuation of conformal moments with even  $n$  and the parameters are specified in Table 1. A few comments are in order. In case (a) we took the conformal moments itself, here in a more appropriate representation that is for  $\eta > 0$  equivalent to  $c_j(1, \eta)$ . They possess the properties we required in the derivation of the Mellin–Barnes integral and of

course, they reduce to polynomials for both even and odd non-integer values of  $n$ . We will use them in the Mellin-Barnes integral (79) within even conformal partial waves (75). Crossing symmetry, see Eq. (43), requires the existence of an analytic continuation to  $\eta > 1$  and this is achieved here by the change of arguments  $c_j(1, \eta) \rightarrow c_j(1 - 2\zeta, 1)$ , see Eq. (44). For the numerical evaluation of the GDAs the conformal partial wave series (43) or alternatively the Mellin-Barnes integral (84) can be used. The projection on the even moments can be achieved by symmetrization:

$$\Phi(z, \zeta) \rightarrow \frac{1}{2} [\Phi(z, \zeta) + \Phi(1 - z, \zeta)] . \quad (135)$$

The case (b) seems to be trivial. But after crossing it results in  $(1 - 2\zeta)^j$ , which leads for odd moments with  $\zeta > 1/2$  to an alternating series with an absolute value that converges to one in the end-points. For the convergence of the conformal partial wave series (44) in terms of polynomials an exponential suppression factor  $2^{-n}$  is required. Hence, this series only converges in the interval  $1/4 < \zeta < 3/4$ . The analytic continuation with respect to  $\zeta$  can be achieved by the Mellin-Barnes integral (85). However, outside of the convergence region, i.e.,  $\zeta < 1/4$  or  $3/4 < \zeta$ , we will find a GDA that does not vanish at the end-points  $z = \{0, 1\}$ .

The cases (c) and (d) differ by the sign of the argument in the hypergeometric function and follows from (e) by an integral transformation (132). They reduce to polynomials for even  $n$  only. The factor  $1/4$  in the argument improves the convergence property after crossing. The second parameter in the upper line of the hypergeometric function, i.e.,  $-199/4 + j$ , can for certain non-integer values of  $j = n < 49$  be a negative integer. As explained above, this does not generate problems. The choice of this “big” constant  $-199/4$  induces a numerical enhancement of  $\mathcal{O}(\eta^2)$  terms. The parameter  $3/2 + 2j$  in the lower line compensates for rather large values of  $j$  the growing of the second argument in the first line. We did not include any poles on the positive  $j$  axis. As a consequence, we have new poles on the negative one. They appear at  $j = -1/3, -4/3, \dots$  and die out in the limit  $\eta \rightarrow 0$ . With our choice  $\alpha = -1/2$ , which determines the small  $x$  behavior of the parton densities and is associated with a pole at  $j = -1/2$ , a new “leading” pole at  $j = -1/3$  arises for non-zero skewness. Its contribution, however, should be suppressed as  $\mathcal{O}(\eta^2)$ . So for instance, in the Compton form factors it should only give rise to a  $\eta^2 \eta^{-2/3} = \eta^{4/3}$  term. Moreover, we changed the normalization of the other poles for  $0 < \eta$ . For not too large values of  $\eta$  this should produce only a numerically small effect. Since we included a numerical enhancement, this might induce some sizeable changes of the GPD and GDA shapes for not too small values of  $\eta$ .

In Fig. 8 we display the  $\eta$  and  $\zeta$  dependence for the second moment, i.e., of  $b_2(\eta^2)$ . The  $\eta$  dependence of the conformal moment in case (a) [(solid line)], i.e.,

$$c_2(\eta, 1) = 1 - \frac{\eta^2}{5} \quad \Rightarrow \quad c_2(1 - 2\zeta, 1) = (1 - 2\zeta)^2 - \frac{1}{5}, \quad (136)$$

is rather weak and so it is “similar” as in case (b) [constant or  $(1 - 2\zeta)^2$  (dash-dotted line)]. In contrast we find for cases (c) [dashed line] and (d) [dotted line] a large deviation in opposite directions. For GPD moments it will die out for  $\eta \rightarrow 0$ , while for the GDA moments the difference



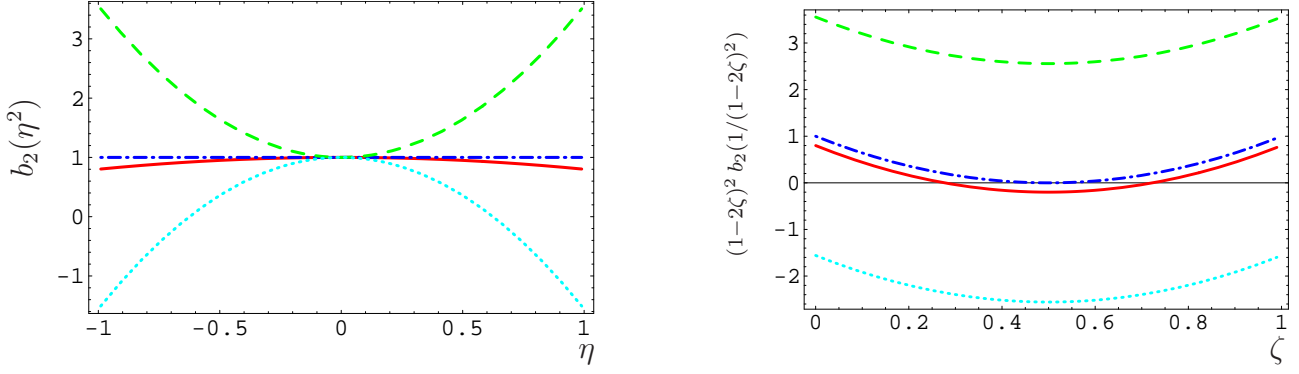


Figure 8: The  $\eta$  (left) and  $\zeta$  (right) dependence of  $b_n(\eta^2)$  and  $(1-2\zeta)^2 b_n(1/(1-2\zeta)^2)$ , respectively, for  $n = 2$  are shown for the parameterizations given in Table 1: (a) solid, (b) dash-dotted, (c) dashed, and (d) dotted lines.

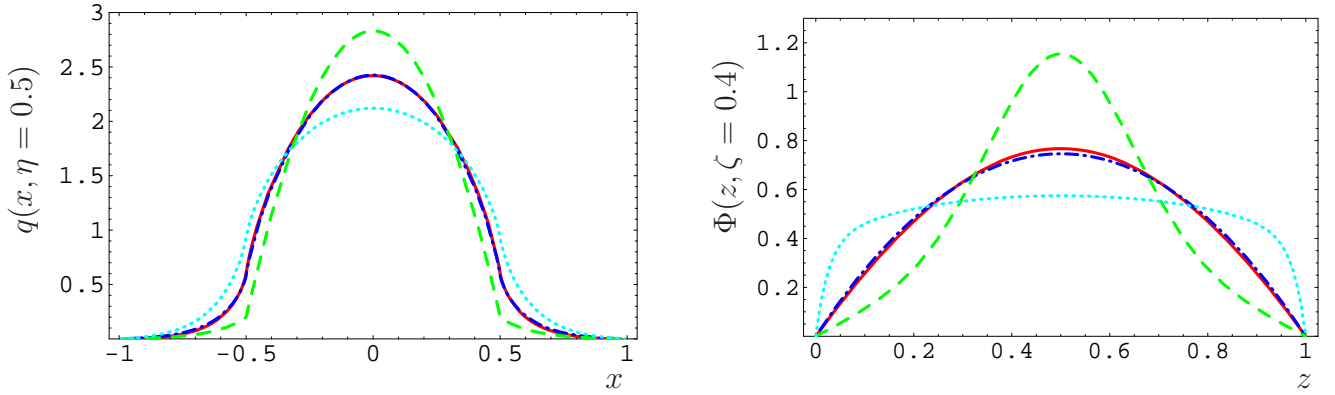


Figure 9: The momentum fraction shape of reduced GPDs with  $\eta = 0.5$  (left) and GDAs with  $\zeta = 0.4$  (right), same labelling as in Fig. 8.

is nearly  $\zeta$  independent and large. We will skip here the detailed discussion of the dependence in higher moments, which are suppressed by the factor  $B(1/2 + n, 4 + n) \sim 1/n^4$  for  $n \rightarrow \infty$ . Note, however, that only the conformal moments (a) for  $\eta^2 > 0$  continuously tend to zero with increasing  $n$ . Also the rescaled conformal moments (a) for all values of  $\zeta$  possess this behaviour. We remark that the conformal moments (e) will mostly not give quantitatively different results as (b), so we will in the following not present them.

In Fig. 9 we show the resulting GPDs for  $\eta = 0.5$  and GDAs for  $\zeta = 0.4$ . As has already been discussed the skewness dependence of the conformal moments in Fig. 8, cases (a) and (b) can be hardly distinguished, for GPDs they are quite the same. In case (c) the area in the central region and the magnitude of the maximum at  $\eta = 0$  are enhanced, while the area of the outer region shrinks (the lowest moment of all functions is normalized to one). Consequently, also the magnitude at the cross-over points  $x = \pm\eta$  decreases. The reverse situation is observed for case (d). This is caused by the analytic properties of the conformal moments with respect to the variable  $j$ , which we explained above. Comparing both panels in Fig. 9, one immediately sees

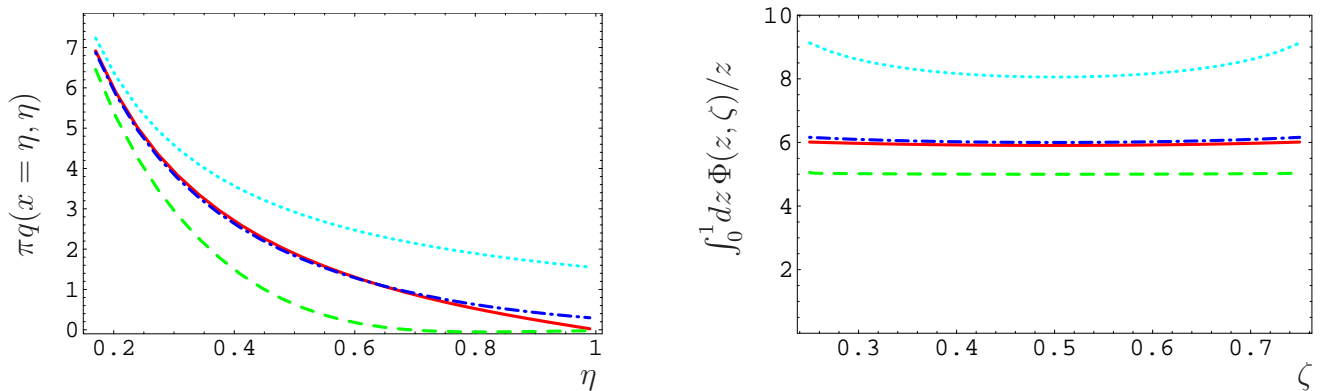


Figure 10: The reduced GPD at the cross-over point  $x = \eta$ , multiplied with the factor  $\pi$ , (left) versus  $\eta$  and the convolution of the GDA with  $1/z$  (right) versus  $\zeta$ , same as in Fig. (8).

that the “width” of GPDs shows up in the end-point behavior of GDAs. It is remarkable that the GDAs (a) and (b) possess shapes that are governed mainly by the first partial wave of the conformal expansion. Indeed, for case (a) it turns out that in the region  $0.05 \leq \zeta \leq 0.95$  the higher partial waves give at most a 10% percent correction. In the much narrower region  $0.3 \leq \zeta \leq 0.7$  this is within the same accuracy also true for the GDA (b). This region starts slightly about or below the value, where the series turns over to be divergent, i.e., for  $\zeta \leq 0.25$  and  $0.75 \leq \zeta$ . A slightly smaller convergency radius holds for the GDA (c) and (d).

In Fig. 10 we show the quantities that enter the scattering amplitude for a hard exclusive process, in which only the virtuality of the incoming photon can be varied. Under such circumstances the Compton form factors, i.e., Eq. (104) or their crossing analogues Eq. (112), are measurable. The non-perturbative distributions can not be directly determined by deconvolution, but at least within our toy ansätze the correspondence between momentum fraction dependence and the amplitudes is clear-cut. In the left panel of Fig. 10 we depict the GPD at the point  $x = \eta$  multiplied by  $\pi$ . This cross-over point trajectory is accessible in single spin asymmetry measurements. Within our ansätze both the normalization and the slope encodes information about the GPD shape. Compared with the left panel in Fig. 9, one realizes that the narrowest (widest) GPD has the smallest (largest) value at the cross over point  $x = \eta$ . The differences of the trajectories diminish with decreasing  $\eta$ . Cases (a) and (b) are only distinguishable when  $\eta$  tends to one. Certainly, the slope of the cross-over point trajectories is dictated by the strength of the skewness dependence of the conformal moments.

In the right panel of Fig. 10 we show the  $\zeta$  dependence of the scattering amplitude, given as convolution of a GDA with a LO hard-scattering amplitude, see Eq. (112). It has been evaluated within the partial wave expansion (113), taking the first thirty terms into account. The result is only displayed for the region in which also the series for the conformal moments (b)-(d) converges, i.e., for  $0.25 \lesssim \zeta \lesssim 0.75$ . The end-point behavior of GDAs determines the normalization of the scattering amplitude while the  $\zeta$  dependence is in all cases (rather) flat. As already mentioned, these convergency problems arise from an exponential growth caused by the factor  $2^n$  that is

contained in the normalized conformal partial waves (39). One would expect that the conformal partial wave expansion of GDAs converges for all physical values of  $\zeta$  and  $z$ . To ensure this, the conformal moments must be exponentially suppressed by a factor  $2^{-n}$  for large  $n$ . We remind that the normalization has been adopted from parton densities and so this factor will drop out in the limit  $\eta \rightarrow 0$ .

We come now to the  $\eta$  dependence of the cross-over point trajectory for smaller values of  $\eta$ . The trajectory is represented by the Mellin-Barnes integral

$$q(\eta, \eta) = \frac{1}{2i} \int_{c-i\infty}^{c+i\infty} dj \eta^{-j-1} \frac{2^{j+1} \Gamma(5/2+j)}{\Gamma(3/2) \Gamma(3+j)} \frac{\Gamma(1/2+j) \Gamma(9/2)}{\Gamma(1/2) \Gamma(9/2+j)} b_j(\eta^2), \quad (137)$$

which can be used to derive, as explained in Sect. 3.2, an analytic expansion in terms of powers in  $\eta$ . The leading terms

$$q(\eta, \eta) = \frac{35}{6\sqrt{2}\pi \sqrt{\eta}} - \frac{105\sqrt{\eta}}{8\sqrt{2}\pi} + \dots \quad (138)$$

are “universal” in all cases and arise from the poles at  $j = -1/2$  and  $j = -3/2$ . The accuracy of this approximation for the cross-over point trajectory is for all cases about 1% for  $\eta = 0.05$  and, of course, starts to be much better with decreasing  $\eta$ . Corrections to the approximation (138) depend on the specific model and will not be discussed here. For large values of  $\eta$  they are smaller for ansatz (a) than for (c) or (d). Remarkably, in case (b) the integral (137) can be exactly calculated:

$$q(\eta, \eta) = \frac{(2-\eta)^{7/2}}{2\sqrt{2}\pi \eta} {}_2F_1\left(\begin{matrix} 1/2, 5/2 \\ 9/2 \end{matrix} \middle| 1 - \frac{2}{\eta}\right). \quad (139)$$

Let us summarize the lessons from this investigation. Unluckily, after crossing it turns out that three of our models, (b)-(d), lead to convergence problems for the conformal partial waves series. Since these series should converge, the conformal moments must for  $\eta > 1$  exponentially decrease as  $2^{-n}$  with increasing  $n$ . Viable ansätze for the conformal moments are holomorphic functions of the conformal spin  $j$  that respect the following requirements:

- they should be bound for  $j \rightarrow \infty$  with  $|\arg(j)| \leq \pi/2$  for  $|\eta| \leq 1$
- An expansion of these functions in  $\eta^2$  should exist
- they should show an exponential suppression for  $\eta^2 > 1$  by a factor  $2^{-n}$  (for integer  $n$ )

In addition they should be flexible enough to be able to generate a large variety of GPD shapes. In our examples only case (a), i.e., the analytic continuation of Gegenbauer polynomials, satisfy the three requirements. Applying suitable integral transformations to them allows to generate “associated” polynomials. We did not study in detail how flexible the GPD shapes can be parameterized within this method but got the impression that only small changes for large  $\xi$  are possible.

We are aware that these examples do not cover all possible types of conformal moments. One important lesson is that the analytic properties of conformal moments determine the qualitative features of GPDs. Certainly, our examples here give only a first insight into this connection. For completeness, we mention the existence of a symmetry relation that arises from the definition (35), namely, the invariance under the replacement  $j \rightarrow -j - 3$  [35]:

$$\frac{2^{1+j}\Gamma(3/2+j)}{\Gamma(3/2)\Gamma(3+j)}\eta^{-j}c_j(x,\eta) = \frac{2^{1+j}\Gamma(3/2+j)}{\Gamma(3/2)\Gamma(3+j)}\eta^{-j}c_j(x,\eta)\Big|_{j \rightarrow -j-3}. \quad (140)$$

Since, however, perturbative QCD, e.g., anomalous dimensions, already violate this symmetry, there is no need to implement it in a non-perturbative ansatz for conformal moments.

#### 4.2.2 Implementation of momentum squared dependence

Now we address the implementation of the  $\Delta^2$  dependence. We might include it by introducing  $\Delta^2$  depended parameters in the ansatz (125) in such a way that no singularities in the first and forth quadrant of the complex  $j$ -plane appear. For the sake of simplicity we write here a factorized ansatz

$$m_j(\eta, \Delta^2 | \alpha, \beta) = \frac{\Gamma(\alpha+1+j)\Gamma(\alpha+\beta+2)}{\Gamma(\alpha+1)\Gamma(\alpha+\beta+2+j)} b_j(\eta^2) F_j(\Delta^2), \quad (141)$$

with the normalization condition  $F_j(\Delta^2 = 0) = 1$ . In the case that the form factors  $F_j(\Delta^2)$  are  $j$  independent the  $x$  and  $\Delta^2$  dependence is obviously factorized, too. Lattice calculations for the first moments of  $u$  and  $d$  quark GPDs suggest that such a factorization is actually not correct. According to these results, the cut-off mass squared in a dipole fit increases with  $j = n$ . Unluckily, the systematic theoretical uncertainties of these results, especially, those associated with the chiral extrapolation are still kind of large, but the preferred fits suggest a linear growth with  $(j+1)$ <sup>13</sup> [72]. A second constraint on the  $\Delta^2$  dependence arises from the lowest moment of GPDs, which is related to partonic form factors, e.g., for the GPD  $H$ :

$$F_1^{p,\text{val}}(\Delta^2) = \int_{-\eta}^1 dx H_{p,\text{val}}(x, \eta, \Delta^2). \quad (142)$$

Where  $F_1^{p,\text{val}}(\Delta^2)$  can be expressed in terms of the proton ( $p$ ) and neutron ( $n$ ) electromagnetic Dirac form factors according to

$$2F_1^{u,\text{val}}(\Delta^2) = 2F_1^p(\Delta^2) + 2F_1^n(\Delta^2), \quad F_1^{d,\text{val}}(\Delta^2) = F_1^p(\Delta^2) + 2F_1^n(\Delta^2). \quad (143)$$

---

<sup>13</sup>The  $m_{d,n}^2 = (n+1)m_{d,0}^2$  dependence for the squared dipole masses  $m_{d,n}^2$ , taken from Table I of Ref. [72] gives a very good fit for the generalized form factors  $A_{n,0}^{u-d}$  ( $m_\pi = 897$  MeV) and  $A_{n,0}^{u+d}$  ( $m_\pi = 744$  MeV) with  $n = 0, 1, 2$ . For the large pion mass  $m_\pi = 897$  MeV one might have the impression that the growth is stronger (weaker) for the (axial-)vector case, which might be caused by a different intercept in the power behavior. Certainly, a definite conclusion can not be drawn from present lattice measurements.

We remark that the lowest moment of a GPD is simply obtained by setting  $j = 0$  in the ansatz (141).

Now we are in the position to build a minimal GPD ansatz for the valence quark GPDs  $H$  which satisfy the theoretical constraints in the forward case and provide for the lowest moment the correct  $\Delta^2$  dependence. Suppose we use the parameterization of the forward parton distribution at a given input scale in the form (127), the conformal GPD moments read then, e.g., for the  $u$  quark

$$m_j^{u,\text{val}}(\eta, \Delta^2) = \frac{2}{1 + A' + B'} [m_j(\eta, \Delta^2|\alpha, \beta) + A' m_j(\eta, \Delta^2|\alpha + 1/2, \beta) + B' m_j(\eta, \Delta^2|\alpha + 1, \beta)] ,$$

$$m_j(\eta, \Delta^2|\alpha, \beta) = \frac{\Gamma(\alpha + 1 + j)\Gamma(\alpha + \beta + 2)}{\Gamma(\alpha + 1)\Gamma(\alpha + \beta + 2 + j)} b_j(\eta^2) F_1^{u,\text{val}}(\Delta^2/(j + 1)) , \quad (144)$$

normalized to 2 for  $j = 0$  and  $\Delta^2 = 0$ . Guided by the lattice results, we rescaled here the dipole masses in the form factor  $F_1^{u,\text{val}}$  by  $j + 1$ , which results in a dependence on the ratio  $\Delta^2/(j + 1)$ . The remaining free parameters  $A', B', \alpha, \beta$  are taken from the parton density parameterization and for  $b_j(\eta^2)$  one can use one of the functions suggested above, where preference is given to case (a). Analogously, one can deal with other species of GPDs that reduce in the forward limit to parton densities. However, for these the  $\Delta^2$  dependence is typically far less known. In particular, unpolarized sea quark GPDs are not constraint by elastic form factor measurements.

Let us have a closer look at the parameterization (144). For  $j = 0$  we obviously find from this parameterization

$$\int_{-\eta}^1 dx H_{u,\text{val}}(x, \eta, \Delta^2) = 2b_0(\eta^2) F_1^{u,\text{val}}(\Delta^2) , \quad (145)$$

where the  $\eta$ -dependence drops out,  $b_0(\eta^2) = 1$  and the correct normalization is ensured. Setting  $\Delta^2 = 0$ , it is also clear from Eq. (141) that we arrive by an inverse Mellin transform at the parton density. It has been mentioned above that the GPD for  $\eta \rightarrow 0$  and small  $x$  is dominated by the leading Regge trajectory. In the following we argue that after a small modification this trajectory is already present in our parameterization. In our case we are dealing with the  $\rho^0$  and  $\omega$  trajectories, which according to the analysis of Ref. [69] are parameterized by a linear  $\Delta^2$ -dependence

$$\alpha_\omega(\Delta^2) = 0.42 + \Delta^2 0.95 \text{ GeV}^{-2}, \quad \alpha_\rho(\Delta^2) = 0.48 + \Delta^2 0.88 \text{ GeV}^{-2}. \quad (146)$$

If we take for the elastic nucleon form factor the standard dipole parameterization and consider only the first pole in the complex  $j$ -plane of the parton density Mellin-moments, i.e., the pole that appears on the negative axis at the largest value of  $j$ , our parameterization for the conformal moments reads

$$m_j^{\text{val}}(\eta, \Delta^2) \propto \frac{1}{\alpha + 1 + j} \frac{(j + 1 + \alpha)}{m_d^2(j + 1 + \alpha) - \Delta^2(1 + \alpha)} \times \left( \frac{A}{4M_N^2 - (1 + c)\Delta^2/(j + 1 + c)} + \frac{B}{m_d^2 - (1 + d)\Delta^2/(j + 1 + d)} \right) . \quad (147)$$

Here  $M_N$  is the nucleon mass,  $m_d$  is the dipole mass appearing the parameterization of the Sachs form factors, e.g., in the electric one of the proton  $G_E^p(\Delta^2) = 1/(1 - \Delta^2/m_d^2)^2$ .  $A$  and  $B$  are two constants, the values of which can be read off, e.g., from Ref. [66]. Moreover, we modified here the rescaling of the  $\Delta^2$  dependence in such a way that the pole at  $j + 1 + \alpha = 0$  cancels against the scaling factor  $(j + 1 + \alpha)$ . The constants  $c$  and  $d$ , appearing in the scaling factors of the remaining  $\Delta^2$  dependence, are chosen to be positive so that they do not interfere with the leading Regge trajectory. This linear trajectory is given by

$$\alpha(\Delta^2) = \alpha(0) + \alpha'(0)\Delta^2, \quad \alpha(0) = -\alpha, \quad \alpha'(0) = \frac{1 + \alpha}{m_d^2} \quad (148)$$

and so we find with Eqs. (144) and (147)

$$m_j^{\text{val}}(\eta, \Delta^2) = \frac{2}{1 + A' + B'} \frac{\Gamma(\alpha + 2 + j)\Gamma(\alpha + \beta + 2)}{\Gamma(\alpha + 1)\Gamma(\alpha + \beta + 2 + j)} \frac{\beta_j(\Delta^2)b_j(\eta^2)}{(j + 1) - \alpha(\Delta^2)} (1 + A' \dots + B' \dots), \quad (149)$$

where the remaining  $\Delta^2$  dependence is accumulated in the function

$$\beta_j(\Delta^2) = \frac{A}{4M_N^2 - (1 + c)\Delta^2/(j + 1 + c)} + \frac{B}{m_d^2 - (1 + d)\Delta^2/(j + 1 + d)}. \quad (150)$$

As we saw, after rescaling of the dipole masses the leading pole at  $j = -1 - \alpha$  in Eq. (144) is in the parameterization (149) shifted to  $j = -1 + \alpha(\Delta^2)$  by an amount proportional to  $\Delta^2$ . The numerical value of the dipole mass is  $m_d = 840$  MeV and that of  $\alpha$  depends on the factorization scale. When we choose the scale to be the intercept of the Regge trajectories (146) we find the following slopes

$$\alpha'_\omega(0) = 0.82 \text{ GeV}^{-2}, \quad \alpha'_\rho(0) = 0.74 \text{ GeV}^{-2}. \quad (151)$$

These values are only about 15% smaller than the ones given in Eq. (146). In view of the fact that we used just the standard dipole parameterization of the elastic form factors and neglected all non-leading Regge trajectories, this agreement is quite astonishing. We interpret it as further evidence that Regge theory or at least Regge phenomenology is indeed applicable to GPDs. A deeper understanding of this issue could provide the key to a dual description of GPDs in terms of hadronic degrees of freedom and certainly warrants dedicated efforts.

#### 4.2.3 Numerical consequences for the probabilistic interpretation of GPD $H$

As mentioned in the introduction, GPDs possesses for  $\eta = 0$  a probabilistic interpretation in the infinite momentum frame. In particular the Fourier transform<sup>14</sup>

$$H_q(x, \vec{b}) = \int \frac{d^2 \vec{\Delta}}{(2\pi)^2} e^{-i\vec{b} \cdot \vec{\Delta}} H_q(x, \eta = 0, \Delta^2 = -\vec{\Delta}^2) \quad (152)$$

---

<sup>14</sup>To avoid a confusion with the definition of the GPD  $\tilde{H}_q(x, \eta, \Delta^2)$  in the axial-vector case, we omit the tilde symbol for the Fourier transform of  $H_q(x, \eta, -\vec{\Delta}^2)$ . The quantities in the two-dimensional impact space  $\vec{b}$  are indicated by their argument  $\vec{b}$ .

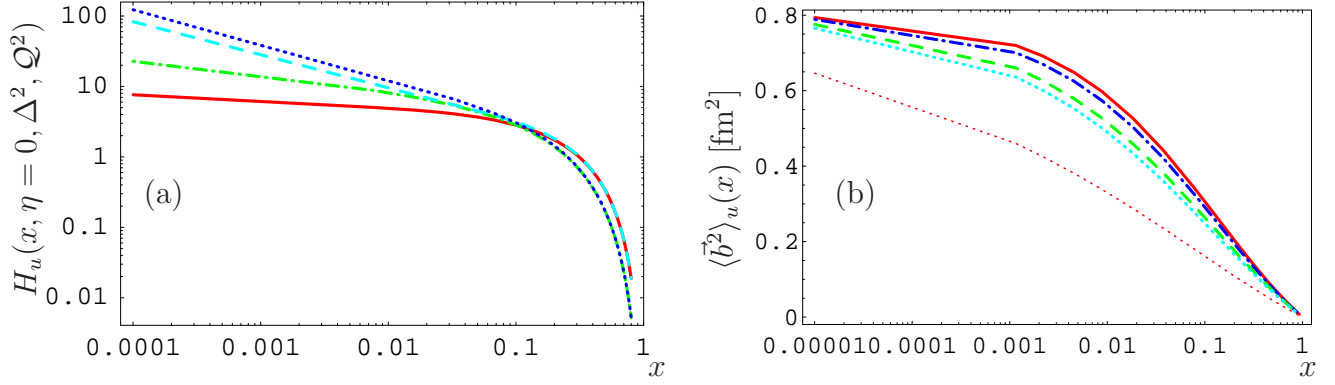


Figure 11: The  $u$ -valence quark GPD  $H_u(x, \eta = 0, \Delta^2, Q^2)$  of the proton is displayed in panel (a) versus  $x$  for fixed  $\Delta^2 = -0.25 \text{ GeV}^2$  with a  $\Delta^2$ -dependence arising from a Regge trajectory via Eqs. (148), (149), and (150) (solid and dash-dotted) and with a rescaled  $1/(j+1)$   $\Delta^2$ -dependence via Eq. (144) (dashed and dotted). The GPD is evolved from the input scale  $Q^2 = 0.5 \text{ GeV}^2$  (solid and dashed) to  $Q^2 = 10 \text{ GeV}^2$  (dash-dotted and dotted). In panel (b) we show for the  $\Delta^2/(j+1)$ -dependent GPD  $H_u$  the expectation value for the square of the impact parameter (154). The different lines correspond to  $Q^2 = 0.5 \text{ GeV}^2$  (solid),  $Q^2 = 1 \text{ GeV}^2$  (dash-dotted),  $Q^2 = 10 \text{ GeV}^2$  (dashed),  $Q^2 = 100 \text{ GeV}^2$  (dotted) and  $Q^2 = 10^{100} \text{ GeV}^2$  (thin dotted). We used the following parameter set:  $A' = B' = 0$ ,  $\alpha = -1/2$ ,  $\beta = 3$  and  $c = d = 1$ .

is the probability to find a quark species  $q$  inside the nucleon with momentum fraction  $x$  at impact parameter  $\vec{b}$ . The latter is defined relative to the center of momentum of the hadron, i.e.,  $\vec{b}$  is the distance of the active parton in the transversal direction from this center. It is worth mentioning that the definition of such a center is based on the existence of a Galilean subgroup of transverse boosts in the infinite moment frame [73]. Within light-cone quantization such transverse boosts have a field theoretical definition in terms of two conserved charges, expressed by the plus components of the energy momentum tensor. Their eigenvalues are good quantum number that labels the states of the hadron. Conveniently, they are chosen to be zero for the center.

This probabilistic interpretation of the GPD (152) has inspired several authors to build GPD ansätze to get a first glimpse of the three-dimensional tomographic picture of the nucleon. This has often been done using an exponential ansatz for the  $\Delta^2$ -dependence, which might serve its purpose in the space like region, however, violates the analytic properties of scattering amplitudes etc. such that crossing relations become meaningless. In the following we study our conformal moments for  $\eta = 0$  under this aspect. The only uncertainty which is left in our GPD representation is the  $j$ -dependence of the form factor. In Fig. (11) we present the momentum fraction dependence for fixed  $\Delta^2 = -0.25 \text{ GeV}^2$  and two different resolution scales. Obviously, the implementation of the Regge trajectory (solid and dash-dotted lines) results in a flatter  $x$ -dependence compared to a simple rescaling of the dipole mass squared with  $j+1$  (dashed and dotted lines).

As a side remark, we comment on the factorized  $\Delta^2$  ansatz for GPDs. Although, it is wrong in principle, this does not necessarily imply that all estimates for observables fail completely, at



least not for smaller values of  $\Delta^2$ . For the ansätze of conformal moments, we discussed in the both previous sections, the normalization of the resulting GPDs between the different versions of  $\Delta^2$ -dependence varies for  $0.08 \lesssim x \lesssim 0.2$  and  $|\Delta^2| < 0.3 \text{ GeV}^2$ , i.e., in the fixed target kinematics, not larger than 20%. Certainly, for lower or larger values of  $x$  the differences especially in the overall size can increase drastically, compare, e.g., the solid and dashed line in Fig. 11 (a). On the other hand the suppression introduced by the Regge motivated ansatz (see solid and dash-dotted lines) is welcome to suppress sea quark and gluonic contributions, which notoriously are overestimated in the factorized  $\Delta^2$  ansatz for hard exclusive electroproduction processes.

The average distance from an active parton to the center of the nucleon is defined as [8, 9]

$$\langle \vec{b}^2 \rangle_q(x, Q^2) = \frac{\int d\vec{b} \vec{b}^2 H_q(x, \vec{b}, Q^2)}{\int d\vec{b} H_q(x, \vec{b}, Q^2)} = 4 \frac{\partial}{\partial \Delta^2} \ln H_q(x, \eta = 0, \Delta^2, Q^2) \Big|_{\Delta^2=0}. \quad (153)$$

Within the parameterization (144), where for simplicity we again rescale the  $\Delta^2$  dependence by  $1/(j+1)$ , this average distance can be exactly calculated and expressed in terms of forward parton distributions

$$\langle \vec{b}^2 \rangle_q(x, Q^2) = \frac{\int_x^1 \frac{dy}{y} q(y, Q^2)}{q(x, Q^2)} 4 \frac{\partial}{\partial \Delta^2} \ln F_1^q(\Delta^2) \Big|_{\Delta^2=0}. \quad (154)$$

The  $1/(j+1)$  factor that arises in Mellin space from the differentiation with respect to  $\Delta^2$  gives in  $x$  space rise to the integral  $\int_x^1 dy/y \dots$ . Obviously, by a more refined rescaling of the  $\Delta^2$  dependence, see Eq. (147), we can express the resulting average by a more complex integral. For small  $x$  this quantity tends to a constant, depending only on the resolution scale, while at large  $x$  it vanishes as  $(1-x)$ . The latter behavior is a consequence of the linear  $j$ -dependence of the dipole masses. Such a behavior has been rejected in Ref. [20]. Namely, the quantity

$$d(x) = \frac{\langle \vec{b}^2 \rangle_q(x)}{(1-x)^2} \quad (155)$$

is interpreted, based on a partonic picture, as the distance of the active parton from the center of momentum of the spectators and should therefore be finite for  $x \rightarrow 1$ . Consequently,  $\langle \vec{b}^2 \rangle_q(x)$  should vanishes at least with  $(1-x)^2$  for  $x \rightarrow 1$ . Although this argumentation is further supported by perturbative QCD arguments [19], it is in our opinion not excluded that the simple parton picture can be misleading for quantities, which have no well-defined field-theoretical analog. Note also that a  $(1-x)^2$  behavior of  $\langle \vec{b}^2 \rangle_q(x)$  for  $x \rightarrow 1$  requires a  $(1+j)^2$  growth of the squared dipole masses. This means in terms of Regge phenomenology that the trajectories should possess a (small) non-linear term.

Let us come back to our ansatz. To include the scale dependence we use for the GPD  $H_q(x, \eta = 0, \Delta^2, Q^2)$  in Eq. (153) the Mellin-Barnes integral and insert the evolution operator, compare with

Eq. (102),

$$\langle \vec{b}^2 \rangle_q(x, \mathcal{Q}^2) = \frac{\int_{c-i\infty}^{c+i\infty} dj \frac{x^{-j-1} \Gamma(1+j+\alpha)}{\Gamma(1+j+\alpha+\beta)(j+1)} e^{\left\{ -\frac{\gamma_j^{(0)}}{2} \int_{\mathcal{Q}_0^2}^{\mathcal{Q}^2} \frac{d\sigma}{\sigma} \frac{\alpha_s(\sigma)}{2\pi} \right\}}}{\int_{c-i\infty}^{c+i\infty} dj \frac{x^{-j-1} \Gamma(1+j+\alpha)}{\Gamma(1+j+\alpha+\beta)} e^{\left\{ -\frac{\gamma_j^{(0)}}{2} \int_{\mathcal{Q}_0^2}^{\mathcal{Q}^2} \frac{d\sigma}{\sigma} \frac{\alpha_s(\sigma)}{2\pi} \right\}}} 4 \frac{\partial}{\partial \Delta^2} \ln F_1^{q\text{val}}(\Delta^2) \Big|_{\Delta^2=0}. \quad (156)$$

For experimental accessible values of  $\mathcal{Q}^2$  and for small  $x$ , both the numerator and denominator are dominated by the leading pole at  $j = -1 - \alpha$ . Shifting the integration path to the left we find for  $x \rightarrow 0$  the constant value

$$\langle \vec{b}^2 \rangle_q(x=0, \mathcal{Q}^2) = -\frac{4}{\alpha} \frac{\partial}{\partial \Delta^2} \ln F_1^{q\text{val}}(\Delta^2) \Big|_{\Delta^2=0}. \quad (157)$$

We remark that a Regge motivated ansatz would induce a double pole in the numerator and, consequently, a logarithmic modification with respect to both the  $x$ - and  $\mathcal{Q}^2$ -dependencies. Within the dipole ansatz for the partonic form factors, taken from Ref. [66], we have

$$\langle \vec{b}^2 \rangle_u(x=0, \mathcal{Q}^2) = -\frac{1}{\alpha} 0.4 \text{fm}^2 \quad \langle \vec{b}^2 \rangle_d(x=0, \mathcal{Q}^2) = -\frac{1}{\alpha} 0.53 \text{fm}^2 \quad (158)$$

for the  $u$  and  $d$  valence quarks. From Fig. 11(b), where we used the generic value  $\alpha = -1/2$ , we can read off the qualitative  $x$ -dependence of  $\langle \vec{b}^2 \rangle_{q\text{val}}(x, \mathcal{Q}^2)$  for given resolution scale  $\mathcal{Q}^2$ . It can be roughly approximated by a logarithmic growth with decreasing  $x$  which changes slope at some “cusp” point  $x_{\text{cusp}}(\mathcal{Q}^2) \sim 10^{-3}$ . With increasing  $\mathcal{Q}^2$  this cusp is washed out. The increase with  $\ln(1/x)$  visible in Fig. 11 (b), will not continue in the limit  $x \rightarrow 0$  but will saturate at a finite value (158). Numerically, we checked this qualitative feature up to  $\mathcal{Q}^2 = 10^{10000} \text{GeV}^2$  and  $1/x = 10^{40}$ .

So within our simple ansatz, which can be easily refined, we reproduce following well-known grand picture. At large  $x$  the valence quarks are in the center of the nucleon. With decreasing  $x$  they become ever more delocalized in the transverse direction and will move away in transversal direction with decreasing momentum fraction  $x$ . In the valence quark region with  $x \sim 0.3$  the average transverse distance is of the order  $\sim 0.4 \text{fm}$ . With increasing resolution scale this value is slowly decreasing. In the small  $x$  region their transverse distance grows, reaches (for the ansatz we used)  $\sim 0.9 \text{fm}$  in the limit  $x \rightarrow 0$  for  $u$  valence quarks and a slightly higher value for  $d$  quarks. Hence, the charge of the proton, which is probed in a scattering experiment, has a non-trivial transverse distribution.

## 5 Summary and conclusions

In this paper we have derived a new representation for leading twist-two GPDs and GDAs in terms of Mellin-Barnes integrals over the complex conformal spin. This representation is rather analogous to the partial wave expansion of scattering amplitudes with respect to complex angular momentum, given in terms of Legendre polynomials or functions, respectively. Indeed, also our

partial waves can be expressed in terms of associated Legendre functions of the first and second kind. Mathematically, there should exist a one-to-one relation to other representations that are based on conformal symmetry. The transformations between different representations, however, still have to be worked out in detail. For instance, taking the Mellin transform of the Mellin-Barnes integral must lead to the integral kernel that maps the “effective forward parton distribution” to GPDs [36, 37] or employing the Fourier transform one must arrive at the light-cone position space representation [33, 34, 35]. We confirm and generalize the results for the gluonic sector given in Ref. [35]. The advantage of our new representation is that the central and outer region are obtained from the same conformal moments of a GPD and polynomiality is manifestly implemented. This has not been done so far in the approaches, we mentioned. Sometimes, the central region was even treated incorrectly, for comments see Ref. [37]. We derived a “spectral” representation of conformal kernels with complex valued conformal spin. However, we are not completely satisfied with this representation, since some support restriction have to be fixed explicitly by step-functions. So far an orthogonal eigenfunction basis for these kernels can only be given as series of mathematical distributions, which are labelled by non-negative integer conformal spin.

To leading order the kernels and hard-scattering amplitudes respect conformal symmetry and so we could provide the solution of the evolution equation and the Compton form factors for DVCS as Mellin-Barnes integral. This representation allows a simple and stable numerical evaluation of these quantities. This has some practical advantages, especially, having efficient numerical routines at hand for the evaluation of the Mellin-Barnes integral, one might be able to evaluate this quantities in “real time” rather than using a database of Compton form factors or GPDs. We even demonstrated for the Compton form factors that by means of the Mellin-Barnes integral a systematic analytic approximation in powers of  $\xi$  is feasible.

Beyond LO order the conformal symmetry is broken in a subtle way by the minimal subtraction scheme, applied to the divergencies of composite operators, and the trace anomaly of the energy momentum tensor. The first effect can be cured by a finite renormalization, while the latter one can be absorbed into either the hard-scattering amplitudes or the evolution of GPDs. Such symmetry breaking effects have been studied for  $\eta = 1$  in connection with the pion distribution amplitude and the pion elastic and  $\gamma\gamma^* \rightarrow \pi^0$  transition form factor. Depending on the model for the pion distribution amplitude one finds a 10% variation of the NLO corrections [74]. For skewness  $\eta < 1$  one would expect an even smaller effect because the conformal symmetry breaking is suppressed by a factor  $\eta^2$ . For realistic experiments typically  $\eta \lesssim 0.4$ . Further studies are desirable to clarify this issue and, hopefully might provide a systematic expansion of the conformal symmetry breaking effects in powers of  $\eta^2$ .

Certainly, the evaluation of the analytic continued conformal moments from a given GPD ansatz is a rather non-trivial task, the difficulty of which depends on the analytic properties of the corresponding GPD. Since, however, GPDs are almost unknown non-perturbative functions, one should rather model the conformal moments directly instead of the GPDs or DDs. This is

a non-trivial task with respect to skewness dependence, since certain analytic properties of the conformal moments must be respected. Some effort is required to tune the internal skewness dependence, arising from the conformal partial waves, accordingly. In the end, however, it turned out that our ansätze generated GDAs with non-vanishing end-point contributions. This illustrates again that known constraints for GPDs are very difficult to fulfill. An important observation one can draw from our examples is that “strong skewness” effects already show up in the first few conformal moments for non-negative integer conformal spin. So it is worthwhile to calculate them on the lattice to get a clue for the strength of the skewness dependence of GPDs.

A partial wave expansion of the conformal moments itself avoids the problems described above yields a most flexible parameterization of GPDs in terms of form factors. These form factors are related to particle exchanges in the  $t$ -channel, but this connection still has to be worked out in detail. For  $\eta = 0$  there is no difference between conformal spin and ordinary spin and the conformal partial wave expansion turns over into one with respect to spin. In this kinematical domain we found some evidence that Regge phenomenology can be used as a reliable guide for modelling the conformal moments. Especially, for unpolarized valence quark GPDs the parameterization of parton densities and elastic electromagnetic form factors can be unified and interpreted as a leading Regge trajectory. Since GPDs depend on the factorization conventions, such a connection can only hold approximatively. Moreover, Regge theory is only applicable for physical amplitudes and going beyond the leading trajectory has its own difficulties. Nevertheless, the Regge analogy provides some guidance for the modelling of conformal moments. This is especially important for those GPDs that are difficult to extract from experiments.

The advantage of the Mellin-Barnes representation has been demonstrated for several analytic and numerical examples, especially, for unpolarized valence quarks in the  $\eta = 0$  case. The only unknown in this limit is the spin, i.e.,  $j$ , dependence of the form factors, which for  $j = 0$ , are measured in elastic electron proton scattering. The momentum fraction dependence of the GPD follows then from the  $t$ - and  $Q^2$ -dependencies, where the boundary condition at the input scale  $Q_0^2$  and at  $\Delta^2 = 0$  can be simply taken from the parameterization of Mellin moments for parton densities. Remarkably, no additional fitting procedure is needed to satisfy the GPD constraints. However, different parameterization of the form factors with respect to  $j$ , can lead to a different holographic picture of the nucleon. Certainly, the important task here is to pin down the remaining degrees of freedom for the  $j$  dependence. No question, improved lattice calculation with a realistic pion mass can provide at least a partial answer.

We would like to add a speculation concerning the experimental access to this dependence in hard exclusive reactions. Suppose it turns out from lattice measurements that the skewness dependence of the conformal moments is weak, the  $\xi$ -dependence for the scattering amplitude is (approximately) known and the only degree of freedom left is the unknown  $j$ -dependence of these form factors, which determines the shape of the trajectory of the cross-over point of a GPD as function of  $\xi$ , in dependence of  $\Delta^2$ . Such a trajectory can be explored in single beam spin experi-

ments. Taking Mellin moments of this trajectory, which requires of course some interpolation, one directly gets the form factors, up to some normalization factor, in dependence of the (conformal) spin.

Let us finally stress that the crossing relation between GPDs and GDAs is very simple for conformal moments. Apart from a trivial rescaling procedure of the skewness dependence it involves only the  $\Delta^2$  or  $W^2$  dependence. One has to perform an analytic continuation of the form factors from the space- to the time-like region, which requires only a suitable parameterization in terms of rational functions (linear combination of monopole or dipole forms), which scale for  $\Delta^2 \rightarrow -\infty$  such as predicted by dimensional counting rules. As there exist also non-perturbative scales, like the hadron masses themselves or  $\Lambda_{\text{QCD}}$ , anomalous, i.e., logarithmical deviations, from the canonical scaling should be present to some extend. Although, we were not able to give for all examples of conformal moments an unified representation of GPDs and GDAs in terms of a Mellin-Barnes integral this is not a restriction in practice. If one has an ansatz for the dependence of the conformal moments on the complex conformal spin, one can employ for GDAs the partial wave expansion with integer conformal spin.

In conclusion, we have introduced a representation that makes it easier to include GPDs and GDAs in phenomenological studies and offers new theoretical possibilities for the investigation of perturbative and non-perturbative aspects.

## Acknowledgement

For discussions on mathematical aspects we are indebted to A. Manashov and for a general discussion on GPDs we like to thank M. Diehl, which inspired us to include several remarks. This project has been supported by the DFG.

## A Integrals

In this appendix we collect several integrals, which appear in the evaluation of moments or the convolution of GPDs with the hard scattering amplitude. The partial waves  $p_j(x, \eta)$ , given in Eqs. (53), (54), and (55), might be expressed by associated Legendre functions of the first and second kind, i.e., by  $\sqrt{1-x^2}P_{j+1}^{-1}(x)$  and  $\sqrt{1-x^2}Q_{j+1}^{-1}(x)$ . The conformal moments  $c_j(x, \eta)$ , see Eq. (35), can be represented within the same basis, however, divided by the weight  $(1-x^2)$  [75]. The integrals, presented in the following, can then be read off from diverse integral tables. Moreover, we give the relation between conformal and ordinary Mellin moments.

The conformal moments of the partial waves for complex valued conformal spin read in the outer region

$$\int_{\eta}^{\infty} dx c_k(x, \eta) p_j(x, \eta) = \frac{\sin(\pi j)}{\pi} \frac{\mathcal{N}_{kj}(\eta)}{k-j}, \quad \Re j > \Re k, \quad (159)$$

where the normalization factor is given by

$$\mathcal{N}_{kj}(\eta) = \frac{2\Gamma(3+k)\Gamma(5/2+j)}{\Gamma(3+j)\Gamma(3/2+k)(j+k+3)} \left(\frac{\eta}{2}\right)^{k-j}, \quad \mathcal{N}_{jj}(\eta) = 1. \quad (160)$$

Note that this integral (159) only converges for  $\Re j > \Re k$ . In the central region we have the following integral

$$\int_{-\eta}^{\eta} dx c_k(x, \eta) p_j(x, \eta) = \left( \frac{\sin(\pi j)}{\pi} - \frac{(j+1)(j+2)}{(k+1)(k+2)} \frac{\sin(k\pi)}{\pi} \right) \frac{\mathcal{N}_{kj}(\eta)}{j-k}. \quad (161)$$

On the r.h.s. two terms appear in the brackets. The sum of the former one and the integral (159) is proportional to the identity  $\delta(j-k)$ , however, the latter one gives an addendum. Fortunately, for integer value  $k = m = 0, 1, 2, \dots$  it will not contribute. Remarkably, if the support of  $c_k(x, \eta)$  is extended to  $x \leq -\eta$  by means of

$$c_k(x, \eta) = \left(\frac{\eta}{2}\right)^{2k+2} \frac{\sin(k\pi)\Gamma(1+k)\Gamma(3+k)}{\Gamma(3/2+k)\Gamma(5/2+k)} x^{-k-3} {}_2F_1\left(\begin{matrix} (k+3)/2, (k+4)/2 \\ 5/2+k \end{matrix} \middle| \frac{\eta^2}{x^2}\right), \quad x \leq -\eta \quad (162)$$

and for  $p_j(x, \eta)$  by analytic continuation into the region  $x < 0$ , we have the following integral

$$\int_{-\infty}^{-\eta} dx c_k(x, \eta) p_j(x, \eta) = \frac{(j+1)(j+2)}{(k+1)(k+2)} \frac{\sin(k\pi)}{\pi} \frac{\mathcal{N}_{kj}(\eta)}{j-k}, \quad \Re k > \Re j. \quad (163)$$

Up to the sign it is equal to the  $\sin(k\pi)$  proportional contribution on the r.h.s. in Eq. (161). Hence, the sum of integrals (159), (161) and (163) might be understood as a limit  $\Re k \rightarrow \Re j$  that yields the identity, formally written as

$$\int_{-\infty}^{\infty} dx c_k(x, \eta) p_j(x, \eta) = -2i \sin(\pi j) \delta(k-j). \quad (164)$$

We add that for non-negative integer values of the conformal spin the integral (161) establishes the orthogonality relation (40) for Gegenbauer polynomials.

Let us also give here the Mellin moments of the partial waves  $p_j(x, \eta)$  for integer value  $n = 0, 1, 2, \dots$ . For the integration in the outer region we have

$$\int_{\eta}^{\infty} dx x^n p_j(x, \eta) = \frac{\eta^{n-j} \sin(\pi j)}{(n-j)\pi} {}_3F_2\left(\begin{matrix} 1/2+j/2, 1+j/2, j/2-n/2 \\ 5/2+j, 1+j/2-n/2 \end{matrix} \middle| 1\right), \quad \Re j > \Re n, \quad (165)$$

while from the central region we find, up to the overall sign, the same expression

$$\int_{-\eta}^{\eta} dx x^n p_j(x, \eta) = \frac{\eta^{n-j} \sin(\pi j)}{(j-n)\pi} {}_3F_2\left(\begin{matrix} 1/2+j/2, 1+j/2, j/2-n/2 \\ 5/2+j, 1+j/2-n/2 \end{matrix} \middle| 1\right). \quad (166)$$

Neglecting the  $\sin(\pi j)$  term, these expressions will contain single poles at  $j = \{0, 2, \dots, n\}$  and  $j = \{1, 3, \dots, n\}$  for even and odd  $n$ , respectively. The values for the two lowest moments are:

$$\int_{-\eta}^{\eta} dx p_j(x, \eta) = \left(\frac{2}{\eta}\right)^j \frac{2^3 \Gamma(5/2+j)}{j \Gamma(1/2) \Gamma(4+j)} \frac{\sin(\pi j)}{\pi}, \quad (167)$$

$$\int_{-\eta}^{\eta} dx x p_j(x, \eta) = \left(\frac{2}{\eta}\right)^{j-1} \frac{2^4 \Gamma(5/2+j)}{(j-1)(4+j) \Gamma(1/2) \Gamma(3+j)} \frac{\sin(\pi j)}{\pi}. \quad (168)$$

Analogous as discussed above, the sum of both integrals (165) and (166) should be understood as a limit that results in a linear combination of “ $\delta$ -functions”, which are concentrated in  $j = \{0, 1, \dots, n\}$ . From the Mellin-Barnes representation of GPDs we explicitly find then the usual Mellin moments, expressed in terms of conformal ones:

$$\int_{-1}^1 dx x^n q(x, \eta, \Delta^2) = \sum_{i=0}^n \left(\frac{\eta}{2}\right)^{n-i} \frac{\left(1 + (-1)^{n-i}\right) n! \Gamma(5/2 + i)}{2 i! \Gamma(1 + n/2 - i/2) \Gamma(5/2 + i/2 + n/2)} m_i(\eta, \Delta^2). \quad (169)$$

The inverse relation can be brought in the form

$$m_n(\eta, \Delta^2) = \sum_{i=0}^{[n/2]} \left(\frac{\eta}{2}\right)^{2i} \frac{(-1)^i n! \Gamma(3/2 + n - i)}{i! (n - 2i)! \Gamma(3/2 + n)} \int_{-1}^1 dx x^{n-2i} q(x, \eta, \Delta^2). \quad (170)$$

In the convolution of the hard-scattering amplitude with generalized parton distributions the following two integrals appear:

$$\int_{-\xi}^{\infty} \frac{dx}{\xi + x} p_j(x, \xi) = \left(\frac{2}{\xi}\right)^{1+j} \frac{\Gamma(5/2 + j)}{\Gamma(3/2) \Gamma(3 + j)}, \quad (171)$$

$$\int_{-\xi}^{\infty} \frac{dx}{\xi - x - i\epsilon} p_j(x, \xi) = e^{-i\pi j} \left(\frac{2}{\xi}\right)^{1+j} \frac{\Gamma(5/2 + j)}{\Gamma(3/2) \Gamma(3 + j)}. \quad (172)$$

We note that the reduction to non-negative integer values of the conformal spin is simply done by the replacement  $j \rightarrow n$ . In this case only the central region contributes in these integrals, especially, the imaginary part will drop out

## B Gluonic sector

Here we present the Mellin-Barnes integral for gluon GPDs, defined in Eq. (2). Let us first note that the index of Gegenbauer polynomials, appearing in the definition of conformal moments, is determined by group theory. To be more general, we consider the light-ray operator

$$\mathcal{O}(\kappa_1, \kappa_2) = \phi(\kappa_2 n) \phi(\kappa_1 n) \quad (173)$$

that contains two quantum fields, which live on the light-cone  $n^2 = 0$ . For gluons the field is build by the field strength tensor. We assume that these fields have definite spin projection  $s$  on the light-cone, i.e.,

$$n^\mu \Sigma_{\mu\nu} \tilde{n}^\nu \phi(\kappa n) = s \phi(\kappa n). \quad (174)$$

Here  $\Sigma_{\mu\nu}$  is the usual generator of Lorentz transformation, acting on a field  $\phi(x)$  at  $x = 0$ . Moreover, the canonical dimension of the field  $\phi(x)$  is denoted as  $\ell$ . The conformal spin of the field is defined as

$$j = \frac{1}{2}(\ell + s). \quad (175)$$



It characterizes the behavior of the field under collinear conformal transformation, which can be viewed as the projective transformations on a line:

$$\begin{aligned}\kappa &\rightarrow \kappa' = \frac{a\kappa + b}{c\kappa + d}, \quad ad - bc = 1, \\ \phi(\kappa n) &\rightarrow \phi'(\kappa n) = (c\kappa + d)^{-2j} \phi\left(\frac{a\kappa + b}{c\kappa + d} n\right).\end{aligned}\quad (176)$$

In four dimensional space the quantum numbers are

$$\ell = \frac{3}{2}, \quad s = \pm \frac{1}{2} \quad \text{for quark fields} \quad (177)$$

$$\ell = 2, \quad s = 0, \pm 1 \quad \text{for gluon field strength tensor} \quad (178)$$

The conformal operators are obtained by the group theoretical decomposition of the light-ray operator (173) into irreducible representations. If both quantum fields have the same conformal spin, then the (local) conformal operators which have definite conformal spin are characterized by Gegenbauer polynomials with index  $\nu = 2j - 1/2$ :

$$\mathcal{O}_{nl} = i^l (\partial_{\kappa_1} + \partial_{\kappa_2})^l C_n^\nu \left( \frac{\partial_{\kappa_1} - \partial_{\kappa_2}}{\partial_{\kappa_1} + \partial_{\kappa_2}} \right) \mathcal{O}(\kappa_1, \kappa_2) \Big|_{\kappa_1 = \kappa_2 = 0}, \quad n \leq l, \quad (179)$$

where the conformal spin of these operators is  $2j + n$ . For each given conformal spin, there appears an infinite tower of operators which are labelled by the quantum number  $l$ , related to their spin or if one likes to their canonical dimension. For leading twist operators the spin projection  $s$  must be maximal so that the twist of the fields  $t = \ell - s$  is minimal. Consequently, to leading twist the quark fields have conformal spin  $j = 1$  and gluon ones  $j = 3/2$ . The index of Gegenbauer polynomials is in the former and latter case  $\nu = 3/2$  and  $\nu = 5/2$ . We remark that the gauge link factor connecting the fields along the light-cone does not change the construction via Eq. (179).

For gluonic GPDs (2) we define the conformal moments for  $n = 1, 2, \dots$

$$G_{c_n}(x, \eta) = \eta^{n-1} G_{c_n}\left(\frac{x}{\eta}\right) \quad \text{with} \quad G_{c_n}(x) = \frac{\Gamma(5/2)\Gamma(n)}{2^{n-1}\Gamma(3/2+n)} C_{n-1}^{5/2}(x). \quad (180)$$

in such a way that in the forward limit the usual normalization of Mellin moments appear:  $\lim_{\eta \rightarrow 0} G_{c_n}(x, \eta) = x^{n-1}$ . Moreover, as in the quark sector, they project on operators with conformal spin  $2 + n$ . Compared to the Mellin moments of parton densities within our convention, one power in  $x$  seems to be missed, however, it is included in the definition of GPDs. For instance, in the vector case we have

$$\lim_{\Delta \rightarrow 0} G_F^V(x, \eta, \Delta^2) = xg(x) \quad \text{for} \quad x \geq 0, \quad (181)$$

where  $g(x)$  is the unpolarized gluon parton density. Analogous convention holds for the axial-vector case. The analytic continuation of the conformal spin  $j$  in the conformal moments is again done in terms of hypergeometric functions

$$G_{c_j}(x, \eta) = \frac{\Gamma(3/2)\Gamma(j+4)}{2^4\Gamma(3/2+j)} \left(\frac{\eta}{2}\right)^{j-1} {}_2F_1\left(-j+1, j+4 \middle| \frac{\eta-x}{2\eta}\right). \quad (182)$$

The conformal partial waves are analogously constructed as described in Sect. 2.3.1. Namely, by including the weight  $(1 - x^2/\eta^2)^2$  with a suitable normalization and from the requirement that the partial waves are vanishing at  $x = -\eta$  and are continuous at the cross-over point  $x = \eta$ :

$$G_{p_j}(x, \eta) = \theta(\eta - |x|)\eta^{-j} {}^G\mathcal{P}_j\left(\frac{x}{\eta}\right) + \theta(x - \eta)\eta^{-j} {}^G\mathcal{Q}_j\left(\frac{x}{\eta}\right) \quad (183)$$

where

$${}^G\mathcal{P}_j(x) = \frac{2^j \Gamma(5/2 + j)}{\Gamma(1/2)\Gamma(j)} (1 + x)^2 {}_2F_1\left(\begin{matrix} -j - 1, j + 2 \\ 3 \end{matrix} \middle| \frac{1 + x}{2}\right), \quad (184)$$

$${}^G\mathcal{Q}_j(x) = \frac{\sin(\pi j)}{\pi} x^{-j} {}_2F_1\left(\begin{matrix} j/2, (j + 1)/2 \\ 5/2 + j \end{matrix} \middle| \frac{1}{x^2}\right). \quad (185)$$

Moreover, Bose symmetry implies definite symmetry of the gluonic GPDs (2) under the transformation  $x \rightarrow -x$ , i.e., in the (axial-)vector case they are always (anti-)symmetric. This property is simply restored by forming symmetric or antisymmetric partial waves, see Eq. (75). Corresponding to our normalization (181), we write

$$G_q(x, \eta, \Delta^2) = \frac{i}{2} \int_{c-i\infty}^{c+i\infty} dj \frac{(-1)}{\sin(\pi j)} [{}^Gp_j(x, \eta) \pm {}^Gp_j(-x, \eta)] m_j(\eta, \Delta^2), \quad (186)$$

where only the analytic continuation of conformal moments for even (odd) integer values of  $n$  is needed for (anti-)symmetric gluon GPDs.

Let us comment on the properties of the gluonic conformal partial waves (183). They are related to the quark ones by a derivation with respect to  $x$ :

$$p_j(x, \eta) = \frac{1}{j} \frac{d}{dx} {}^Gp_j(x, \eta). \quad (187)$$

As a simple consequence, the first derivative of the gluonic partial wave is smooth at the cross-over point, while the second one has a jump as it is the case in the quark sector. Also at the point  $x = -\eta$  the gluonic partial waves vanish as  $(x + \eta)^2$  rather than  $(x + \eta)$  as for the quark ones. Consequently, the convolution with the following hard-scattering amplitudes, which appear in the electroproduction of transversely polarized vector mesons [76], exist

$$\int_{-\xi}^{\infty} \frac{dx}{(\xi + x)^2} {}^Gp_j(x, \xi) = \left(\frac{2}{\xi}\right)^{1+j} \frac{j \Gamma(5/2 + j)}{\Gamma(3/2)\Gamma(3 + j)}, \quad (188)$$

$$\int_{-\xi}^{\infty} \frac{dx}{(\xi - x - i\epsilon)^2} {}^Gp_j(x, \xi) = e^{-i\pi(j-1)} \left(\frac{2}{\xi}\right)^{1+j} \frac{j \Gamma(5/2 + j)}{\Gamma(3/2)\Gamma(3 + j)}. \quad (189)$$

It has been argued already in Ref. [76] that this integrals without any further regularization exist, which is shown here from a more general point of view. We add that in the convolution of the gluonic GPDs with the hard-scattering amplitude at leading twist-two the integrals appear

$$\int_{-\xi}^{\infty} \frac{dx}{\xi + x} {}^Gp_j(x, \xi) = \left(\frac{2}{\xi}\right)^j \frac{4 \Gamma(5/2 + j)}{\Gamma(3/2)\Gamma(4 + j)}, \quad (190)$$

$$\int_{-\xi}^{\infty} \frac{dx}{\xi - x - i\epsilon} {}^Gp_j(x, \xi) = e^{-i\pi(j-1)} \left(\frac{2}{\xi}\right)^j \frac{4 \Gamma(5/2 + j)}{\Gamma(3/2)\Gamma(4 + j)}. \quad (191)$$

Finally, the convolution with conformal kernels is analogous done as outlined in Sect. 3 and yields in the Mellin-Barnes integral representation of GPDs to a multiplication of the conformal moments with its eigenvalues. Here we only mention that in correspondence with our normalization these eigenvalues follows from the Mellin transform of the forward limit, i.e., from the Mellin moments of the usual DGLAP kernels.

## C Mellin–Barnes representation of conformal kernels

In the following we derive the Mellin–Barnes integral for a generic kernel (87), which is conformal covariant and possess only non-negative eigenvalues  $k_n$ . This is analogously done as for GPDs in Sect. 2.3. Let us first remind on the support extension of the spectral representation (87). The procedure for the kernel  $K(x, y)$  is well-known and arise from the representation

$$K(x, y) = \int_0^1 dw_+ \int_{-1+w_+}^{1-w_+} dw_- \delta(x - yw_+ - w_-) \kappa(w_+, w_-). \quad (192)$$

Here  $\kappa(w_+, w_-)$  is the analog of the DD in the case of GPD, see Eqs. (10) and (21). Such a kernel appears in the convolution with a light-ray operator (173) and it is in the mathematical sense a distribution. The support in the whole  $(x, y)$ -plane can be read off from Eq. (23) and is written here as

$$K(x, y) = \theta(y - x)\theta(x + 1) [k(x, y) - \theta(x - 1)k(-x, -y)] + \left\{ \begin{array}{l} x \rightarrow -x \\ y \rightarrow -y \end{array} \right\}, \quad (193)$$

where the distribution  $k(x, y)$  has the integral representation

$$k(x, y) = \int_0^{\frac{1+x}{1+y}} dw_+ \kappa(w_+, x - yw_+). \quad (194)$$

Analogous as in the case of a GPD, see discussion in Sec. 2.1, this integral is only uniquely defined in the central region, i.e.,  $|x| \leq 1$ , while in the outer region  $1 \leq |x|$  only the difference  $k(x, y) - k(-x, -y)$  enters. Here the ambiguities in the support extension of  $\kappa(w_+, x - yw_+)$  drop out. The support extension from the region  $|x|, |y| \leq 1$  to the whole support is unique [2], see analogous discussion as in the last paragraph of Sect. 2.2.

Now we are in the position to derive the Mellin-Barnes integral representation for the kernel  $K(x, y)$ . To do so, we represent the series (87) in the region  $|x|, |y| < 1$  as integral in the complex plane that includes the positive real axis

$$K(x, y) = \frac{1}{2i} \oint_{(0)}^{(\infty)} dj \frac{1}{\sin(\pi j)} p_j(x) k_j c_j(y). \quad (195)$$

Here the functions  $c_j(x) = c_j(x, 1)$  and  $p_j(x) = p_j(x, 1)$  are defined in Eqs. (35) and (46), respectively, and  $k_j$  is the analytic continuation of the eigenvalues  $k_n$ . They coincide with the Mellin

moments of the corresponding DGLAP kernel and might possess a logarithmical growing for  $j \rightarrow \infty$ . The integrand has simple poles at  $j = n = 0, 1, 2, \dots$  and so the residue theorem leads to the series (87). Next, we deform the integration contour in such a way that it includes the imaginary axis and is closed by an arc with infinite radius, see Fig. 3 (a). It remains to show that this latter contribution vanishes. The behavior of the integrand for large  $j$  with  $|\arg(j)| \leq \pi/2$  can be estimated from the behavior of hypergeometric functions and is in our case given by [56]

$$\frac{1}{\sin(\pi j)} p_j(x + i\epsilon) c_j(y - i\epsilon) \sim \frac{e^{\pm j \{ \operatorname{arccosh}(-x - i\epsilon) \pm \operatorname{arccosh}(y - i\epsilon) \}}}{\sin(\pi j)}. \quad (196)$$

Here the analytic continuation in the complex plane by the  $i\epsilon$  prescription determines the branch of the  $\operatorname{arccosh}$  function, not uniquely defined for real valued  $x, y < 1$ . It is done in such a way that the estimate (196) is applicable for  $-1 < y$  and  $x < 1$  and  $|\arg(j)| \leq \pi/2$ . Obviously, on the infinite arc, both the denominator and numerator in Eq. (196) will exponentially grow and the integrand will vanish as long as the condition  $|\operatorname{arccosh}(-x - i\epsilon) \pm \operatorname{arccosh}(y - i\epsilon)| \leq \pi$  is satisfied. This is the case for  $-1 < x < y < 1$ . Thus, for this region we arrive at the Mellin–Barnes representation for the Kernel  $K(x, y)$ , i.e., for the function

$$k(x, y) = \frac{i}{2} \int_{c-i\infty}^{c+i\infty} dj \frac{1}{\sin(\pi j)} p_j(x) k_j c_j(y). \quad (197)$$

From the spectral representation (192) it follows that the convolution of the kernel with a holomorphic test function  $\tau(x)$  yield a holomorphic function, depending on  $y$ . Thus, we might now employ analytic continuation to extend the representation (197) into the region  $1 \leq y$ . This will not alter the convergency properties of the integral, since  $\arg(\operatorname{arccosh}(y)) = 0$  for  $1 \leq y$ . We remind that  $p_j(x)$  coincides for  $x \leq 1$  with the holomorphic function  $\mathcal{P}_j(x)$ , defined in Eq. (54).  $\mathcal{P}_j(x)$  has a branch cut, starting at  $x = 1$ , along the positive real axis and we might define its value on the this cut by  $(\mathcal{P}_j(x + i\epsilon) + \mathcal{P}_j(x - i\epsilon))/2$ . Hence, within this procedure the function  $k(x, y)$  is uniquely continued into the region  $1 \leq y$  for all values  $-1 \leq x$ , cf. with the prescription (16).

The Mellin–Barnes integral for the kernel  $K(x, y)$  follows now in a unique way from the result (197) and its support, cf. Eq. (193). For  $1 \leq x$  we can write  $K(x, y)$  as the difference

$$K(x, y) = k(x, y) - k(-x, -y) \quad \text{for } 1 \leq x \leq y. \quad (198)$$

We represent  $k(-x, -y)$  via the Mellin–Barnes integral (197), where  $p_j(-x)$  is obtained by analytic continuation while  $c_j(-y)$  has now for  $1 \leq y$  a branch cut and a single pole at  $y = 1$  on the real axis. We have now to employ the principal value prescription, as above for  $\mathcal{P}_j(x)$ , and so its value on the cut is

$$\frac{1}{2} [c_j(-y + i\epsilon) + c_j(-y - i\epsilon)] = \cos(\pi j) c_j(y) + \sin(\pi j) d_j(y), \quad (199)$$

where the function  $d_j(y)$  is defined in Eq. (67). Using the asymptotic behavior of hypergeometric functions for large  $j$ , it can be shown that in the region  $1 \leq x < y$  the contribution  $\mathcal{P}_j(-x) k_j d_j(y)$ ,

appearing in the integral (197), exponentially vanishes for  $j \rightarrow \infty$  with  $|\arg(j)| \leq \pi/2$ . Hence, we can close the integration path so that the positive real axis is encircled. Since it is a holomorphic function, the corresponding integral vanishes. So we can drop this contribution and find that for  $1 \leq x < y$  the extension of the integral kernel,

$$\frac{k_j}{\sin(\pi j)} p_j(x) c_j(y) = \frac{k_j}{\sin(\pi j)} \left[ \frac{1}{2} \mathcal{P}_j(x + i\epsilon) + \frac{1}{2} \mathcal{P}_j(x - i\epsilon) - \cos(\pi j) \mathcal{P}_j(-x) \right] c_j(y), \quad (200)$$

of the Mellin–Barnes integral for  $K(x, y)$

$$K(x, y) = \frac{i}{2} \int_{c-i\infty}^{c+i\infty} dj \frac{k_j}{\sin(\pi j)} p_j(x) c_j(y) \quad \text{for } x < y. \quad (201)$$

The formula (200) defines the continuation of  $p_j(x)$  for  $1 \leq x$ , which coincides with Eqs. (53)–(55) for  $\eta = 1$ . The missing part of the kernel, i.e., for  $y < x$ , follows by the symmetry transformation  $x, y \rightarrow -x, -y$  from Eq. (201). Hence, the integral kernel can be written as

$$K(x, y) = \frac{i}{2} \int_{c-i\infty}^{c+i\infty} dj \frac{k_j}{\sin(\pi j)} [\theta(y - x) p_j(x) c_j(y) + \theta(x - y) p_j(-x) c_j(-y)]. \quad (202)$$

We excluded in our analyze here the line  $x = y$ . As long  $jk_j$  is vanishing for  $j \rightarrow \infty$ , we can use analytic continuation to approach it. In all other cases a more advanced analyze is required. However, this is in fact not necessary here, since it is obvious that a constant or logarithmic behavior of  $k_j$  for  $j \rightarrow \infty$  is associated with  $\delta$ -functions and  $+$ -prescriptions for singularities at  $x = y$ . It is easy to check by forming the lowest moment that the Mellin-Barnes integral is correct in that case, too.

## References

- [1] F.-M. Dittes, B. Geyer, D. Müller, D. Robaschik, and J. Hořejši, Phys. Lett. **209B**, 325 (1988).
- [2] D. Müller, D. Robaschik, B. Geyer, F.-M. Dittes, and J. Hořejši, Fortschr. Phys. **42**, 101 (1994), hep-ph/9812448.
- [3] X.-D. Ji, Phys. Rev. Lett. **78**, 610 (1997), hep-ph/9603249.
- [4] A. V. Radyushkin, Phys. Lett. **B380**, 417 (1996), hep-ph/9604317.
- [5] J. Collins, L. Frankfurt, and M. Strikman, Phys. Rev. **D56**, 2982 (1997), hep-ph/9611433.
- [6] M. Diehl, T. Gousset, B. Pire, and O. Teryaev, Phys. Rev. Lett. **81**, 1782 (1998), hep-ph/9805380.
- [7] J. Ralston and B. Pire, Phys. Rev. **D66**, 111501 (2002), hep-ph/0110075.

- [8] M. Burkardt, Phys. Rev. **D62**, 071503 (2000), hep-ph/0010082.
- [9] M. Burkardt, Int. J. Mod. Phys. **A18**, 173 (2003), hep-ph/0207047.
- [10] M. Diehl, Eur. Phys. J. **C25**, 223 (2002), hep-ph/0205208.
- [11] A. V. Belitsky and D. Müller, Nucl. Phys. **A711**, 118 (2002), hep-ph/0206306.
- [12] A. V. Belitsky, AIP Conf. Proc. **698**, 607 (2004), hep-ph/0307256.
- [13] X.-D. Ji, Phys. Rev. Lett. **91**, 062001 (2003), hep-ph/0304037.
- [14] M. Diehl, Phys. Rept. **388**, 41 (2003), hep-ph/0307382.
- [15] A. V. Belitsky and A. V. Radyushkin, *Unraveling hadron structure with generalized parton distributions*, (2005), hep-ph/0504030.
- [16] M. Guidal and M. Vanderhaeghen, Phys. Rev. Lett. **90**, 012001 (2003), hep-ph/0208275.
- [17] A. V. Belitsky and D. Müller, Phys. Rev. Lett. **90**, 022001 (2003), hep-ph/0210313.
- [18] A. V. Belitsky and D. Muller, Phys. Rev. D **68**, 116005 (2003), hep-ph/0307369.
- [19] F. Yuan, Phys. Rev. **D69**, 051501 (2004), hep-ph/0311288.
- [20] M. Burkardt, Phys. Lett. **B595**, 245 (2004), hep-ph/0401159.
- [21] LHPC, P. Hagler *et al.*, Phys. Rev. **D68**, 034505 (2003), hep-lat/0304018.
- [22] QCDSF, M. Gockeler *et al.*, Phys. Rev. Lett. **92**, 042002 (2004), hep-ph/0304249.
- [23] LHPC, P. Hagler *et al.*, Eur. Phys. J. **A24S1**, 29 (2005), hep-ph/0410017.
- [24] S. Brodsky, Y. Frishman, G. Lepage, and C. Sachradja, Phys. Lett. **91B**, 239 (1980).
- [25] A. V. Efremov and A. V. Radyushkin, Phys. Lett. **94B**, 245 (1980).
- [26] D. Müller, Phys. Rev. **D58**, 054005 (1998), hep-ph/9704406.
- [27] B. Melić, D. Müller, and K. Passek-Kumerički, Phys. Rev. **D68**, 014013 (2003), hep-ph/0212346.
- [28] D. Müller, Nucl. Phys. **A755**, 71 (2005), hep-ph/0501158.
- [29] A. V. Belitsky, B. Geyer, D. Müller, and A. Schäfer, Phys. Lett. **B 421**, 312 (1998).
- [30] L. Mankiewicz, G. Piller, and T. Weigl, Eur. Phys. J. **C5**, 119 (1998), hep-ph/9711227.

- [31] A. V. Belitsky, D. Müller, L. Niedermeier, and A. Schäfer, Phys. Lett. **B437**, 160 (1998), hep-ph/9806232.
- [32] A. V. Belitsky, D. Müller, L. Niedermeier, and A. Schäfer, Nucl. Phys. **B546**, 279 (1999), hep-ph/9810275.
- [33] I. Balitsky and V. Braun, Nucl. Phys. **B311**, 541 (1989).
- [34] N. Kivel and L. Mankiewicz, Nucl. Phys. **B557**, 271 (1999), hep-ph/9903531.
- [35] A. Manashov, M. Kirch, and A. Schäfer, Phys. Rev. Lett. **95**, 012002 (2005), hep-ph/0503109.
- [36] A. Shuvaev, Phys. Rev. **D60**, 116005 (1999), hep-ph/9902318.
- [37] J. D. Noritzsch, Phys. Rev. **D62**, 054015 (2000), hep-ph/0004012.
- [38] M. Polyakov and A. Shuvaev, *On 'dual' parametrizations of generalized parton distributions*, (2002), hep-ph/0207153.
- [39] D. Müller and A. Schäfer, *Next-to-next-to leading order corrections to deeply virtual Compton scattering: the non-singlet case*, in preparation.
- [40] X.-D. Ji, J. Phys. **G24**, 1181 (1998), hep-ph/9807358.
- [41] E. R. Berger, F. Cano, M. Diehl, and B. Pire, Phys. Rev. Lett. **87**, 142302 (2001), hep-ph/0106192.
- [42] M. Bordag and D. Robaschik, Theor. Math. Phys. **49**, 1063 (1982).
- [43] I. I. Balitsky, Phys. Lett. **B124**, 230 (1983).
- [44] A. D. Martin and M. G. Ryskin, Phys. Rev. **D57**, 6692 (1998), hep-ph/9711371.
- [45] B. Pire, J. Soffer, and O. Teryaev, Eur. Phys. J. **C8**, 103 (1999), hep-ph/9804284.
- [46] A. V. Radyushkin, Phys. Rev. **D59**, 014030 (1999), hep-ph/9805342.
- [47] P. V. Pobylitsa, Phys. Rev. **D66**, 094002 (2002), hep-ph/0204337.
- [48] P. V. Pobylitsa, Phys. Rev. **D67**, 034009 (2003), hep-ph/0210150.
- [49] M. Diehl, T. Feldmann, R. Jakob, and P. Kroll, Nucl. Phys. **B596**, 33 (2001), hep-ph/0009255.
- [50] B. Geyer, D. Robaschik, M. Bordag, and J. Hořejši, Z. Phys. **C26**, 591 (1985).
- [51] A. V. Radyushkin, Phys. Rev. **D56**, 5524 (1997), hep-ph/9704207.



- [52] A. V. Belitsky, D. Müller, A. Kirchner, and A. Schäfer, Phys. Rev. **D64**, 116002 (2001), hep-ph/0011314.
- [53] M. V. Polyakov and C. Weiss, Phys. Rev. **D60**, 114017 (1999), hep-ph/9902451.
- [54] O. V. Teryaev, Phys. Lett. **B510**, 125 (2001), hep-ph/0102303.
- [55] V. M. Braun, G. P. Korchemsky, and D. Müller, Prog. in Part. and Nucl. Phys. **51**, 312 (2003), hep-ph/0306057.
- [56] Y. L. Luke, *The Special Functions and their Approximations Vol. 2.* (Academic Press New York and London, 1969).
- [57] D. Müller, Phys. Rev. **D49**, 2525 (1994), hep-ph/9411338.
- [58] R. Crewther, Phys. Lett. **B397**, 137 (1997), hep-ph/9701321.
- [59] A. V. Belitsky and D. Müller, Phys. Lett. **B417**, 129 (1997), hep-ph/9709379.
- [60] A. V. Belitsky and D. Müller, Nucl. Phys. **B527**, 207 (1998), hep-ph/9802411.
- [61] A. V. Belitsky and D. Müller, Nucl. Phys. **B537**, 397 (1999), hep-ph/9804379.
- [62] S. J. Brodsky, G. T. Gabadadze, A. L. Kataev, and H. J. Lu, Phys. Lett. **B372**, 133 (1996), hep-ph/9512367.
- [63] S. Moch, J. A. M. Vermaseren, and A. Vogt, Nucl. Phys. **B688**, 101 (2004), hep-ph/0403192.
- [64] A. Vogt, S. Moch, and J. A. M. Vermaseren, Nucl. Phys. **B691**, 129 (2004), hep-ph/0404111.
- [65] E. B. Zijlstra and W. L. van Neerven, Nucl. Phys. **B383**, 525 (1992).
- [66] A. V. Belitsky, D. Müller, and A. Kirchner, Nucl. Phys. **B629**, 323 (2002), hep-ph/0112108.
- [67] Y. L. Luke, *The Special Functions and their Approximations Vol. 1.* (Academic Press New York and London, 1969).
- [68] P. V. Landshoff, J. C. Polkinghorne, and R. D. Short, Nucl. Phys. **B28**, 225 (1971).
- [69] M. Diehl, T. Feldmann, R. Jakob, and P. Kroll, Eur. Phys. J. **C39**, 39 (2005), hep-ph/0408173.
- [70] I. Balitsky and E. Kuchina, Phys. Rev. **D 62**, 074004 (2000), hep-ph/0002195.
- [71] M. Penttinen, M. V. Polyakov, and K. Goeke, Phys. Rev. **D62**, 014024 (2000), hep-ph/9909489.

- [72] LHPC and SESAM, P. Hägler *et al.*, Phys. Rev. Lett. **93**, 112001 (2004), hep-lat/0312014.
- [73] J. Kogut and D. Soper, Phys. Rev. **D1**, 2901 (1970).
- [74] D. Müller, Phys. Rev. **D59**, 116003 (1999), hep-ph/9812490.
- [75] M. Abramowitz and I. Stegun, *Handbook of Mathematical Functions*. (Dover Publications Inc. New York, 1970).
- [76] L. Mankiewicz and G. Piller, Phys. Rev. **D61**, 074013 (2000), hep-ph/9905287.